1989

Structural and Functional Studies of the Plant Lectin Peanut Agglutinin

Eugene J. Zaluzec
Loyola University Chicago

STRUCTURAL AND FUNCTIONAL STUDIES OF THE PLANT LECTIN PEANUT AGGLUTININ

by

Eugene J. Zaluzec

A Dissertation Submitted to the Faculty of the Graduate School of Loyola University of Chicago in Partial Fulfillment the of the Requirements for the Degree of Doctor of Philosophy

September

1989

ACKNOWLEDGMENTS

I would like to express my sincere gratitude to Drs. Stephen F. Pavkovic and Kenneth W. Olsen for the training, support, and guidance they provided throughout this thesis project. I also extend my appreciation to Drs. Duarte Mota De Freitas, Albert W. Herlinger, and Mir Shamsuddin for serving in my thesis committee.

I am exceedingly thankful to Dr. Mir Shamsuddin, Ghaus Ansari, and Children's Memorial Hospital (Chicago) for their assistance in the amino acid analysis of PNA, Dr. Larry Fox, Salley Dorwin and Abbott Laboratories (Abbott Park, Il.) for the help they provided in the amino acid sequencing of PNA, Dr. Paula M. Fitzgerald (Merck Sharp and Dohme Research Laboratories) for supplying the MERLOT computer programs for the determination of crystal structures by molecular replacement, Dr. Fred L. Suddath (Georgia Institute of Technology) for supplying the pea lectin atomic coordinates, Dr. David Ollis (Northwestern University) for supplying the PROTEIN computer programs for the determination of crystal structures and his help in data analysis, Dr. Bruno Jaselskis (Loyola University of

Chicago) for the use of his HPLC in the manual sequence analysis of PNA, Drs. Leslie W. M. Fung and Duarte Mota De Freitas (Loyola University of Chicago) for the use of their laboratories and equipment in various aspects of this thesis project, and Marianne Yung (Loyola University of Chicago) for providing crystals of PNA-BAP complex and her help in the PNA binding assays.

I would finally like to thankfully acknowledge Loyola University of Chicago for providing financial support, and the faculty, staff, and students of the chemistry department for making my graduate education an enlightening experience.

VITA

The author, Eugene J. Zaluzec, is the fourth son of John and Nettie Zaluzec. He was born March 25, 1956, in Chicago, Illinois.

He received his primary education at Oliver H. Perry Public School in Chicago. His secondary education was from Mendel Catholic High School in Chicago. In August, 1973, Mr. Zaluzec entered Thorton Community College in South Holland, Illinois, from where he received the degree of Associate of Applied Science in electronics technology. From January, 1976, to January, 1981, Mr. Zaluzec was on active duty in the United States Air Force with a primary specialty of airborne avionic communications specialist attaining the rank of E-4 sergeant. In August, 1981, he entered Southern Illinois University, receiving the degree of Bachelor of Science in chemistry in May, 1984.

In August, 1984, Mr. Zaluzec was admitted as a Ph.D. candidate to the Chemistry Department of Loyola University of Chicago. This thesis is being submitted in partial fulfillment of the requirements for the degree of Doctor of Philosophy.

TABLE OF CONTENTS

Page

ACKNOWLEDGMENTS....ii

VITA....iv

TABLE OF CONTENTS....v

LIST OF TABLES....x

LIST OF ILLUSTRATIONS....xiii

ABBREVIATIONS OF VARIABLE NAMES....xix

Chapter Page

I. INTRODUCTION....1

A. LECTINS....1

Historical Background....1

Occurrence and Distribution....3

Molecular Properties....4

Biological Functions....6

Applications and Utilizations....8

B. LEGUMINOUS LECTINS.....11
Primary Structure Homology.....11
Species Heterogeneity.....17
Metal Binding Sites.....23
Hydrophobic Binding Sites.....28
Glycosylation Site.....33
Three Dimensional Structures.....35

C. PEANUT AGGLUTININ.....37
Species Heterogeneity.....37
Carbohydrate Specificity.....38
Macromolecular Properties.....40
Primary Structure.....41
Crystallographic Studies.....41
Biological Functions.....44

II. STATEMENT OF RESEARCH.....45

III. MATERIALS AND METHODS.....48

A. MATERIALS.....48

B. PREPARATION OF PEANUT AGGLUTININ.....50
Saline Fractionation.....50
Affinity Chromatography.....51
1. Preparation of Lactosyl-Sepharose 6B...51
2. Isolation of Peanut Agglutinin.....52

Gel Electrophoresis.....52

1. Dissociating (SDS) Gels.....53

2. Dissociating (Urea) Gels.....54

3. Non-dissociating Gels.....55

C. AMINO ACID COMPOSITION.....56

Acid Hydrolysis.....56

Performic Acid Oxidation (Cystine).....57

N-Bromosuccinimide Assay (Tryptophan).....57

Amino Acid Analysis.....58

D. AMINO ACID SEQUENCING.....58

Chemical Digestion.....58

1. Cyanogen Bromide Cleavage.....58

2. CNBr Peptide Isolation.....60

3. CNBr Peptide Composition.....60

Enzymatic Digestion.....60

1. Trypsin Cleavage.....60

2. Tryptic Peptide Isolation.....61

3. Tryptic Peptide Composition.....62

Manual Sequence Analysis.....62

1. Edman Degradation.....62

2. Phenylthiohydantoin Chromatography.....64

Automated Sequence Analysis.....64

E. BINDING ASSAYS.....65

Carbohydrate Binding.....65
1. Preparation of N-Dansyl Galactosamine..65
2. Fluorometric Titrations.....66
Hydrophobic Binding.....67
1. Fluorometric Titrations.....67
Gel Filtration.....69
F. CRYSTALLOGRAPHY.....69
Crystallization of Peanut Agglutinin.....69
1. Peanut Agglutinin/Lactose.....69
2. Peanut Agglutinin/N^6-Benzylaminopurine.70
Heavy Metal Derivatization.....70
1. Crystal Soaking Derivatization.....70
2. Co-crystallization.....71
X-Ray Diffraction.....71
1. Crystal Mounting.....71
2. Data Collection.....72

IV. RESULTS 74

A. ISOLATION OF PEANUT AGGLUTININ.....74

B. THE PRIMARY STRUCTURE OF PEANUT AGGLUTININ..81
Amino Acid Composition.....81
Cyanogen Bromide Fractionation.....88
Trypsin Fractionation.....93

Sequence Analysis.....95

C. THE BINDING OF LIGANDS TO PEANUT AGGLUTININ.116

Preparation of N-Dansylgalactosamine.....116

Binding of Ligands to PNA.....120

1. Binding of DnsGalN and Lactose.....124

2. Binding of TNS and BAP.....128

3. Binding of ANS.....143

4. Effects of BAP on DnsGalN Binding.....143

5. Determination of Ligand Stoichiometry..144

D. CRYSTALLOGRAPHY OF PEANUT AGGLUTININ.....146

Crystallization of PNA-Lactose.....146

Crystallization of PNA-BAP.....148

Heavy Atom Derivatization of PNA.....148

Diffraction Data Analysis.....150

Heavy Atom Derivative Assays.....158

V. CONCLUSIONS.....162

Primary Structure of PNA.....163

Hydrophobic Binding of PNA.....166

Crystallography of PNA.....175

REFERENCES.....179

APPENDIX 189

LIST OF TABLES

Table | Page

I.1. Blood Type-Specific Lectins.....9

I.2. Characteristics of Legume Lectins.....13

I.3. Metal Binding Regions of Legume Lectins.....27

I.4. Carbohydrate Binding Residues of Legume Lectins Determined by X-ray Diffraction.....29

I.5. Homology of Legume Lectins to the Subunit Hydrophobic Binding Region of Con A.....31

I.6. Glycosylation Sites of Legume Lectins.....34

I.7. Inhibition of Hemagglutinating Activity of Peanut Agglutinin.....39

I.8. Amino Acid Composition Reported for Peanut Agglutinin.....42

IV.1. Composition of Amino Acids Found in Peanut Agglutinin.....84

IV.2. Amino Acid Composition of Cyanogen Bromide Peptides of Peanut Agglutinin.....92

IV.3. Amino Acid Composition of Tryptic Peptides Peanut Agglutinin.....96

IV.4. Composition of PNA Tryptic Peptides Compared to Non-Digested PNA.....96

IV.5. Sequence Analysis of PNA Tryptic Peptides....98

IV.6. Total Composition of Segments Not Sequenced in the Primary Structure of PNA.....115

IV.7. Predicted Composition of Cyanogen Bromide Peptides Not Fully Sequenced in PNA.....117

IV.8. Lattice Parameters of PNA-Lactose Crystals..152

IV.9. Axis Intensity Scans of Native PNA Compared Heavy Atom Treated PNA.....160

IV.10. Degree of Agreement Between Equivalent Reflections of PNA-Lactose and Heavy Atom Treated PNA.....161

V.1. Properties of Interactions Between Lectins and Hydrophobic Ligands.....168

LIST OF ILLUSTRATIONS

Figure		Page
I.1.	Chemotaxonomy of Sequenced Legume Lectins	15
I.2.	Circularly Permuted Sequence Homology of Legume Lectins	16
I.3.	Primary Structure of Legume Lectins	18
I.4.	Model for the Gene Representation of Legume Lectins	24
I.5.	Schematic Diagram Showing Relative Locations of the Various Binding Sites on a Single Protomer of Con A	32
III.1.	Beckman 121M Amino Acid Analyzer Instrument Control Program	59
IV.1.	Affinity Chromatogram of Peanut Agglutinin	76

IV.2. Affinity Chromatogram of Peanut Agglutinin...77

IV.3. UV Absorption Spectrum of Peanut Agglutinin..78

IV.4. SDS Polyacrylamide Disc Electrophoresis of Peanut Agglutinin.....79

IV.5. Subunit Molecular Weight of PNA Determined by SDS-PAGE.....80

IV.6. Urea Polyacrylamide Disc Electrophoresis of Peanut Agglutinin.....82

IV.7. Native Polyacrylamide Disc Electrophoresis of Peanut Agglutinin.....83

IV.8. Amino Acid Analysis of a PNA 24 Hour Hydrolyzate.....86

IV.9. Indole-Oxindole Conversion of Tryptophan by N-Bromosuccinimide Oxidation.....87

IV.10. Gel Chromatogram of Cyanogen Bromide Peptides of PNA.....89

IV.11. Gel Chromatogram of Cyanogen Bromide Band II.....90

IV.12. Gel Chromatogram of Cyanogen Bromide Band III.....91

IV.13. HPLC Separation of Peptides Obtained from the Digestion of PNA with Trypsin.....94

IV.14. HPLC Separation of Calibration Standard PTH Amino Acids.....100

IV.15. Primary Structure of Peanut Agglutinin.....101

IV.16. Reaction Scheme for the Preparation of N-Dansylgalactosamine.....118

IV.17. Thin Layer Chromatography of N-Dansyl-Galactosamine Reaction Mixture.....119

IV.18. Reverse Phase HPLC of N-Dansylgalactosamine Reaction Mixture.....121

IV.19. Ultra Violet Absorption Spectrum of N-Dansyl-Galactosamine in Methanol.....122

IV.20. Proton NMR Spectrum of N-Dansyl Galactosamine.....123

IV.21. Molecular Structure of Probes Used in PNA Binding Assays.....125

IV.22. Fluorescence Emission Enhancement of DnsGalN in the Presence of PNA.....129

IV.23. Fluorescence Emission Intensity of DnsGalN Extrapolated to Infinite PNA Concentration..130

IV.24. Titration of DnsGalN with PNA.....131

IV.25. Graphical Representation for the Determination of the Association Constant of DnsGalN Binding to PNA.....132

IV.26. Fluorescence Emission Quenching of PNA-DnsGalN Complex by Lactose.....133

IV.27. Titration of PNA-DnsGalN Complex with Lactose.....134

IV.28. Graphical Representation for Determination of the Association Constant from the Competitive Binding of Lactose to PNA-DnsGalN Complex...135

IV.29. Fluorescence Emission Enhancement of TNS in the Presence of PNA.....137

IV.30. Titration of PNA with TNS.....138

IV.31. Graphical Representation for Determination of the Association Constant of TNS Binding to PNA.....139

IV.32 Fluorescence Emission Quenching of PNA-TNS Complex by BAP.....140

IV.33. Titration of PNA-TNS Complex with BAP.....141

IV.34. Graphical Representation for Determination of the Association Constant from the Competitive Binding of BAP to PNA-TNS Complex.....142

IV.35. Crystals of PNA Grown in the Presence of Lactose.....147

IV.36. Crystals of PNA Grown in the Presence of N^6-Benzylaminopurine.....149

IV.37. X-Ray Precession Photograph (μ=10°) of the h0l Reciprocal Lattice Section of PNA-BAP Complex.....154

IV.38. X-Ray Precession Photograph (μ=10°) of the hk0 Reciprocal Lattice Section of PNA-BAP Complex.....155

IV.39. Gel Filtration of PNA in the Presence of 17.8% Methanol and 200mM Lactose on Shephadex G100-50.....157

ABBREVIATIONS OF VARIABLE NAMES

Lectins

PNA, *Arachis hypogaea*, peanut agglutinin

Con A, *Canavalia ensiformis*, concanavalin A

SL, *Onobrychis viciifolia*, sainfoin lectin

SBL, *Glycine max*, soybean lectin

KBL, *Phaseolus vulgaris*, kidney bean lectin

HGL, *Dolichos biflorus*, horse gram lectin

LL, *Lens culinaris*, lentil lectin

FBL, *Vicia faba*, fava bean lectin

PL, *Pisum sativum*, pea lectin

Reagents

ANS, 1,8-anilinonaphthalene sulfonate

TNS, 2,6-toluidinylnaphthalene sulfonate

DnsGalN, 2-amino-2-deoxy-N-(5-dimethylamino-1-naphthalene sulfonyl)-galactose, N-dansylgalactose amine

BAP, N^6-benzyladenine, N^6-benzylaminopurine

TRIS, TRISMA, tris(hydroxymethyl)aminomethane

NaCl-TRIS, 0.1M NaCL, 0.05M TRIS, 5mM $CaCl_2$, 5mM $MgCl_2$, 0.02% NaN_3, pH=7.20

Gal, galactose

GalNAc, 2-acetamido-2-deoxy-D-galactopyranose

SDS, sodium dodecyl sulphate

PAGE, polyacrylamide gel electrophoresis

DPCC, diphenyl carbamyl chloride

DPTU, diphenylthiourea

DPU, diphenylurea

PEG, polyethylene glycol

DMSO, dimethyl sulfoxide

pCMB, p-chloromercuribenzoic acid

PTH, phenylthiohydantoin

Instrumental

HPLC, high performance liquid chromatography

TCL, thin layer chromatography

AUFS, absorbance units full scale

TOA, take-off angle

Amino Acids

A, Ala, Alanine

R, Arg, Arginine

N, Asn, Asparagine

D, Asp, Aspartic acid

C, Cys, Cysteine

Q, Gln, Glutamine

E, Glu, Glutamic acid

G, Gly, Glycine

H, His, Histidine

I, Ile, Isoleucine

L, Leu, Leucine

K, Lys, Lysine

M, Met, Methionine

F, Phe, Phenylalanine

P, Pro, Proline

S, Ser, Serine

T, Thr, Threonine

W, Trp, Tryptophan

Y, Tyr, Tyrosine

V, Val, Valine

I. INTRODUCTION

I.A. LECTINS

Historical Background

That the seeds of some plants are toxic to both man and animal has been known for a long time. In the late 1880's, an investigation into the toxic constituents contained in the seeds of some plants belonging to the Euphorbiaceae family was begun by Stillmark (1). From the seeds of the castor bean, an aqueous extract called ricin was obtained and experiments were designed to test its effects on whole blood. Stillmark discovered that ricin caused red blood cells to aggregate, and that red blood cells from different animal species did not react to ricin in the same way. Afterwards, it was found that toxins isolated from the seeds of other plants showed agglutinating activities different from that of ricin, even towards erythrocytes of the same animal species.

Due to their ability to clot red blood cells, these toxins were first called hemagglutinins. And since they were first isolated from plants, they were more

specifically known as phytohemagglutinins. But eventually, it was discovered that these substances could agglutinate not only erythrocytes, but also lymphocytes, fibroblasts, spermatozoa, bacteria, and fungi. And furthermore, it became apparent that they were present not only in plants, but also in some vertebrates and invertebrates as well (2).

In 1936, Sumner and Howel (3) found that phyto-hemmagglutinins bind to carbohydrates. Watkins and Morgan (4) later confirmed that phytohemagglutinins have a binding specificity towards particular carbohydrates, and simple sugars inhibit their agglutinating activity. This suggested that the selective agglutination observed for phytohemagglutinins is due to their ability to react with specific carbohydrates present on the surface of cells. Inhibitory sugars blocked cell agglutination by occupying combining sites on the phytohemagglutinin, thus interfering with their attachment to the cell membrane.

In 1954, the term "lectin" (from the latin legere, to pick out or choose) was introduced (5) to describe the class of plant protein which can agglutinate cells and exhibit antibody-like sugar binding specificity. Lectins are presently defined as a carbohydrate-binding protein of non-immune origin that agglutinates cells or precipitates polysaccharides or glycoconjugates (6,7). The emphasis on lectins being from a non-immune origin is included so that these proteins can be distinguished from anti-carbohydrate

antibodies which may act as cell agglutinins. This definition has been adopted by the Nomenclature Committee of the International Union of Biochemistry (1981).

Occurrence and Distribution of Lectins

Lectins have been found to be widespread in the plant kingdom. The majority of lectins studied belong to the Leguminoseae family. In these plants, lectins are found to be particularly abundant in the seed, especially during the later stages of maturation. Within the cell, most of the lectin is found to be localized in the cytoplasm of the cotyledons, or associated with the protein bodies. Both of these tissues function as major protein storage organelles of the plant. Small amounts of lectin are also found in cells of the leaves, stem, and roots (8). Lectins isolated from these vegetative parts can have different carbohydrate specificity and molecular structure from those found in the seed of the same plant (9,10).

Two classifications of lectins have recently been discovered in vertebrate tissue: soluble lectins obtained from aqueous extracts and membrane lectins which require detergents for solubilization. One property that characterizes many of the soluble lectins is that the amounts found in tissues may change dramatically with embryonic development. The membrane lectins are believed to be an integral part of the cell membranes (although this

is not rigorously established). Most of the membrane lectins have been discovered in mammalian liver tissue (11).

Cellular slime molds are also found to synthesize lectins as they differentiate from a unicellular to a multicellular form. Each species synthesize more than one type of lectin. These lectins are primarily intracellular in their early developmental stages and are later found to be extracellular.

In addition to plant, vertebrate and slime mold lectins, a small number of bacterial lectins have been isolated and investigated. They can be described as surface lectins which occur in the form of filamentous proteins distributed on the bacterial cells. A few intracellular bacterial lectins are also known to exist (12).

Molecular Properties of Lectins

Besides being widely distributed in many different forms of living organisms, lectins are also found to be molecularly diverse. Many contain covalently bound sugars and can be classified as glycoproteins, while some are completely devoid of sugar residues. Values for the molecular weight can vary from 43,200 for dimeric wheat germ agglutinin (13), to 500,000 for the lectin isolated from the Indian horseshoe crab which is thought to be

composed of 18 to 20 subunits (14). Some lectins are rich in sulfur-containing amino acids and disulfide bonds, while others have none. The number of binding sites range from 2 as found in the sweet pea lectin (15), to 6 for the lectin found in the snail (16). Lectins can be composed of a single chain subunit, or discrete polypeptide chains which form an intact subunit. But despite these differences in molecular structure, lectins share in common the ability to specifically bind carbohydrates to more than one binding site.

The type of interaction involved between lectins and carbohydrates has generated some controversy. The polyhydroxylic nature of carbohydrates suggest that polar interactions such as hydrogen bonding and dipolar attractions are dominant in the binding of these ligands to lectins. Precipitation inhibition studies employing a variety of deoxy, O-alkyl, halogeno, thio, and acetamido derivatives (17,18) support this view. Inhibition studies obtained from chemical modifications of concanavalin A (19), and the three dimensional structures of the concanavalin A-methyl α-mannopyranoside (20) and favin-glucose complexes (21) are also in agreement with these results. In addition, the thermodynamic parameters that characterize the binding of wheat germ agglutinin to the α2-3 isomer of (N-acetylneuraminyl) lactose by ^{1}H NMR (22) indicate stabilization through hydrogen bonds and van der

Waals forces.

However, there is conflicting evidence that the lectin-carbohydrate interaction is hydrophobic rather than polar in nature. In this hypothesis (23), the involvement of oligosaccharide hydroxyl groups is not precluded, but does not dominate the driving force for the complex formation. It is suggested that lectins (and antibodies) recognize carbohydrates based on their topographical features rather than as the sugar units that comprise them. Since hydrophobic bonding is not atom-atom specific but related to the complementary shapes and hydrophobicities of ligands, the driving force of the lectin-carbohydrate binding interaction is thought to be hydrophobic in nature.

Most evidence suggest that lectins bind to carbohydrates via polar interactions. A site has been identified in Con A and soybean agglutinin which provides for a hydrophobic interaction with the binding sugar. With these lectins, phenyl and methyl derivatives are found to bind stronger than their parent sugars (24,25).

Biological Functions of Lectins

The widespread occurrence of lectins, especially in plants, suggest that they may be involved in some fundamental biological role. However, it has been 100 years since the first documentation of a hemagglutinin, and these functions still remain unclear and are much debated.

It is possible that a fundamental biological role of lectins may not exist since these proteins have not been found in all the organisms examined for them. But this view could be misleading because screening assays for lectins are dependant on their carbohydrate specificity which can elude detection.

Hemagglutinating activity has been detected in extracts from over 800 plant species. More than 100 different plant lectins have been characterized, most of them belonging to the Leguminosae family whose seeds are particularly rich in lectins. Numerous physiological roles have been attributed to plant lectins. However, definitive evidence to support any particular role has yet to be found.

The functional role of lectins has been investigated via two approaches. The first is by determination of their distribution, both cellulary and subcellulary, in various tissues during various stages in the life cycle of the plant. The second is by experiments designed to establish whether lectins participate in a hypothetical role. Some of the proposed functions for lectins in plants are (26):

Storage of proteins,

Packaging and/or mobilization of storage materials,

Transportation of carbohydrates,

Mechanisms of defense against disease,

Attractants for Rhozobial symbiosis,

Mitogenic stimulators of plant embryonic cells,

Recognition of cells,

Extension of cell walls,

Enzymes that are carbohydrate specific.

In animals, it is proposed that cell surface lectins may participate in receptor mediated pinocytosis of degraded glycoproteins, or play a role in intercellular interactions during tissue differentiation of developing vertebrates (27). Slime mold lectins appear to be involved in cell-cell adhesion (28). Bacterial lectins are thought to be involved in bacterial-eukaryotic cell recognition in the initiation of the infectious process (29).

In retrospect, all these proposed roles for lectins share a common chemical activity related to specific binding of cells (either of the same or different species), or the binding of glycoproteins for pinocytosis and the organization of extracellular materials.

Applications and Utilizations of Lectins

Because of their ability to specifically interact with the carbohydrates that extend from the cell membrane, lectins preferentially agglutinate specific cell types. A popular clinical application of lectins was found in distinguishing between erythrocytes of different blood types (30, Table I.1.). In addition to being specific for blood types A, B, O(H), M, and N, the specificity of some

Table I.1. **Blood Type-Specific Lectins (1)**

Specificity	Source of Lectin
Anti-A	Griffonia(Bandeirae) simplicifolia I (A_4) Helix pomatia Phaseolus lunatus Vicia cracca
Anti-A_1	Dolichos biflorus
Anti-B	Griffonia(Bandeirae) simplicifolia I (B_4)
Anti-O(H)	Anguilla anguilla Lotus tetragonolobus Ulex europeus
Anti-A + N	Molucella laevis
Anti-N	Vicia graminea
Anti-T	Arachis hypogaea
Anti-Tn	Salvia sclare

1. Ref. 30.

lectins can be used to distinguish among blood subgroups. For example, the lectin from Dolichos biflorus agglutinates A_1 type RBC more readily than type A_2 (31). Some lectins, such as those of Arachis hypogaea and Salvia scarea interact with cells carrying an antigen that are tumor-specific (T-antigen).

The interaction of lectins with membrane bound sugars has made them applicable in following changes that occur on the cell surface during physiological and pathological processes. This has been found to be useful in the area of cancer research. Wheat germ agglutinin (32), concanavalin A (33), soybean agglutinin (34), and other lectins are found to agglutinate malignant cells when present in concentrations that do not agglutinate normal cells. Subsequent studies revealed a difference in the surface distribution between lectins bound to normal and tumor cells. Whereas lectins are randomly distributed on the surface of normal cells, they aggregate in small areas on tumor cells. This suggests a rearrangement of saccharide receptors on the surface of malignant cells (35). Proposals have subsequently been made suggesting that one difference between malignant and normal cells lay in alterations of the cell surface detectable by lectins. Research into the possibility of using lectins as carriers for chemotherapeutic agents is currently underway.

Lectins are also widely used as a tool in chromosome

and immunological chemistry because they are found to stimulate the division of lymphocytes (36). Other current applications for lectins are in the area of affinity chromatography of glycoproteins and the fractionation of cells bearing different surface carbohydrates.

I.B. LEGUMINOUS LECTINS

The leguminosae are the second largest family of flowering plants containing about 550 genera with more than 12,000 species. With but few exceptions, all seeds examined from these plants contain lectins. In some seeds like the soybean and jackbean, as much as 2 to 10 percent of the total protein content is lectin. Such abundances have made legume lectins the most extensively studied and widely used proteins of their kind.

Although legume lectins are classified according to their unique carbohydrate binding specificity, they also share a number of other common molecular and biochemical properties.

Primary Structure Homology

All legume lectins are composed of monomers with a molecular weight of about 25,000 to 30,000 daltons. Some monomers are made up of a single polypeptide chain, while others have subunit structure (an α-chain of about 6000 daltons and a β-chain of about 18,000 daltons) which

together form a pseudo $\alpha\beta$-monomer (Table I.2.). Amino acid analysis of legume lectins show a high content of aspartic acid, serine and threonine, and a very low abundance of sulfur containing residues. Terminal amino acid sequences of 26 lectins isolated from two of the three groups comprising the Leguminosae have been compared (37). A striking feature of this data is that the subunits which make up the legume lectins are extensively conserved in their primary structure. And as expected from their evolutionary origins, the proteins from the same group (or tribe) are more homologous to each other than to those outside their group (or tribe). Presently, eight complete sequences are available for legume lectins spanning 4 tribes of the Papilionaceae group of the Leguminosae (Figure I.1.). Alignment of these sequences shows a circularly permuted relationship (48,49) among their primary structures (Figure I.2.). As shown in figure 2, the α-chains of favin, pea, and lentil lectins are homologous to a 50 residue segment of Con A spanning residues 70-121. The β-chains are homologous to a region that begins at residue 122 of Con A and continues without interruption through its carboxy and amino terminals to residue 45 for lentil and 69 for favin. The actual length of the pea β-subunit is uncertain since the pea sequence was deduced by gene cloning. The sequences of sainfoin, soybean, and the lectin isolated from Dolichos biflorus

Table I.2. Characteristics of Legume Lectins

Lectin	Native Molecular Weight	Subunit Molecular Weight	Molecular Form	Metals
Canavalia ensiformis (jack bean)	100,000 (50)	25,500 (51)	α_4	Ca,Mn,Mg,Zn (52)
Arachis hypogaea (peanut)	110,000 (53)	27,500 (53)	α_4	Ca,Mg,Mn,Zn (52)
Onobrychis viciifolia (sainfoin)	53,000 (54)	26,509 (55)	α_2	Ca,Mn,Mg (54)
Glycine max (soybean)	122,000 (56)	30,000 (56)	α_4	Ca,Mn (57)
Phaseolus vulgarus (kidney bean)	115,000 (58)	31,000 (59)	α_4	Mn,Ca,Mg,Zn (52)
Dolichos biflorus (horse gram)	110,000 (60)	27,398 (44)	α_4	Ca,Mg,Mn,Zn (61)
Pisum sativum (pea)	49,000 (62)	5753 17,000 (63)	$(\alpha\beta)_2$	Ca,Mn,Mg,Zn (52)
Lens culinaris (lentil)	46,000 (45)	5710 17,572 (45)	$(\alpha\beta)_2$	Mn,Ca,Mg,Zn (52)
Vicia faba (fava)	51,000 (64)	5571 20,700 (64)	$(\alpha\beta)_2$	Ca,Mg,Zn,Mn (52)

Table I.2. cont.

Lectin	Carbohydrate Specificity	Binding Sites Per Protein	Isolectins	Glycoprotein
Canavalia ensiformis (jack bean)	Mannose, Glucose (65)	4 (66)	-	0 (67)
Arachis hypogaea (peanut)	GalNAc, Galactose (65)	4 (68)	7 (69)	0 (53)
Onobrychis viciifolia (sainfoin)	Mannose, Glucose (65)	-	2 (56)	4.2% (70)
Glycine max (soybean)	GalNAc, Galactose (65)	4 (71)	4 (72)	7.0% (73)
Phaseolus vulgaris (kidney bean)	GalNAc, Galactose (65)	-	5 (74)	+ (75)
Dolichos biflorus (horse gram)	GalNAc, Galactose (65)	2 (76)	2 (60)	1.2-2.5% (77)
Pisum sativum (pea)	Mannose, Glucose (65)	2 (62)	2 (62)	0 (47)
Lens culinaris (lentil)	Mannose, Glucose (65)	2 (78)	1-2 (79)	0 (79)
Vicia faba (fava)	Mannose, Glucose (65)	2 (80)	-	2.3-7.7% (64)

Figure I.1. Chemotaxonomy of Sequenced Legume Lectins (1)

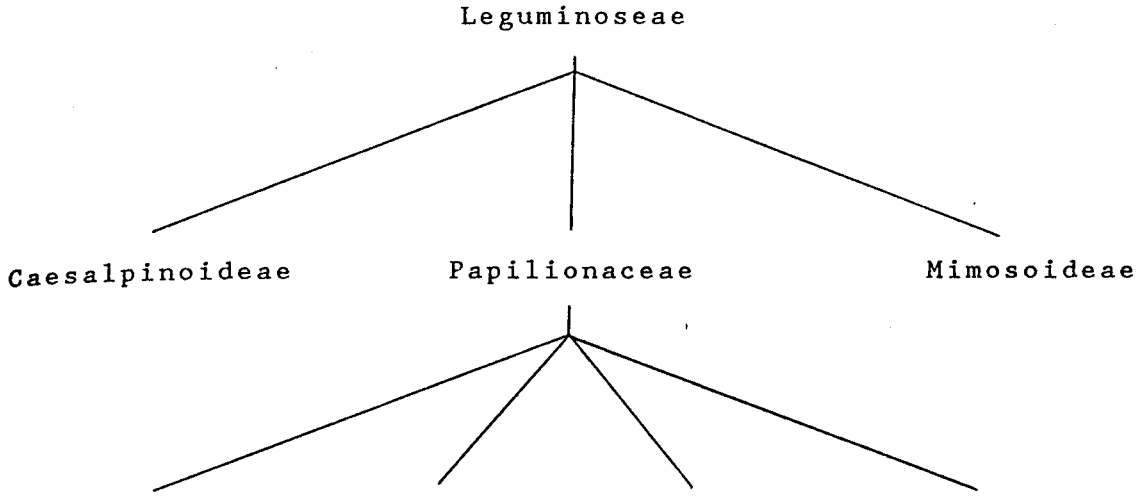

Diocleae	Hedysareae	Phaseoleae	Vicieae
Canavalia ensiformis (jack bean) (38) Con A	Onobrychis viciifolia (sainfoin) (39) SL	Glycine max (soybean) (42) SBL	Lens culinaris (lentil) (45) LL
	Arachis hypogaea (peanut) (40,41) PNA	Phaseolus vulgaris (kidney bean) (43) KBL	Vicia faba (fava bean) (46) FBL
		Dolichos biflorus (horse gram) (44) HGL	Pisum sativum (pea) (47) PL

1. Only partial sequence available for Arachis hypogaea.

Figure I.2. Circularly Permuted Sequence Homology of Legume Lectins (1)

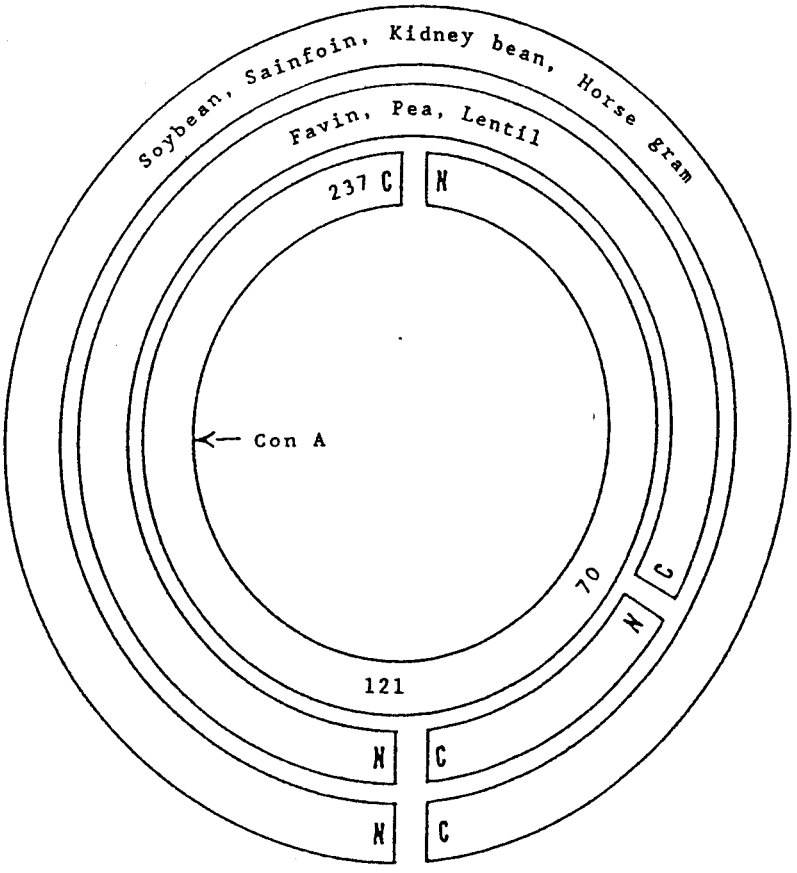

1. Refs. 48, 49.

seeds can be aligned to Con A in this permuted fashion also. Their primary structures are found to mimic that of Con A beginning at residue 122 and terminating where residue 238, 255, and 253 would be for sainfoin, soybean, and the Dolichos biflorus seed lectin, respectively. The complete primary structures for these 8 legume lectins are shown in Figure I.3. Of these lectins, the three dimensional structures have been determined for Con A (88), pea (89), and favin (90) lectins.

Species Heterogeneity

Extensive variations are found to exist in the electrophoretic mobility of many purified lectins suggesting species heterogeneity. The red kidney bean lectin is found to be comprised of five isolectins (69) made up of two distinct subunits R and L. These subunits only differ in their primary structure from residues 1 to 7. The tetrameric forms found to make up the red kidney bean lectin consist of L_4, L_3R, L_2R_2, LR_3, and R_4 combinations (74). Similarly, two affinity purified lectins were isolated from the seeds of Vicia cracca. One of these lectins is of the single subunit type, while the other is composed of a pseudo $\alpha\beta$-monomer. The primary structure of these isolectins are found to differ in the first 25 N-terminal amino acids (81). The isolectins found in both of these two species of legume seeds show

Figure I.3. Primary Structures of Legume Lectins

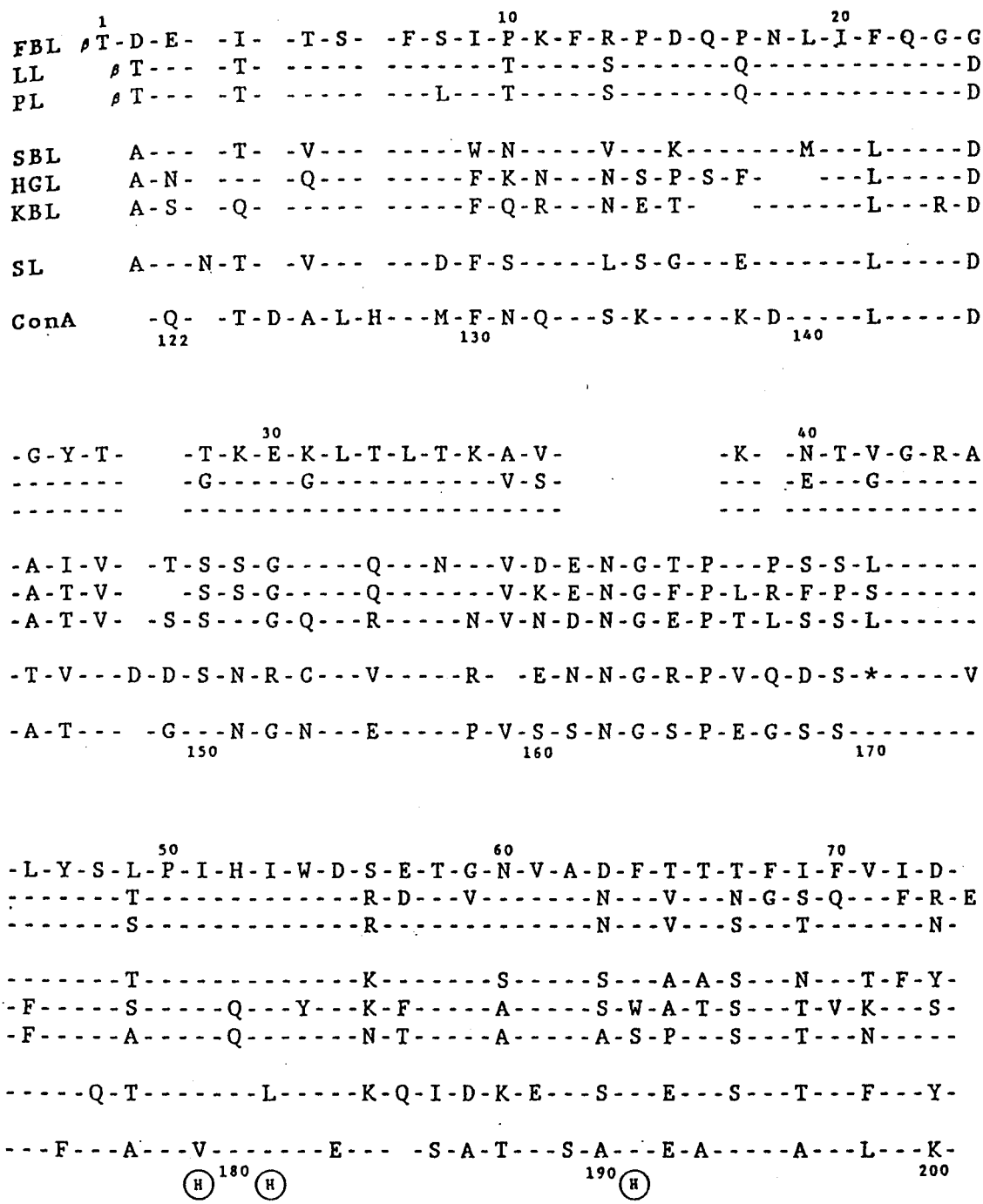

Figure I.3. cont.

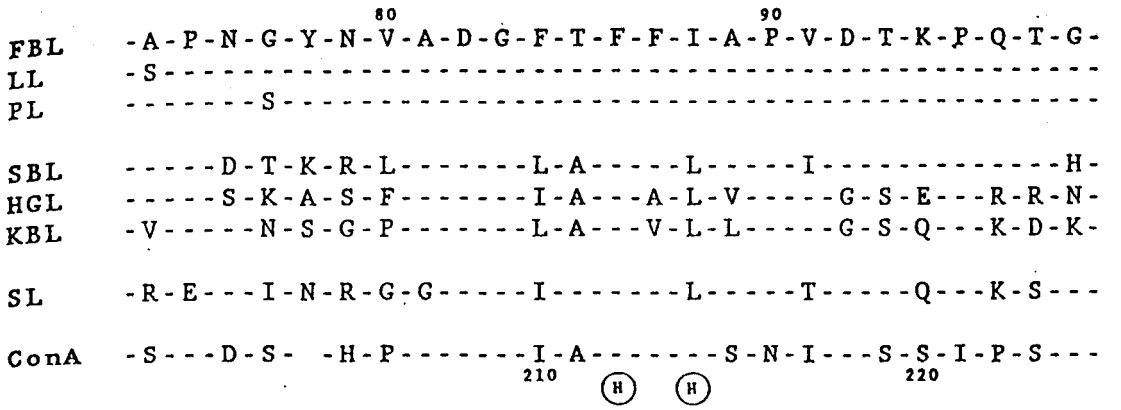

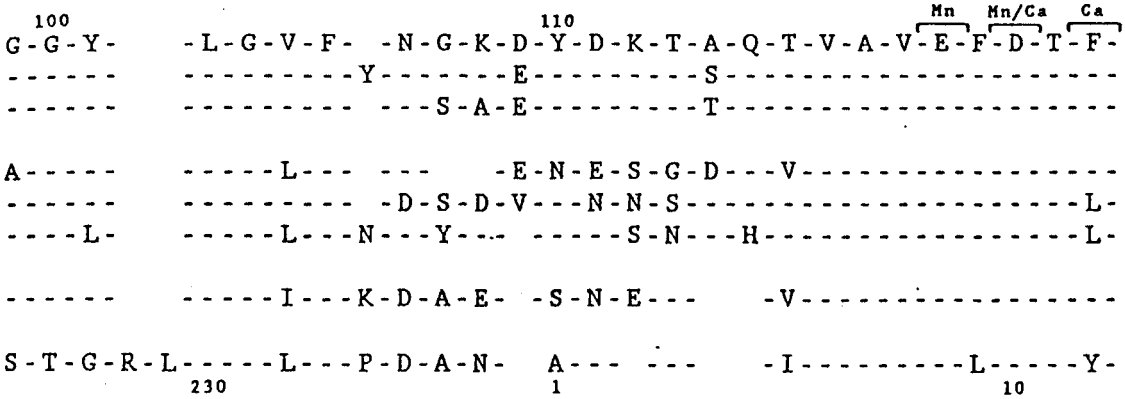

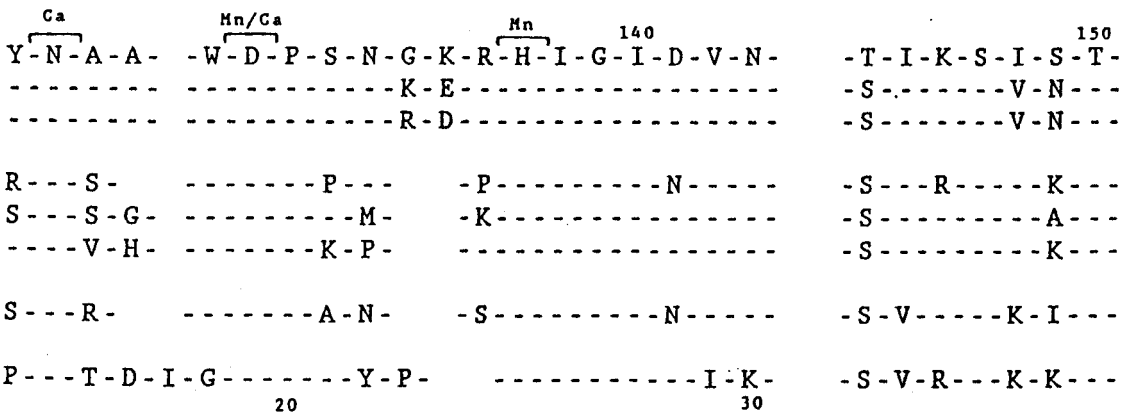

Figure I.3. cont.

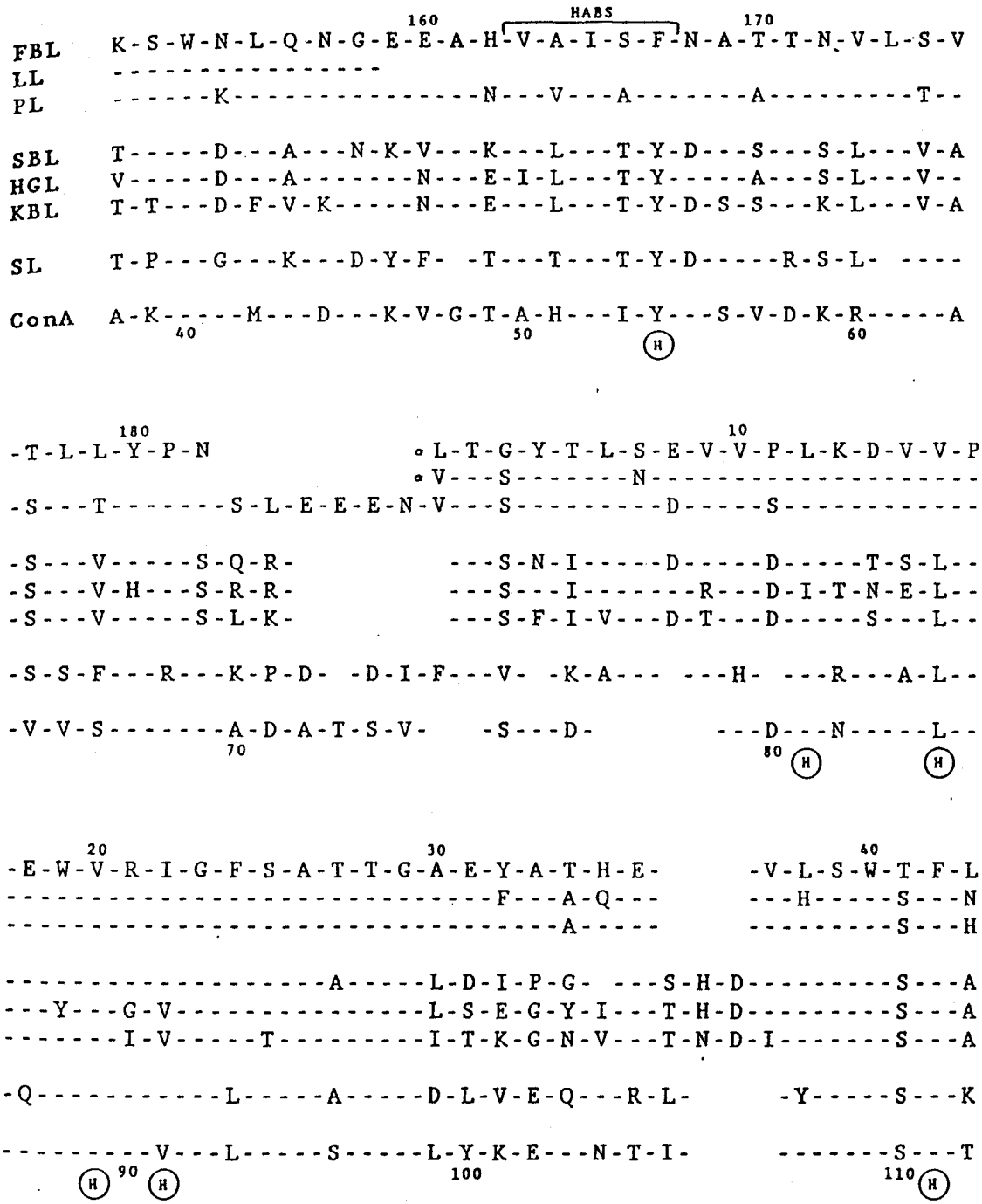

Figure I.3. cont.

```
                          50
FBL     -S-E-L-T-G-P-S-N
LL      ---Q---G-H-T---K-S
PL      -------S---T---S-S-K-Q-A-A-D-A

SBL     ---N---P-H-A---S-N-I-D-P-L-D-L-T-S-F-V-L-H-E-A-I
HGL     ---R---P-D-D---T- -A-E-P-L-D-L-A-R-Y-L-V-R-N-V-L
KBL     ---K---S-D-G-T-T-S-E-A-L-N-L-A-N-F-A-L-N-Q-I-L

SL      ---V---P-L-D---S-T

ConA    ---K---K-S-N---T-H-
        (H)             120
```

notes:

1. Ca and Mn represent the calcium and manganese binding sites identified on Con A, pea and favin lectins by x-ray crystallography.

2. H represents the residues found in the subunit hydrophobic binding site identified in Con A by x-ray crystallography.

3. HABS represents the residues found in the high affinity hydrophobic binding site identified in the red kidney bean lectin by photoaffinity labeling and sequence analysis.

differences in their carbohydrate binding specificities (81) and/or erythroagglutinating and lymphocyte-stimulating properties (82). Structural variations of this type have been ascribed to genetic polymorphism in the genome of the plant.

Other isolectins, such as those isolated from the green pea, have been found to differ only at their C-termini. The α-chains of the pea isolectin B are identical to that of the pea isolectin A except that it is two residues longer (83). Furthermore, the α-chains of both lectins are shorter than would be predicted from the nucleotide sequence of a cDNA clone for the pea lectin. Likewise, two isolectins isolated from the seeds of Dolichos biflorus also differ at their C-termini by 10 residues (84). Variations at the carboxy terminal of this type have been suggested to arise from specific post-translational proteolytic processing of a single polypeptide precursor molecule in the biosynthesis of these proteins. Post-synthetic modifications can also account for the presence of two chain monomeric subunits homologous to the single subunit lectins by a cleavage which yields the larger amino terminal β-chain and the smaller α-chain (45).

Molecular genetics can also be used to explain the circularly permuted homology that exists between the legume lectins and Con A. A primary structure rearrangement may

have resulted from the existence of a duplicate pair of genes coding for a single polypeptide chain of about 240 residues in the evolution of Con A. Three protein coding nucleotide sequences are distinguished in this model (Figure I.4.). The first, $\beta 2$, codes for the 69 amino terminal residues of Con A or the homologous segment spanning the carboxy terminal of the β-chains of the two chain lectins. The second, α, corresponds to residues 70 to 122 in Con A and the α-chains of the two chain lectins. And the third, $\beta 1$, codes for the carboxy terminal of Con A and the homologous region spanning the amino terminal of the β-chain of the two chain lectins (45). Non-coding nucleotide sequences (depicted as loops in Figure I.4.) may separate the coding regions to facilitate alternate rearrangements of lectin genes. Con A would have resulted from the use of genetic material of two adjacent genes. In conflict with this proposal is one which suggests that Con A is first synthesized as a glycoprotein precursor that is deglycosylated and cleaved into fragments that become reannealed with a post-translational peptide bond to become the mature protein (85).

Metal Binding Sites

The legume lectins are metalloproteins which mainly contain the divalent cations Ca^{2+}, Mn^{2+}, and Mg^{2+} with trace amounts of Zn^{2+} (Table I.2.). These metal ions are

Figure I.4. Model for the Gene Representation of Legume Lectins (1)

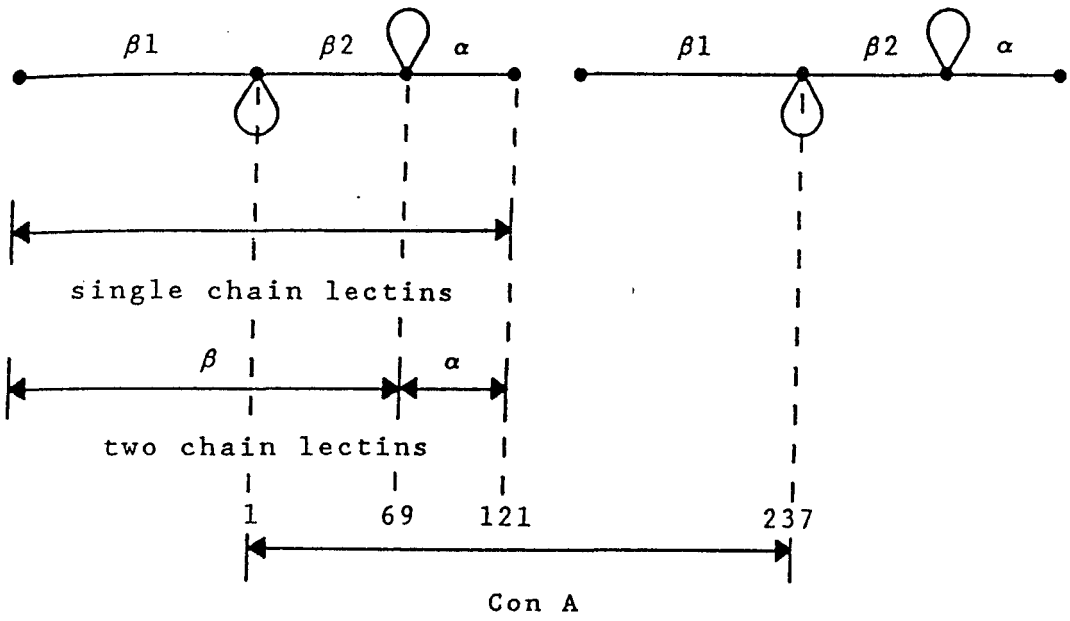

1. Ref. 45.

required for the sugar binding activity of lectins. Removal of the cations causes the loss of carbohydrate binding activity (52).

The binding of metal ions to legume lectins is strong. Consequently, metal free lectins are difficult to prepare. Methods of preparation usually involve extensive dialysis at a low pH and in the presence of chelators like ethylenediaminetetraacetic acid or ethylene-glycol bis-(β-aminoethyl ether)-N,N'-tetraacetic acid. In spite of this treatment, several lectins still retain a significant amount of calcium, and to a lesser extent, manganese. Retention of metal ions is thought to be a consequence of metal binding sites located in integral parts of the lectin (52).

Lectins have different specificities for metal ions as cofactors. Some lectins, such as those from the soybean, lentil, and pea require both Ca^{2+} and Mn^{2+} for their binding capability. However, the Dolichos biflorus seed lectin requires only one type of metal ion, Ca^{2+}, to exhibit its carbohydrate binding activity (61). No correlation has been detected between the type of metal ion present and the carbohydrate specificity of the lectin. Substitution of the metal ions commonly found in lentil (86), pea (86) and Dolichos biflorus lectin (61) with metals such as Co^{2+}, Ni^{2+}, Cd^{2+}, and Cu^{2+} results in derivatives identical in their intrinsic molecular

properties when compared to their native protein.

The regulatory role of metal ions in lectins has been most extensively studied in Con A. Each monomer of Con A possesses two metal ion binding sites. One is referred to as the transition metal binding site, S1, and the second as the calcium ion site, S2 (87). The transition metal must bind to its site first in order to induce a conformational transition in the protein for the calcium ion to bind. Both metal ion sites must be fully occupied in order for Con A to exhibit its carbohydrate binding activity.

The three dimensional structures of Con A, pea and favin have described the divalent metal ion binding sites. The amino acid residues participating in these two regions are found to be highly conserved in the crystal structures (Table I.3.) as well as the primary structures (Figure I.3.) of all the legume lectins for which sequence information is available. In Con A, pea and favin, the Mn^{2+}, is bound in a octahedral environment by the side chains of two aspartic acids, one glutamic acid, and one histidine residue. The coordination is completed by two water molecules. The Ca^{2+} is bound to the side chains of one asparagine, and two aspartic acids, one of which is also bound to the Mn^{2+} and serves to bridge the Ca^{2+} and Mn^{2+} together. The Ca^{2+} is further coordinated to the backbone carbonyl of Tyr-12 for Con A, Phe-123 for Pea, and

Table I.3. Metal Binding Regions of Legume Lectins

Con A (1)

Mn^{2+}	Ca^{2+}
Glu - 8	Asp - 10
Asp - 10	Tyr - 12
Asp - 19	Asn - 14
His - 24	Asp - 19

Pea (2)

Mn^{2+}	Ca^{2+}
Glu - 119	Asp - 121
Asp - 121	Phe - 123
Asp - 129	Asn - 125
His - 136	Asp - 129

Favin (3)

Mn^{2+}	Ca^{2+}
Glu - 120	Asp - 122
Asp - 122	Phe - 124
Asp - 130	Asn - 126
His - 137	Asp - 130

1. Ref. 88.
2. Ref. 89.
3. Ref. 90.

Phe-124 for favin. The coordination environment of Ca^{2+} is also made octahedral by bonds to two water molecules.

Hydrophobic Binding Sites

Besides having the ability to bind specific carbohydrates, legume lectins have recently been shown to bind a variety of hydrophobic ligands. Three classes of non-polar binding sites have presently been identified. The first is a non-polar site which is adjacent to the carbohydrate binding site. This was identified in many lectins (such as Con A) which bind stronger to carbohydrates containing phenyl substituents than to their parent sugars (91). A low resolution crystallographic study of the Con A-methyl α-mannopyranoside complex (20, 92) showed the presence of two tyrosyl residues in the vicinity of the carbohydrate binding region (Table I.4.). It is postulated that pi-pi interactions at the sugar binding site account for the increased affinities of carbohydrates with aryl substitutents (20).

The second class of non-polar binding sites has become known as the low affinity or subunit binding site. It has been identified in a large number of the legume lectins (92) suggesting that this site is conserved in the biosynthesis of these proteins. Fluorescent probes like 1,8-anilinonaphthalene sulfonate (ANS), and indoleacetic acid bind to this site in the ratio of 1 ligand per subunit

Table I.4. **Carbohydrate Binding Residues of Legume Lectins Determined by X-ray Diffraction**

Con A (1)	Favin (2)
Tyr - 12	Asn - 40
Asn - 14	Asp - 82
Asp - 16	Gly - 100
Leu - 99	Ala - 212
Tyr - 100	Thr - 213
Asp - 208	Asn - 126
Arg - 228	

1. Refs. 20, 92.
2. Ref. 90

in the respective case of lima bean lectin and Con A (94,95). The subunit binding site in Con A has been identified by x-ray crystallography as a deep pocket surrounded by many non-polar side chains (Table I.5.), with dimensions of about 9 x 6 x 15 Å (95). It is located approximately 35 Å away from the carbohydrate binding site (figure 5), (91). Of the twelve residues making up the Con A subunit hydrophobic binding pocket, 4 are completely conserved in other legume lectins that have been sequenced. Val-179 is replaced by Ile in all the other lectins, and the residues Leu-81, Ile-181 only differ in Dolichos biflorus seed lectin and sainfoin, being replaced by Ile and Leu respectively. Most of the other amino acids forming the hydrophobic cavity of Con A are replaced by chemically homologous residues also. For example Tyr-54, Leu-85, Val-92, and Ile-214 are replaced only by Phe, Val, Ile, and Leu respectively. Only Phe-191 differs in a chemically homologous replacement, being replaced by Ser in the red kidney bean lectin.

The third class of non-polar binding exhibited by many of the legume lectins (93) is one which interacts with the fluorescent probe 2,6-toluidinylnaphthalene sulfonate (TNS). This site has become known as the high affinity binding site since association constants for the interaction between TNS and a particular lectin are usually an order of magnitude larger than ANS and the same lectin.

Table I.5. Homology of Legume Lectins to the Subunit Hydrophobic Binding Region of Con A

			(site deviations)				
Con A	FBL	LL	PL	SBL	HGL	KBL	S L
Tyr - 54	Phe		Phe	-	-	-	-
Leu - 81	-	-	-	-	Ile	-	-
Leu - 85	Val	Val	Val	-	-	Val	-
Val - 89	-	-	-	-	-	-	-
Val - 91	Ile	Ile	Ile	Ile	-	-	Ile
Phe - 111	-	-	-	-	-	-	-
Ser - 113	-	-	-	-	-	-	-
Val - 179	Ile	Ile	Ile	Ile	Ile	Ile	Ile
Ile - 181	-	-	-	-	-	-	Leu
Phe - 191	-	-	-	-	Trp	Ser	-
Phe - 212	-	-	-	-	-	-	-
Ile - 214	-	-	-	Leu	Leu	Leu	Leu

Figure I.5. Schmatic Diagram Showing Relative Locations of the Various Binding Sites on a Single Protomer of Con A (1)

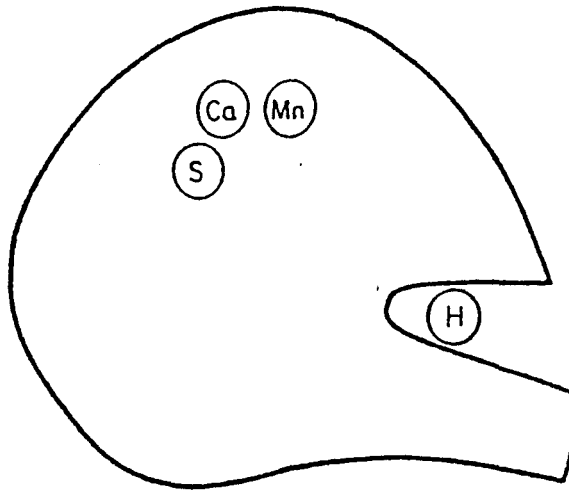

1. Ref. 95.

Studied most thoroughly in Con A (96) and the lima bean lectin (97), this site is also found to bind ligands like adenine and adenine derivatives (97) in the ratio of 1 ligand per tetramer. The photoactive compound 8-azidoadenine was used as an affinity probe to label the high affinity site of the lima bean and red kidney bean lectin (97). Identity was found between the amino acid sequence of a labeled peptide isolated from the lima bean and red kidney bean lectin (Figure I.3.). This region corresponds to residues 50 to 54 of Con A which is part of the antiparallel β-structure responsible for contacts between two Con A dimers to form a tetramer (88). It is possible for this region to provide a single site stoichiometry as found for the high affinity hydrophobic binding of TNS and adeninine to legume lectins.

Glycosylation Site

Except for Con A, pea, and lentil lectin, the sequenced legume lectins are found to be glycosylated. The identified sites of carbohydrate attachment (Table I.6.) conforms to the Asn-X-Ser/Thr sequence requirement found in both plant (98) and animal (99) glycoproteins. However, these sites are only found in homologous positions in the sainfoin and horse gram lectins. The lack of site conservation of covalently bound carbohydrates suggests that these sugars may not be involved in an important

Table I.6. Glycosylation Sites of Legume Lectins

Sainfoin (1)	Asn_{118}	- Glu - Thr
Kidney bean (2)	Asn_{12}	- Glu - Thr
	Asn_{60}	- Thr - Thr
	Asn_{80}	- Asn - Ser
Soybean (3)	Asn_{75}	- Phe - Thr
Horse gram (4)	Asn_{114}	- Asn - Ser
Favin (5)	Asn_{168}	- Ala - Thr

1. Ref. 39.
2. Ref. 44.
3. Ref. 100.
4. Ref. 44.
5. Ref. 46.

biological role. But a variation in the degree of glycosylation of the two isolectins of the red kidney bean lectin may account for their difference in vitro biological activities (44).

Three-dimensional Structures

The three dimensional structures for Con A (88), pea (89), and favin (90), are known from crystallographic studies. They are very similar in all respects other than their metal binding sites as previously described. The secondary structure of all three lectins are dominated by two large antiparallel β-structures. The first is comprised of six strands forming the rear of each protomer. A portion of one strand is bent sharply forward such as to form the left side surface. This same sheet is also hydrogen bonded to its symmetry related surface of an adjacent protomer to form a dimer. As a whole, the back surface of each dimer is therefore in the form of a 12 stranded sheet. The second β-structure is comprised of seven strands which forms a β-barrel that twists through the center of the front side of the protomer.

All three lectins are also found to contain a rare cis peptide bond. Aside from carboxypeptidase A, these are the only cis peptides reported that do not involve the peptide bond of proline (101). The cis peptide is found in a highly conserved region of the primary structures; Ala_{81}-

Asp_{82} of favin, Ala_{80}-Asp_{81} of pea, and Ala_{207}-Asp_{207} of Con A. Crystallographic data shows that one of the water molecules bound to the calcium in these structures is hydrogen bonded to the carbonyl oxygen of the aspartic acid residue in this cis peptide. It is thought that the hydrogen bonding stabilizes the thermodynamically unfavorable cis linkage. Removal of the metals can disrupt the cis peptide bond which can change the conformation of the protein in the carbohydrate binding region. This would explain the inactivity of lectins following the removal of divalent metal ions.

Con A differs from pea and favin lectins in that it is a tetramer while the latter are dimers. In the Con A dimer, 54 residues were identified in the non-covalent interaction between dimers. Of these, only 14 are conserved in favin and 12 in the pea lectin. All of these residues project from the back β-structure of the Con A dimer. Lack of these same residues in favin and pea may remove a source of stabilization needed to form a tetramer. Other differences between Con A and pea or favin are found at the amino and carboxy terminals, as would be expected from their circularly permuted sequence homology.

On the basis of the observed sequence homology, Con A was described (102) in terms of three functional or structural domains that can result from an evolutionary model requiring three exons. Modifications to the three

dimensional structure of Con A can produce models of the other legume lectins that are consistent with sequence data. This suggests that homologous primary structures produce three dimensional structures that are conserved.

I.C. PEANUT AGGLUTININ

Species Heterogeneity

Seeds of the peanut (Arachis hypogaea) contain an agglutinin known as peanut agglutinin or PNA. This lectin agglutinates neuraminidase treated ABO human blood types. It also exhibits the same immunological reaction as the anti-T antibody found in mammalian sera (103). Therefore, PNA is also known as the anti-T agglutinin.

Peanut agglutinin, or a immunological indistinguishable material, is present in the seeds of 4556 genotypes of the peanut (104). A study of the seeds of 116 lines of Arachis hypogaea was undertaken to resolve isolectin heterogeneity. Isoelectric focusing in the pH range of 5 to 7 showed four profile types. One hundred and one were of the V type containing 8 isolectins. Nine were of the S type containing 6 isolectins (lacking 2 bands present in the V type). And five were of the V_2 type which also contained 8 isolectins (lacking one, and containing one additional band to the V type profile). The remaining line exhibited a complex and unique isolectin profile not related to the others (104).

Carbohydrate Specificity

Hemagglutination experiments (53,105) conclude that of the simple saccharides, Galβ(1-3)GalNAc is the most potent inhibitor of PNA activity. Among galactosides differing in their anomeric C1 configuration, there is a slight preference for the α anomers except for melibiose (Table I.7.). Aromatic aglycons of galactose did not inhibit hemagglutination activity of PNA over methyl galactosides. The lack of enhanced hemagglutination by aromatic aglycons excludes a hydrophobic binding region adjacent to the carbohydrate site as proposed for Con A and soybean agglutinin (24,25). Both galactose and galactosamine are inhibitors of the hemagglutinating activity of PNA, however, N-acetylgalactosamine and 2-deoxy-galactose are not. Therefore, a free hydroxyl or amino group must be present at C2. The configuration at C4 also plays a role in the activity of PNA because neither glucose or methyl-α-glucoside are inhibitors. Galactose 6-sulfate, galacturonic acid, fucose, and L-arabinose are not inhibitors of PNA. This indicates a essential role of a C6 hydroxymethyl group since all these sugars are isomeric with D-galactose at positions C2, C3, and C4, but lack a free hydroxyl at C6 (53). The enhanced inhibition of PNA

Table I.7. **Inhibition of Hemagglutinating Activity of Peanut Agglutinin (1)**

Sugar	Concentration needed for 50% inhibition(2)	Relative inhibitory activity(3)
A. Monosaccharides		
Galactose	100	1
Methyl-α-galactopyranoside	40	2.5
Methyl-β-galactopyranoside	80	1.25
p-Nitrophenyl-α-galactopyranoside	60	1.66
p-Nitrophenyl-β-galactopyranoside	80	1.25
Galactosamine	70	1.43
B. Di- and Tetrasaccharides		
Melibiose	125	0.8
Lactose	60	1.66
N-Acetyllactosamine	60	1.66
Lacto-N-tetrose	60	1.66
Lacto-N-neotetrose	60	1.66
Galβ(1-3)GalNAc	2	50
C. Glycoproteins (desialylated)		
α_1-Acid glycoprotein	0.4	250
Fetuin	0.1	1000
Glycophorin	0.01	10,000
T-Antigen	0.008	12,500

(1) Ref. 53.

(2) The concentration (mM) of inhibitors before the addition of 1 ml of neuraminidase treated human type B erythrocyte suspension.

(3) The hemagglutination inhibitory activity of galactose was taken as 1.

by methyl-α-galactopyranoside (which is fixed in the six member ring) over galactose (which exists as an equilibrium mixture of open chain and ring forms) suggests that sugars in the pyranose form bind better. And the increased affinity of PNA for Gal-GalNAc relative to galactose may indicate the presence of an extended combining site (53). Extended sugar binding sites have been proposed for Con A (106).

The binding of mono- and disaccharides by PNA has been studied by ultraviolet difference spectroscopy. Titrations of the lectin with methyl-α- and methyl-β-galactopyranoside and lactose were found to perturb the UV spectrum with positive maxima at 286 or 285nm and at 278nm (107). This can be attributed to perturbation of tyrosine residues on the protein upon binding. The enthalapy change upon binding of disaccharides to the lectin is much larger than found for the binding of monosaccharides. This also suggests the existence of an extended carbohydrate binding site (108).

Macromolecular Properties

Values for the native molecular weight of PNA vary from 98,000 to 110,000 daltons at neutral pH, and 24,500 to 27,500 daltons in the presence of denaturants (109,53). Peanut agglutinin is tetrameric in neutral solution and dissociates reversibly into dimers below pH 5.1. Below pH

3.4, the lectin is totally dimeric (110). Amino terminal sequence analysis showed identity between the 4 subunits (53). No traces of amino or neutral sugar is observed by amino acid analysis or the colorimetric phenolsulfuric method of analysis (53,105). Amino acid analysis (Table I.8.) showed a high content of acidic and hydroxyamino acids, a low content of methionine, tryptophan, and histidine, and the absence of cysteine and cystine (53,69).

Primary Structure

Two partial sequences are available for peanut agglutinin. The first identified 161 residues of PNA that were homologous to portions of favin and soybean lectin (40). Additional data could not be obtained because of peptide insolubility, and resistance of the lectin to hydrolysis. Also, a number of tryptic peptides showed alternate sequences suggesting the interference of isolectins. The second sequence identified 198 residues of PNA that were homologous to portions of Con A and pea lectin (41). Three fragments of the protein were obtained by a CNBr cleavage. Using tryptic and chymotryptic digestions, the two smaller fragments have been fully sequenced. The third was only partially sequenced.

Crystallographic Studies of PNA

Crystals of PNA have been grown at neutral pH in the

Table I.8. Amino Acid Composition Reported for Peanut Agglutinin (3)

Amino Acid	Lotan, et al. (1)	Miller (2)
Aspartic acid	32	32
Threonine	25	20
Serine	28	25
Glutamic acid	13	12
Proline	9	8
Glycine	21	20
Alanine	14	14
Valine	22	25
Methionine	3	2
Isoleucine	12	15
Leucine	12	12
Tyrosine	5	7
Phenylalanine	12	14
Histidine	3	3
Lysine	9	10
Tryptophan	2	3
Arginine	6	7
Cysteine	0	0

1. Ref. 53.
2. Ref. 69.
3. Values shown are moles per 24,500g protein (nearest integers)

presence (111, 112) and absence (111) of a carbohydrate. Two independent studies reported the crystallization of PNA in the orthorhombic space group $P2_12_12$ with cell dimensions of **a**=130, **b**=127, and **c**=78 Å. The crystals grown in the presence of lactose diffracted beyond 3.0 Å resolution and contain a tetramer in the asymmetric unit. The crystals grown in the absence of lactose were twinned and its space group has not been determined. Three new crystal forms of PNA were grown at pH 4.6 (113). Two of these were in the monoclinic space group $P2_1$ with cell dimensions of **a**=70.3 and 70.5, **b**=101.1 and 107.3, **c**=84.5 and 85.0 Å, and β=114.0°. The third is in the triclinic space group P1 with cell constants of **a**=52.0, **b**=71.1, **c**=83.6 Å, and α=65.4, β=77.1, and γ=71.5°. The crystals grown at low pH are also suitable for high resolution work.

Diffraction data from the native (orthorhombic form) crystals of PNA have been collected using oscillation photography (114). A rotation function showed the four subunits in the asymmetric unit of the crystal are related to one another by three mutually perpendicular non-crystallographic 2-fold axes. The two monomers in a dimer are related by a 2-fold axis. The two dimers are in turn related by another 2-fold axis perpendicular to the one that relates the two monomers in the dimer. Thus the PNA tetramer is a dimer of dimers.

Biological Functions

Peanut agglutinin is found to interact with Rhizobium B.TG-3 and Rhizobium 5A which nodulate peanut, but did not bind to Rhizobium japonicum or Rhizobium meliloti, which do not nodulate peanut (115). The rhizobia has dual binding sites for PNA in the form of exopolysaccharides and lipopolysaccharides. Peanut agglutinin may therefore play a role in the legume-rhizobium recognition process in the initiation of nitrogen fixation.

II. STATEMENT OF RESEARCH

The research proposed in this project examines aspects of both the molecular structure and chemical activity of the plant lectin peanut agglutinin (PNA). At the molecular level, both the primary and three dimensional structure of PNA were studied by means of conventional protein sequencing and X-ray crystallography. Chemically, the ability of PNA to bind various types of hydrophobic and hydrophilic molecules was studied by means of fluorescence spectroscopy.

Three Dimensional Structure

Although the X-ray structures of the legume lectins concanavalin A (88), pea (89), and favin (90), have been completed, the structure of PNA would provide for the following structural details lacking in legume lectins.

1. A low resolution structure of Con A crystallized in the presence of a carbohydrate is available which does not provide details of sugar binding. Also, the crystal structure of favin in the presence of bound glucose is poorly refined with the sugar not unambiguously orientated. Crystals of PNA grown in the presence of lactose diffract to high resolution (111). Thus the high

resolution structure of the PNA/lactose complex would afford details to the nature of the lectin-carbohydrate interaction. The high resolution structure of PNA would show the size, shape, and participating amino acid and/or metal ions involved in carbohydrate binding.

2. While Con A, favin, and pea lectins are glucose/mannose binding lectins, PNA belongs to the class of N-acetylgalactosamine/galactose binding lectins. When compared to these lectins, the structure of PNA would help to explain the sugar binding specificity exhibited by this class of proteins.

3. Crystals of PNA have also been grown in the absence of carbohydrate (111). A comparison of the structures of PNA in the presence and absence of a bound carbohydrate would describe the conformational changes that occur to facilitate sugar binding.

4. In this study, Peanut agglutinin has been crystallized in the presence of the cytokinin N^6-benzyladenine (BAP). These cystals provide the first opportunity to identify one of the hydrophobic binding sites known to exist in legume lectins by crystallographic means. The structure of the PNA/BAP complex would demonstrate plant hormone action at the molecular level and could be used to suggest physiological roles to the binding of phytohormones to lectins.

Primary Structure

Only a partial primary structure of PNA is currently available (40, 41). The amino acid sequence, needed to compliment this study, will determine the complete three dimensional structure of PNA by X-ray crystallography. When compared to other sequenced lectins, the PNA sequence can also be used to describe common evolutionary origins and probable gene divergence that occurred in the development of legume lectins.

Chemical Activity

Although lectins have been known to exist for over 100 years, their biological functions remain unknown. Lectins are most widely known for their ability to specifically bind carbohydrates, and most of the proposed physiological functions are related to their sugar binding activity. Recently, several legume lectins have been shown to bind a variety of hydrophobic ligands, including adenine and adenine derivatives (93, 97). This class of compounds, the cytokinins, are known to be present in plants and serve as phytohormones. This study of the binding activity of PNA will provide evidence to distinguish among several proposed chemical features and physiological roles of legume lectins in plants.

III. MATERIALS AND METHODS

III.A. MATERIALS

Sigma Chemical Company, St. Louis, MO. USA

TRIZMA base
Sodium azide
Sepharose 6B
Sodium borohydride
α-Lactose
N,N'-Methylene bisacrylamide
Acrylamide
Ammonium persulfate
N,N,N',N'-Tetramethylethylenediamine
Glycine
Bromophenol blue
Dalton Mark VI SDS molecular weight standards
Coomassie blue
DPCC Trypsin
Trifluoroacetic acid (sequential grade)
Methanol (sequential grade)
2-Amino-2-deoxy-D-galactopyranose
5-Dimethylamino-1-naphthalenesulfonyl chloride
2,6-Toluidinylnaphthalene sulfonate
1,8-Anilinonaphthalene sulfonate
N^6-Benzyladenine
Gel filtration molecular weight markers (kit MW-GF-200)

Pierce, Rockford, IL. USA

Ammonium sulphate
Sodium dodecyl sulphate
Cyanogen bromide
0.2 Micron filters (Nylon-66)
Reacti-Vials (1 ml, amber, with Mininert valves)
Triethylamine (sequential grade)
Pyridine (sequential grade)
Phenylisothiocyanate (sequential grade)
Ethyl acetate (sequential grade)
Benzene (sequential grade)

PTH Amino acid standard kit

Mallinckrodt, Inc., Paris, KY. USA

Sodium chloride
Calcium chloride
Magnesium chloride

Aldrich Chemical Company, Milwaukee, WI. USA

1,4-Butanedioldiglycidylether
β-Mercaptoethanol
N-Bromosuccinimide
Ammonium acetate (gold label)
Tetrahydrofuran (HPLC grade)
Deuterium oxide

J.T. Baker Chemical Company, Phillipsburg, NJ. USA

Urea
Sodium phosphate, dibasic
Sodium phosphate, monobasic

Fisher Scientific Company, Pittsburgh, PA. USA

Hydrochloric acid
Glacial acetic acid
30% Hydrogen peroxide
Ammonium bicarbonate
Heptane (HPLC grade)
Sodium acetate
Polyethylene glycol (PEG 6000)

Allied Chemical, Morristown, NJ. USA

88% Formic acid

Beckman Instruments, Palo Alto, CA. USA

0.2N Sodium citrate buffer, pH=2.20
0.2N Sodium citrate buffer, pH=3.49
0.2N Sodium citrate/0.2N sodium chloride buffer, pH=4.12
0.2N Sodium citrate/0.8N sodium chloride buffer, pH=6.40
DMSO ninhydrin reagent
Beckman Systems 6300 Amino Acid Standards

Pharmacia Fine Chemicals Inc., Piscataway, NJ. USA

Sephadex G-25-300
Sephadex G-100-40

Curtin Matheson Scientific Inc., Houston, TX. USA

Acetonitrile

Applied Biosystems Inc., Foster City, CA. USA

PTH Amino Acid Standard Kit

Gelman Sciences Inc., Ann Arbor, MI. USA

0.2 Micron filters

Stohler Isotope Chemicals, Waltham, MA. USA

Dimethylsulfoxide-d_6

Charles Supper Company, Natick, MA. USA

0.7 mm Quarzkappillaren

Mann Research Laboratories, Inc. New York, NY. USA

p-Chloromercuribenzoic acid

III.B. PREPARATION OF PEANUT AGGLUTININ

Saline Fractionation

The preparation of peanut agglutinin followed the procedure of Olsen and Miller (111). Raw peanuts (200 g), (purchased locally, variety unknown) were ground by mortar and pestle, then homogenized in (500 ml) cold saline solution (0.9% NaCl) with a Sunbeam blender at top speed (60 sec). The mixture was centrifuged (16,000 x g, 30 min) with a Sorvall RC5B refrigerated (4°C) centrifuge using a GSA rotor. Lipids were removed from the mixture by passing the supernatant through glass wool. The material left in the form of a pellet was removed from the centrifuge vessels and subjected to the same extraction described

above a second time. The combined extracts (ca. 1000 ml) were made 40% saturated in ammonium sulphate and allowed to stand (5.0 hrs) refrigerated (4°C). The resulting precipitate was pelleted by centrifuging (16,000 x g, 20 min) and discarded. The supernatant was made 60% saturated in ammonium sulphate and allowed to stand overnight refrigerated (4°C). The resulting precipitate was pelleted by centrifuging (16,000 x g, 20 min) and dialyzed against buffer containing 0.1 M NaCl, 0.05 M TRIS, 5 mM $CaCl_2$, 5 mM $MgCl_2$, and 0.02% NaN_3 at pH=7.20 (NaCl-TRIS buffer). The protein solution was stored in this buffer refrigerated (4°C).

Affinity Chromatography

1. Preparation of Lactosyl-Sepharose 6B

The preparation of epoxy-activated Sepharose 6B followed procedures of Sundberg and Porath (116). Sedimented Sepharose 6B gel (7 ml) was washed with distilled water on a glass filter and dried by suction. The gel was suspended in NaOH (1 M, 5 ml) containing $NaBH_4$ (2 mg/ml) and 1,4-butanediol-diglycidylether (5 ml). The reaction mixture was tumbled end-over-end (10 hrs) at ambient temperature. The activated gel was washed with distilled water (4°C) on a glass filter and stored refrigerated (4°C).

The synthesis of lactosyl-Sepharose followed the

procedure of Olsen and Miller (111). The swollen, epoxy-activated gel (9 ml) was suspended in NaOH (0.1 M, 20 ml) containing lactose (2.16 g/20 ml) and mixed by end-over-end tumbling (overnight). The lactosyl-Sepharose 6B was washed in a scintered glass funnel with NaCl (0.5 M, 100 ml) and then with NaCl-TRIS buffer (100 ml). The resin was stored in NaCl-TRIS buffer refrigerated (4°C).

2. Isolation of Peanut Agglutinin

The protein solution obtained from saline fractionation was loaded onto a column (30 x 1 cm) of lactosyl-Sepharose 6B (20 ml/hr). The column was washed with NaCl-TRIS buffer until a baseline absorbance (280 nm) was recorded on the system detector (ISCO UA-5 Absorbance/Fluorescence Monitor). The bound PNA was then eluted by washing the column with NaCl-TRIS buffer made 100 mM in lactose. The concentration of PNA was determined spectrophotometrically using an extinction coefficient of ϵ(280 nm, 1 mg/ml)= 0.96 (109). The PNA isolated from affinity chromatography was stored lyophilized or precipitated in 80% ammonium sulphate. Lactose bound to the protein was removed by extensive dialysis in NaCl-TRIS buffer.

Gel Electrophoresis

Protein homogeneity was assayed by native or sodium

dodecyl sulfate (SDS) polyacrylamide electrophoresis (Laemmli system) as outlined by Hames (117). Slab gels were used for both the dissociating and non-dissociating systems with dimensions of 22 x 16 x 0.2 cm as follows.

1. Dissociating (SDS) Gels

The resolving gel solution was prepared by mixing 12 ml of (1.875 M TRIS-HCl buffer, pH=8.8) and 24 ml of (15 g of acrylamide and 0.41 g of N,N'-methylene bisacrylamide dissolved in 50 ml of water) to 0.6 ml of (10% SDS and 22.96 ml of water). The resolving gel was degassed under vacuum and polymerized by adding 0.8 ml of 10% ammonium persulfate and 0.16 ml of N,N,N',N'-tetramethylethylene-diamine. The stacking gel solution was prepared by mixing 3.75 ml of (1.0 M TRIS-HCl buffer, pH=6.8) and 1.5 ml of (15 g of acrylamide and 0.41 g of N,N'-methylene bisacrylamide dissolved in 100 ml of water) to 0.15 ml of 10% SDS and 9.48 ml of water. The stacking gel was degassed by vacuum and polymerized by adding 0.1 ml of 10% ammonium persulphate and 0.02 ml of N,N,N'N'-tetramethylethylenediamine. The final acrylamide concentrations for the resolving and stacking gels were 12.0% and 3.0%, respectively. The electrode buffer was made 0.025 M TRIS-HCL, pH=8.8, 0.192 M glycine, and 1% SDS. The protein samples (50 μg) were digested for 3-12 minutes at 100° C in 50 μl of a solution made 0.23 M TRIS-HCl,

pH=6.8, 3.7% SDS, 18.3% glycerol, 8.3% β-mercaptoethanol, and 0.02% bromophenyl blue as the marker dye. Bovine albumin (66,000 daltons), egg albumin (45,000 daltons), pepsin (34,700 daltons), PMSF treated trypsinogen (24,000 daltons), β-lactoglobulin (18,400 daltons), and lysozyme (14,300 daltons) were used as molecular weight standard markers and were treated in the same digestion mixture as the was the PNA. The electrophoresis was carried out at a constant current of 25 mA and 100 VDC for about 6 hours or until the marker dye reached the bottom of the gel. Proteins were fixed and stained by soaking the gel in water:methanol:glacial acetic acid (5.3:4:0.7 by volume) and 0.1% by weight in Coomassie blue stain (8 hrs). The gel was destained in the same solution excluding the coomassie blue stain.

2. Dissociating (Urea) Gels

The resolving gel solution was prepared by mixing 20 ml of (30 g of acrylamide and 0.8 g of N,N'-methylene bisacrylamide dissolved in 100 ml of water) and 10 ml of (43.2 ml of glacial acetic acid and 4.0 ml of N,N,N',N'-tetramethylethylenediamine in 100 ml of water) to 50 ml of (10 M urea containing 0.2 g ammonium persulphate per 100 ml). The resolving gel was degassed by vacuum and polymerized by adding 0.150 ml of N,N,N',N'-tetramethylethylenediamine and 0.05 g of ammonium

persulphate. The stacking gel solution was prepared by mixing 2 ml of (30 g of acrylamide and 0.8 g of N,N'-methylene bisacrylamide dissolved in 100 ml of water) and 1 ml of (43.2 ml of glacial acetic acid and 4.0 ml of N,N,N',N'-tetramethylethylenediamine in 100 ml of water) to 17 ml of (10 M urea containing 0.2 g ammonium persulphate per 100 ml). The stacking gel was degassed by vacuum and polymerized by adding 0.150 ml of N,N,N',N'-tetramethylethylenediamine and 0.03 g ammonium persulphate. The final concentration of acrylamide in the resolving and stacking gels were 7.5% and 3%, respectively. The electrode buffer was made by mixing 0.9 M glacial acetic acid and 10 M urea (1:1.6 by volume). Protein samples (40 μg) were prepared by diluting with electrode buffer made 0.04% in methyl green as the marker dye. The electrophoresis and fixing/staining of the proteins in the gel were carried out as described in the dissociating (SDS) gel system.

3. Non-dissociating Gels

The resolving gel solution was prepared by mixing 3.75 ml of (36.3 g TRIS-HCl and 0.23 ml of N,N,N',N'-tetramethylethylenediamine in 100 ml water, pH=8.8) and 10 ml of (28.0 g acrylamide and 0.74 g N,N'-methylene bisacrylamide dissolved in 100 ml of water) to 14.75 ml of water. The resolving gel was degassed by vacuum and

polymerized by adding 0.15 ml of N,N,N',N'-tetramethylethylenediamine and 1.5 ml of 1.5% ammonium persulphate. The stacking gel solution was prepared by mixing 5 ml of (5.98 g TRIS-HCl and 0.46 ml N,N,N',N'-tetramethylethylenediamine in 100 ml water, pH=6.6) and 2.5 ml of (28.0 g acrylamide and 0.74 g of N,N'-methylene bis acrylamide dissolved in 100 ml water) to 10 ml of water. The stacking gel was degassed by vacuum and polymerized by adding 0.15 ml of N,N,N',N'-tetramethylethylenediamine and 1.5 ml of 1.5% ammonium persulphate. The final concentration of acrylamide in the resolving and stacking gels were 10% and 4%, respectively. The electrode buffer was made by adding 3.0 g TRIS-HCl and 14.4 g of glycine to 1000 ml of water, pH=8.2). Protein samples (40 μg) were prepared by diluting with electrode buffer made 0.002% in bromophenyl blue as the marker dye. The electrophoresis and fixing/staining of the proteins in the gel were carried out as described in the dissociating (SDS) gel system.

III.C. AMINO ACID COMPOSITION

Acid Hydrolysis

Acid hydrolysis of protein and/or peptides followed procedures of Darbre (118). Lyophilized samples (1 mg) of PNA were placed in 10 x 75 mm glass culture tubes that were cleaned by boiling (30 min) in distilled HCl (6 N). Each sample was frozen in distilled HCl (6 N, 1.5 ml) by placing

the culture tube into a CO_2-acetone bath followed by vacuum evacuation. The culture tubes were then sealed with a gas-oxygen flame into ampules while under vacuum, and heated in mineral oil (110°C) for 16, 24, and 72 hours. After hydrolysis, the ampules were broken open, vacuum dried, and stored refrigerated (4°C) in a sodium citrate buffer (0.2 N, pH=2.2).

Performic Acid Oxidation (Cystine Analysis)

Performic acid reagent was prepared as described by Darbre (119). To 90 ml of 88% formic acid was added 10 ml of 30% hydrogen peroxide. The mixture was allowed to stand at room temperature for one hour, then cooled in a ice bath. The cooled oxidant (2 ml) was added to lyophilized samples (1 mg) of PNA, and allowed to react (20 hrs) in an ice bath, after which 48% HBr was added (0.30 ml) to stop the reaction. The samples were dried by vacuum, and subjected to acid hydrolysis as described previously.

N-Bromosuccinimide Assay (Tryptophan Analysis)

Tryptophan content was analyzed by the spectrophotometric method described by Spande and Witkop (120). To a lyophilized sample (1 mg) of PNA was added 3.5 ml of urea (10 M, pH=3.84 with acetic acid) in a 1 x 1 x 4.5 cm quartz cuvette containing a teflon coated stir bar. The PNA-urea solution was titrated with 10 μl additions of N-

bromosuccinimide (0.178 g/100 ml 10 M urea, pH=4.05). The optical density was recorded at 280 nm with a Hewlett Packard 8451A Diode Array Spectrophotometer after stirring the solution (3 min) at room temperature upon each addition. Titration was continued until no further decrease in absorbance was observed. Spectra baseline were corrected using a 10 M urea blank solution at pH=3.84.

Amino Acid Analysis

Amino acid analyses were performed on a Beckman Model 121M Microcolumn Amino Acid Analyzer equipped with an automatic sample injector at Children's Memorial Hospital, Chicago, IL. Samples were diluted (1.0 ml) with sodium citrate buffer (0.2 N, pH=2.2). Sample storage coils were loaded with aliquots (50 μl) for use with a 20 μl sample metering loop. The column contained Beckman Type AA-15 resin, and its temperature was maintained at 55°C. All buffers and the DMSO ninhydrin reagents were obtained from Beckman Instruments, Inc., and stored refrigerated (4°C) and under nitrogen. Sample detection was monitored at both 440 and 570 nm (2.0 AUFS) with a Beckman Dual Drag-Pen Recorder and a Hewlett Packard 3390A Reporting Integrator. The amino acid analyzer was run automatically by the instrument control program shown in Figure III.1. Amino acid identification and quantification were in reference to a mixture of seventeen amino acid calibration standards

Figure III.1. Beckman 121M Amino Acid Analyzer Instrument Control Program

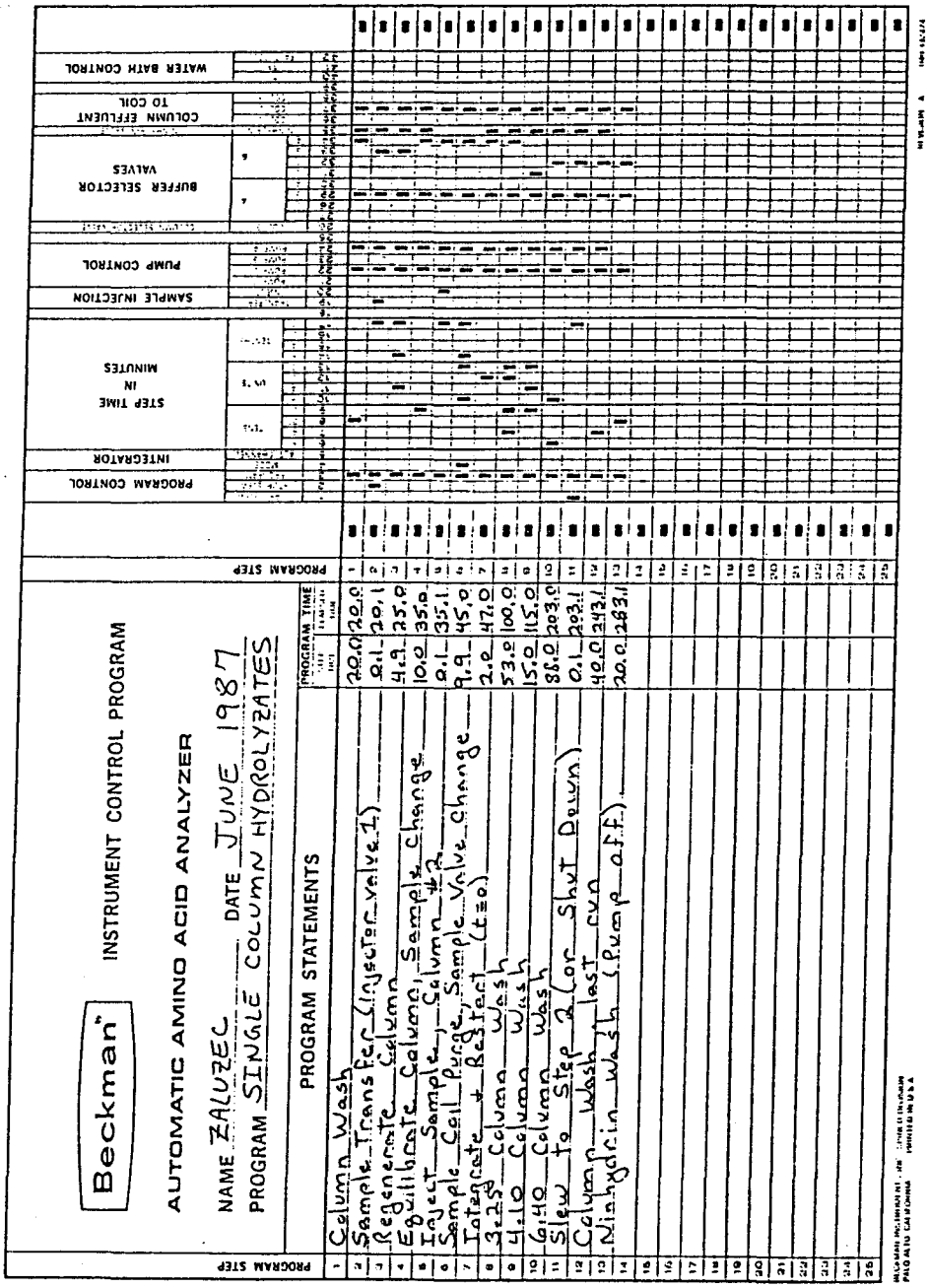

obtained from Beckman Instruments.

III.D. AMINO ACID SEQUENCING

Chemical Digestion

1. Cyanogen Bromide Cleavage

Digestion of PNA by the cyanogen bromide reaction followed procedures described by Fontana and Gross (121). To a solution of 70% formic acid (3.0 ml) were added 21 mg of lyophilized PNA and 47 mg of CNBr. The reaction mixture was allowed to digest at room temperature for 23 hours, following dilution with 3.0 ml of water and vacuum drying.

2. CNBr Peptide Isolation

The CNBr peptides were isolated using a column (110 x 1 cm) packed with Sephadex G-25-300 swollen in water and equilibrated with 88% formic acid. The digestion sample was dissolved in 3.0 ml of 88% formic acid, and eluted by gravity flow (3.3 ml/hr). Elution was detected by collecting fractions every 5.0 ml and measuring the absorbance at 230 nm. The fractions were pooled into four major zones and vacuum dried. Each of the four major zones was solubilized by 88% formic acid (1.0 ml) and passed down the gel filtration column a second time as described for the total digestion mixture. The samples were washed with water, vacuum dried, and stored refrigerated (4°C).

3. CNBr Peptide Composition

The total amino acid composition of the four major zones isolated by gel filtration were determined as described in III.C.

Enzymatic Digestion

1. Trypsin Cleavage

Digestion of PNA by trypsin followed procedures described by Wilkinson (122). To 160 mg of lyophilized PNA suspended in 32 ml of ammonium bicarbonate buffer (0.1 M, pH=7.85) maintained at 40.5°C was added 0.1 ml aliquots of DPCC treated trypsin (80.4 mg trypsin/5.0 ml 0.01 N HCl) three times and allowed to digest for 4, 5, and 6 hours, respectively. The digestion mixture was filtered through a 0.2 micron filter, and lyophilized. A control self-digestion experiment was simultaneously performed on a solution containing no PNA. The total enzyme-substrate ratio was 3.0%.

2. Tryptic Peptide Isolation

The peptides generated from the digestion of PNA with trypsin were fractionated using a Du Pont 8820 Series Gradient Liquid Chromatographic System, an Altex Ultrasphere-ODS C18 column (0.46 x 25 cm, 5 micron), and a Altex Ultrasphere-ODS C18 guard column (0.46 x 2 cm, 5

micron). Elution was at ambient temperature by a non-linear gradient (Du Pont -3 exponent program) of 25 mM ammonium acetate/water, pH=4.0 (solvent A), and 25 mM ammonium acetate/70% acetonitrile, pH=4.0 (solvent B). The solvent concentration profile was from 0 to 100% solvent B in 60 minutes at a flow rate of 1.5 ml/minute. Solvents were filtered through a 0.2 micron filter and degassed prior to use. Samples (1.8 mg lyophilized digestion material) were applied by a Rheodyne 7010 injector using a 54 μl sample loop. Sample elution was detected at 254 nm, and collected on a modified Packard 850 fraction collector. Thirty two fractions were isolated from the tryptic digestion.

3. Tryptic Peptide Composition

The total amino acid composition of peptides generated by digestion with trypsin used fractions isolated from 5 injections (ca. 9 mg lyophilized digestion material), and was determined as described in III.C.

Manual Sequence Analysis

1. Edman Degradation

Manual sequencing methods followed the procedures described by Tarr (123,124). The combined fractions from 17.3 mg of PNA lyophilized after digestion with trypsin were used for sequence analysis. Each peptide was placed in a 1 ml amber Reacti-Vial modified according to Tarr

(125) and flushed with nitrogen. While under nitrogen, the peptide was solubilized with 20 μl of 25% triethylamine:pyridine (1:1) in water, followed by the addition of 20 μl of a stock solution of phenylisothiocyanate:pyridine (1:3) kept under N_2 at 0°C. The mixture was vortexed for 60 seconds and the peptide was coupled to the phenylisothiocyanate by heating at 50°C for 20 minutes. After coupling, excess reagents were removed by extraction with 400 μl of heptane:ethyl acetate (10:1) x 1, then with 300 μl of heptane:ethyl acetate (2:1) x 2. The phenylthiocarbamyl derivative was then vacuum dried and cleaved with 20 μl of trifluoroacetic acid at 50°C for 5 minutes while under N_2. Excess trifluoroacetic acid was removed by vacuum drying. Separation of the resulting amino terminal anilinothiazolinone derivative and the remaining peptide was by solubilizing the dried material with 40 μl of 0.1 N HCl, and extracting with 100 μl of benzene:ethyl acetate (1:2) x 2. The aqueous phase of the extraction mixture was vacuum dried and subjected to subsequent Edman degradation cycles. The combined organic extracts were vacuum dried and converted to the corresponding phenylthiohydantoin by heating in 40 μl of 1 N HCL in methanol at 50°C for 10 minutes under N_2. Excess methanolic hydrochloride was removed by vacuum drying.

2. Phenylthiohydantoin Chromatography

Analysis of the phenylthiohydantoins isolated from the Edman degradation cycles was by high pressure liquid chromatography. The same chromatographic system described in III.D.2. was used for characterization with the following changes. Both the column and guard column were jacketed and maintained at 46°C. Elution was by a non-linear gradient (Du Pont -2 exponent program) of 5 mM sodium acetate/5% tetrahydrofuran, pH=5.16 (solvent A), and 60% solvent A/10% tetrahydrofuran in acetonitrile (solvent B). The solvent concentration profile was from 0 to 100% solvent B in 17.5 minutes (segment 1), and 100% solvent B for 10 minutes (segment 2) at a flow rate of 1.5 ml/minute. Samples were solubilized in solvent A and applied with a 10 μl sample loop. Detection was at 254 nm and identification and quantification were in reference to calibration standards obtained from Pierce and Applied Biosystems, Inc.

Automated Sequence Analysis

Automated peptide sequence analysis was performed on either an Applied Biosystems Model 470 Sequenator equipped with a Applied Biosystems Model 120 PTH Analyzer, or a Applied Biosystems Model 477 Sequenator at Abbott Laboratories, Abbott Park, IL.

III.E. BINDING ASSAYS

Carbohydrate Binding

1. Preparation of N-Dansyl Galactosamine

The preparation of 2-amino-2-deoxy-N-(5-dimethylamino-1-naphthalene sulfonyl)-galactose (N-dansyl galactosamine) followed the procedures described by Lartey (125) for the preparation of 2-amino-2-deoxy-N-(5-dimethylamino-1-naphthalene sulfonyl)-glucose. A suspension of sodium methoxide (0.25 g in 20 ml of methanol at 5°C) was added to a stirred solution of 2-amino-2-deoxy-D-galactopyranose (1.0 g in 10 ml of methanol). The suspension was stirred for 15 minutes, mixed with 1.22 g of 5-dimethylamino-1-naphthalenesulfonyl chloride solubilized in 10 ml of methanol, and allowed to react under N_2 for 15 hours at room temperature in the dark. A white precipitate was filtered from the suspension and discarded. The remaining yellow filtrate was dried by rotary-evaporation and after the resulting oil was washed with hexanes, a yellow/green precipitate formed. The yellow/green precipitate was dissolved in methanol and purified by column chromatography using either (1) silica gel column chromatography (45 x 1 cm column and a 10% methanol/methylene chloride mobile phase), or (2) reverse phase high pressure chromatography (Whatman Partisil 10/25

ODS-2 column and 70% methanol isocratic elution). The isolated product was detected by irradiating the column eluant with short wave ultra violet light. Purity of product was checked by TLC (silica gel using 10% methanol/methylene chloride for development). The product was characterized by proton NMR (Varian VXR300) in DMSO-d_6 after exchange with D_2O. The concentration of N-dansyl galactosamine was determined spectroscopically using a molar absorptivity of 4400 cm^{-1} at 330 nm (126).

2. Fluorometric Titrations

Fluorometric titrations of PNA with N-dansyl galactosamine were performed using a Perkin Elmer LS-5 Fluorescence Spectrophotometer. Samples were titrated at room temperature (21.5°C) in a 1.0 x 0.4 x 4.0 cm quartz cuvette and mixed with a cuvette plunger-mixer. Excitation was at 328 nm (5 nm slit) and emission was recorded at 540 nm (10 nm slit) after equilibrating for 60 seconds. The fluorimeter was equipped with a microprocessor which integrated the emission signal over a 16 second time interval. Excitation scans were made with a scan speed of 60 nm/minute and recorded between 475 to 600 nm. All solutions were filtered through a 0.2 micron filter before use.

Association constants for the binding of N-dansyl galactosamine to PNA were determined from the fluorescence

enhancement observed by titrating a fixed amount of the fluorescent probe (5.00 μM, 850 μl) with protein (185 μM, 20 μl additions x 10) using a 50 μl Hamilton syringe. Baseline correction was with NaCl-TRIS, and emission was corrected for dilution. The binding of lactose to PNA was studied by a competitive substitution titration. Association constants for the binding of lactose to a complex of PNA and N-dansyl galactosamine were determined from the fluorescence quenching observed by titrating a fixed amount of fluorescent probe (4.05 μM) and protein (35.2 μM) in 1050 μl with lactose (100 mM, 3.0 μl additions x 10) using a 10 μl Hamilton syringe. The concentration of lactose was determined by adding a weighed amount to a fixed volume of buffer.

Hydrophobic Binding

1. Fluorometric Titrations

Fluorometric titrations of PNA with the hydrophobic ligands 2,6-toluidinylnaphthalene sulfonate (TNS) and 1,8-anilinonaphthalene sulfonate (ANS) were performed as described for N-dansyl galactosamine with the following changes.

Association constants for the binding of TNS to PNA were determined from the fluorescence enhancement observed by titrating a fixed amount of the fluorescent probe (11.66 μM, 890 μl) with protein (183 μM, 40 μl additions x 7). The

binding of N^6-benzyladenine (BAP) to PNA was studied by a competitive substitution titration. Association constants for the binding of BAP to a complex of PNA and TNS were determined from the fluorescence quenching observed by titrating a fixed amount of fluorescent probe (8.87 μM) and protein (43.80 μM) in 1170 μl with BAP (8.00 mM in 50% methanol/TRIS buffer, pH=7.20, 30 μl additions x 7). Excitation was at 350 nm (5 nm slit) and emission was recorded at 425 nm (10 nm slit). The concentration of TNS and BAP were determined by adding a weighed amount to a fixed volume of buffer.

Association constants for the binding of ANS to PNA were determined from the fluorescence enhancement observed by titrating a fixed amount of the fluorescent probe (5.62 μM, 890 μl) with protein (185 μM, 40 μl additions x 7). Excitation was at 350 nm (5 nm slit) and emission was recorded at 470 nm (10 nm slit). The concentration of ANS was determined by adding a weighed amount to a fixed volume of buffer.

Determination of the stoichiometry of hydrophobic ligand binding was performed as described by Wang and Edelman (143). Fluorescence enhancement experiments were performed by titrating fixed amounts of protein (13.6, 27.3, 54.5, 81.8, and 109.1 μM PNA, 900 μl) with hydrophobic probe (272 μM TNS, 30 μl additions x 6). Excitations was at 350 nm (10 nm slit) and emission was

recorded at 450 nm (10 nm slit). The concentration of TNS was determined spectrophotometrically, using a extinction coefficient of 1.89×10^4 $M^{-1}cm^{-1}$ at 317 nm (96).

2. Gel Filtration

Gel filtration of PNA was performed using a column (53 x 1 cm) packed with Sephadex G100-40 swollen in water and equilibrated with NaCl-TRIS buffer made 200 mM in lactose. Cytochrome C (12,400 daltons), carbonic anhydrase (29,000), bovine serum albumin (66,000), and alcohol dehydrogenase (150,000) were used as molecular weight standard markers. Column void volume was determined from the elution volume of blue dextran. Elution of proteins was detected at 280 nm using a flow rate of 2.2 ml/hr.

III.F. CRYSTALLOGRAPHY

Crystallization of Peanut Agglutinin

1. Peanut Agglutinin/Lactose

Crystals of the PNA/lactose complex were obtained following a modification to the procedures described by Olsen and Miller (111). To a 5.0 ml glass vial, 50 μl of a 0.10 M sodium phosphate buffer (pH=7.0), 50 μl of a 50 mM lactose solution that is 0.2% in sodium azide, and 50 μl of a 50% polyethylene glycol (PEG 6000) precipitant in water were pipetted and mixed. Enough of a stock PNA solution

and water were then added to give a final protein concentration of 6.5 mg/ml in a total volume of 500 μl. The vials are stored at ambient temperature for 5-10 days. If crystal growth was not apparent at the end of this period, then 10 μl aliquots of a saturated ammonium sulfate solution were added every 2-4 days with gentle mixing until the crystals developed.

2. Peanut Agglutinin/N^6-Benzyladenine

To a 5.0 ml glass vial, 98 μl of a 12.43 mM N^6-benzyladenine stock solution (in methanol), 40 μl of a 50% polyethylene glycol (PEG 6000) precipitant in water were added and mixed. Enough of a stock PNA solution and NaCl-TRIS buffer were then added to give a final protein concentration of 6.4 mg/ml in a total volume of 550 μl, and the vials are stored at ambient temperature.

Heavy Metal Derivatization

1. Crystal Soaking Derivatization

To a 5.0 ml glass vial, 100 μl of a 0.05 M TRIS buffer (pH=6.8), 100 μl of a 50 mM lactose solution made 0.2% in sodium azide, 190 μl of a 50% polyethylene glycol (PEG 6000) precipitant in water, 100 μl of a solution containing a heavy metal salt, and 510 μl of water were pipetted and mixed. Heavy metal salts (final concentration, time of soak) used were K_2HgI_4 (1.0 mM, 3

days), K_2PtCl_4 (0.1 to 1.7 mM in the presence of 0.1 M NaCl, 6.0 hours and 3.0 days), K_2PtCl_6 (1.0 to 5.0 mM in the presence of 0.1 M NaCl, 12.0 hours and 3.0 days), $UO_2(NO_3)_2$ (1.0 to 2.0 mM, 15.0 hours and 3.0 days), $Sm(NO_3)_3$ (2.0 mM, 3.0 days), $Hg(CH_3CO_2)_2$ (1.0 mM, 3.0 days), and $UO_2(CH_3CO_2)_2$ (1.0 to 2.0 mM, 15.0 hours and 3.0 days). Crystals were soaked in these solutions at ambient temperature.

2. Co-Crystallization Derivatization

To a 5.0 ml glass vial, 50 µl of a 0.1 M sodium phosphate (pH=7.0), 50 µl of a 50 mM lactose solution made 0.2% in sodium azide, 47 µl of a 50% polyethylene glycol (PEG 6000) precipitant in water, and 50 µl of a 27 mM p-chloromercuribenzoic acid solution made 6.0 M in ammonium sulphate were pipetted and mixed. Enough of a PNA stock solution and water were then added to give a final protein concentration of 6.50 mg/ml in a total volume of 500 µl.

X-Ray Diffraction

1. Crystal Mounting

Crystals were mounted in 0.7 mm quartz capillary tubes. A 1.0 cc syringe, attached to the capillary by rubber tubing, was used to draw the crystal and mother liquor halfway into the capillary. The crystal was then pushed out of the capillary by a glass fiber. The

capillary was sealed at both ends with wax and mounted on a aluminum goniometer head pin with epoxy or clay.

2. Data Collection

Diffraction data of the PNA/lactose complex and the heavy atom derivatives were collected on a modified four-circle Picker diffractometer using Ni-filtered Cu Kα radiation, λ=1.5418 Å, operated at 34,000 VDC and 14 mA, and at a TOA of 2.0°. The diffractometer was equipped with a helium tube mounted between the receiving collimator and detector. The detector was mounted 51 cm from the crystal. Three rectangular crystals with dimensions of about 0.2 x 0.4 x 0.8 mm were used to collect the native data set. Lattice parameters were determined from the least squares refinement of $K\alpha_1$, $K\alpha_2$ peak positions using step scans of $\pm 2\theta = |6\text{-}20°|$ for 10 reflections. Relative absorption corrections were derived from ø scans of the 6,0,0 reflection at χ=90°, and applied to the data as a function of the ø setting. Data was collected by the θ-2θ method in the indice ranges of h=0-43°, k=0-42°, l=0-25°, with a scan rate of 1°/min and a scan width of 0.75 + 0.35(tan θ). Background correction was determined from 5 sec counts at both extremities of the scan. Three standard alignment reflections were collected every 100 reflections, and five standard decay reflections were collected every 250 reflections. An initial group of 1000 standard reflections

was measured with each crystal and used for scaling purposes. Crystal decay was corrected by assuming a linear decrease in intensity with time. Diffraction data for the PNA/BAP complex were collected on an Enraf Nonius Diffractis Generator equipped with a Type Y 925 Integrating Precession Camera using Kodak direct exposure X-ray film. The generator was operated at 37,000 VDC and 16 mA with a film-to-crystal distance of 100 mm. A 10° precession angle and 10 hour exposure was used for each film.

IV. RESULTS AND DISCUSSION

IV.A. ISOLATION OF PEANUT AGGLUTININ

The seeds of the peanut contain a galactose specific lectin that was isolated by affinity chromatography. Lactosyl-Sepharose 6B column resin was prepared according to the methods of Olsen and Miller (111). These columns had a maximum capacity of about 5 mg PNA/ml moist resin. However, lactosyl-Sepharose obtained from Sigma had a higher capacity of about 15 mg PNA/ml moist resin. Conditions for optimal coupling of bisoxiranes to agarose were investigated by Sunberg and Porath (116). Although coupling pH, temperature, reaction time, and reagent concentrations of laboratory preparations were adjusted for optimal resin capacity, commercially purchased resins had a 3-fold greater binding capacity. A technical grade (70%) of 1,4-butanedioldiglycidyl ether was used in all lactosyl -Sepharose 6B preparations. This could account for less reactive oxirane groups in the resin because impurities would create side reactions or crosslinking.

Lactosyl-Sepharose 6B affinity columns produced one major symmetrical absorbance peak after washing first with

NaCl-TRIS buffer, then with the same buffer made 100 mM in lactose (Figure IV.1.). Two well resolved minor peaks (combined relative area about 2%) were detected when large amounts of the saline fractionated protein mixture was applied to high capacity affinity columns (Figure IV.2.). The near uv absorption spectrum of all affinity fractions showed a double maxima occurring at 278 and 284 nm with a shoulder at 292 nm (Figure IV.3.). Sodium dodecyl sulfate polyacrylamide disc electrophoresis of the major affinity fraction yielded a single molecular weight species (Figure IV.4.). Electrophoretic analysis of the minor affinity fractions was not performed. Although these fractions had the same spectral characteristics of the major affinity fraction, they were not used in any subsequent research. The occurrence of these fractions can be accounted for by secondary and tertiary binding sites within the affinity resin, or species heterogeneity of the PNA. A calibration curve of $\log_{10}$ molecular weight to distance of migration relative to the tracking dye was used to estimate the molecular weight of PNA. Relative to the Sigma Dalton Mark VI molecular weight standards, PNA migrated a distance corresponding to a molecular weight of 30,000 ± 3000 daltons (Figure IV.5.). This molecular weight agrees with the SDS-PAGE values of 29,200 reported by Fish, et al. (110), and 27,000 ± 1500 reported by Lotan, et al. (105). Denaturation of PNA in the SDS digestion mixture for 12

Figure IV.1. Affinity Chromatogram of Peanut Agglutinin

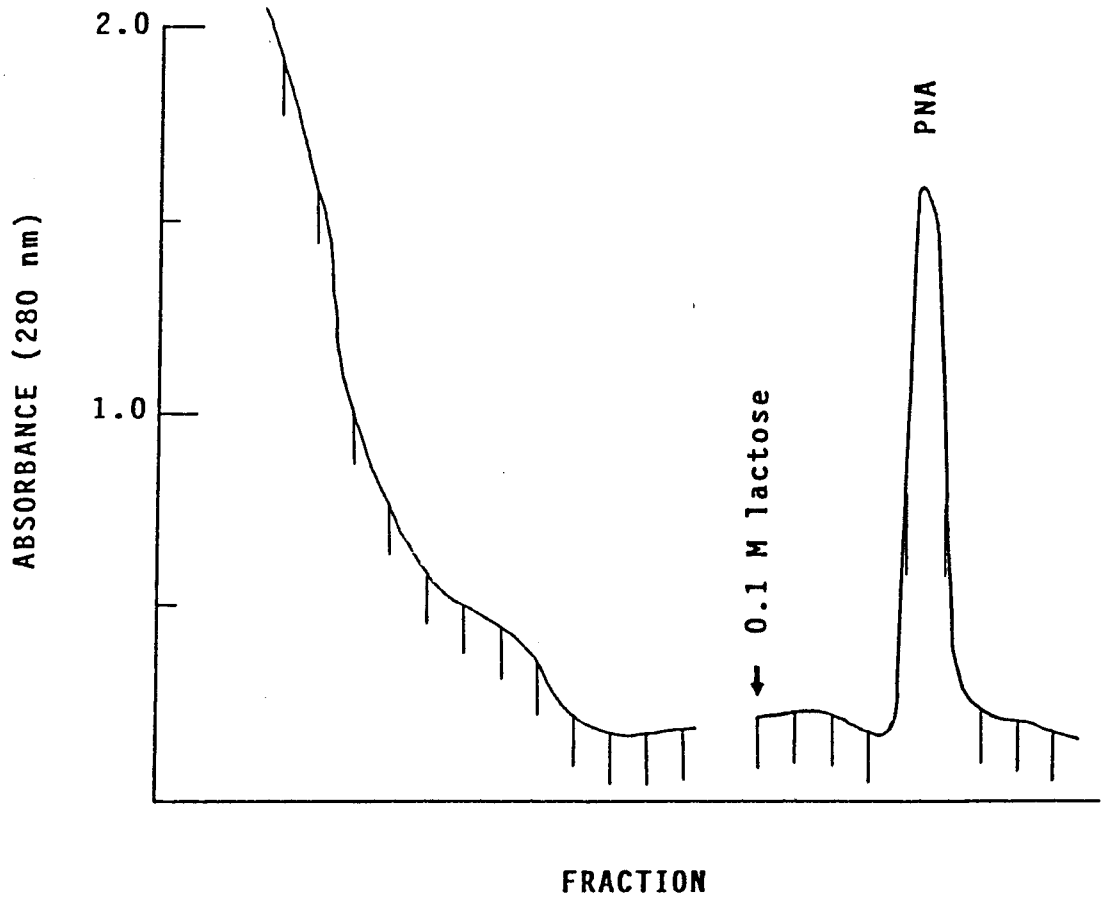

Column was washed with NaCl-TRIS buffer to remove non-lectin material, and PNA was eluted by NaCl-TRIS buffer made 100 mM in lactose. Fractions were collected every 5.0 ml at a flow rate of 12 ml/hr. Elution profile shown yielded 65 mg of PNA.

Figure IV.2. Affinity Chromatogram of Peanut Agglutinin

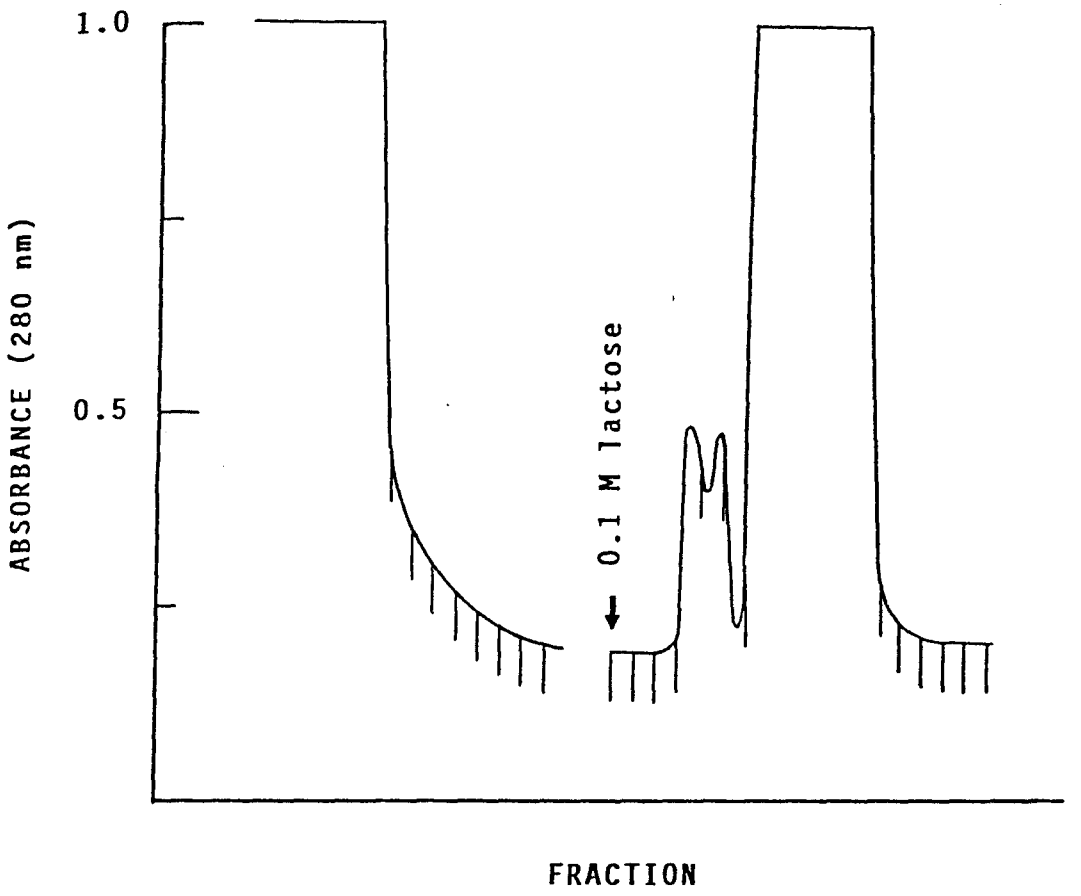

Column was washed with NaCl-TRIS buffer, and PNA was eluted by NaCl-TRIS buffer made 100 mM in lactose. Fractions were collected every 5.0 ml at a flow rate of 12 ml/hr. Elution profile shown yielded 380 mg of PNA.

Figure IV.3. UV Absorption Spectrum of Peanut Agglutinin

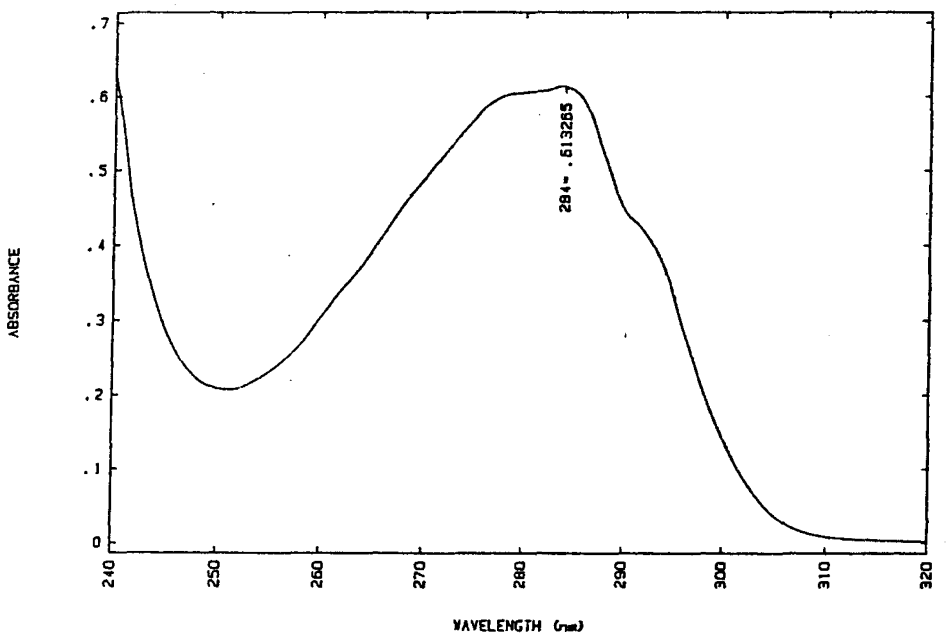

Absorption spectrum shown was recorded in NaCl-TRIS buffer made 100 mM in lactose at a PNA concentration of 0.6 mg/ml.

Figure IV.4. SDS Polyacrylamide Disc Electrophoresis of Peanut Agglutinin

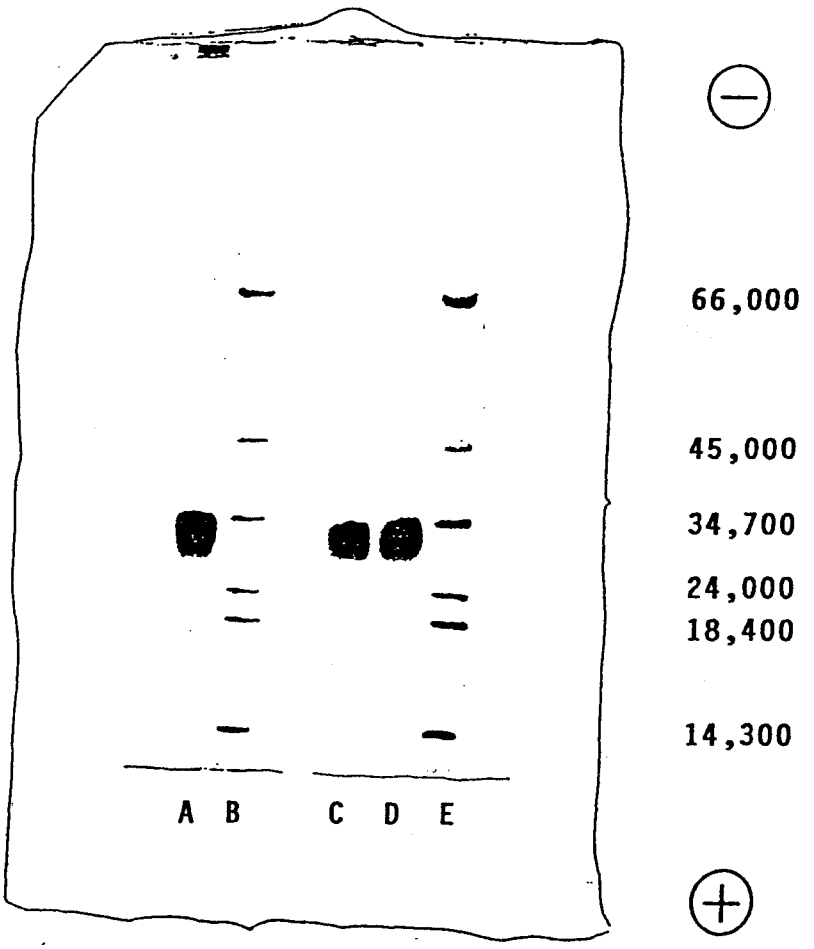

SDS-PAGE of PNA and molecular weight standards (50 μg samples) were run in a resolving gel made 12% in acrylamide at pH=8.8 for 6.0 hours at 100 VDC and 25 mA. Molecular weight standards are bovine albumin (66,000), egg albumin (45,000), pepsin (34,700), PMSF treated trypsinogen (24,000), β-lactoglobulin (18,400), and lysozyme (14,300). Sample A,C, and D are 3, 6, and 12 minute digests, respectively, of native PNA in SDS at 100°C. Samples B and E, are 3 minute digests of molecular weight standards in SDS at 100°C.

Figure IV.5. Subunit Molecular Weight of PNA Determined by SDS-PAGE

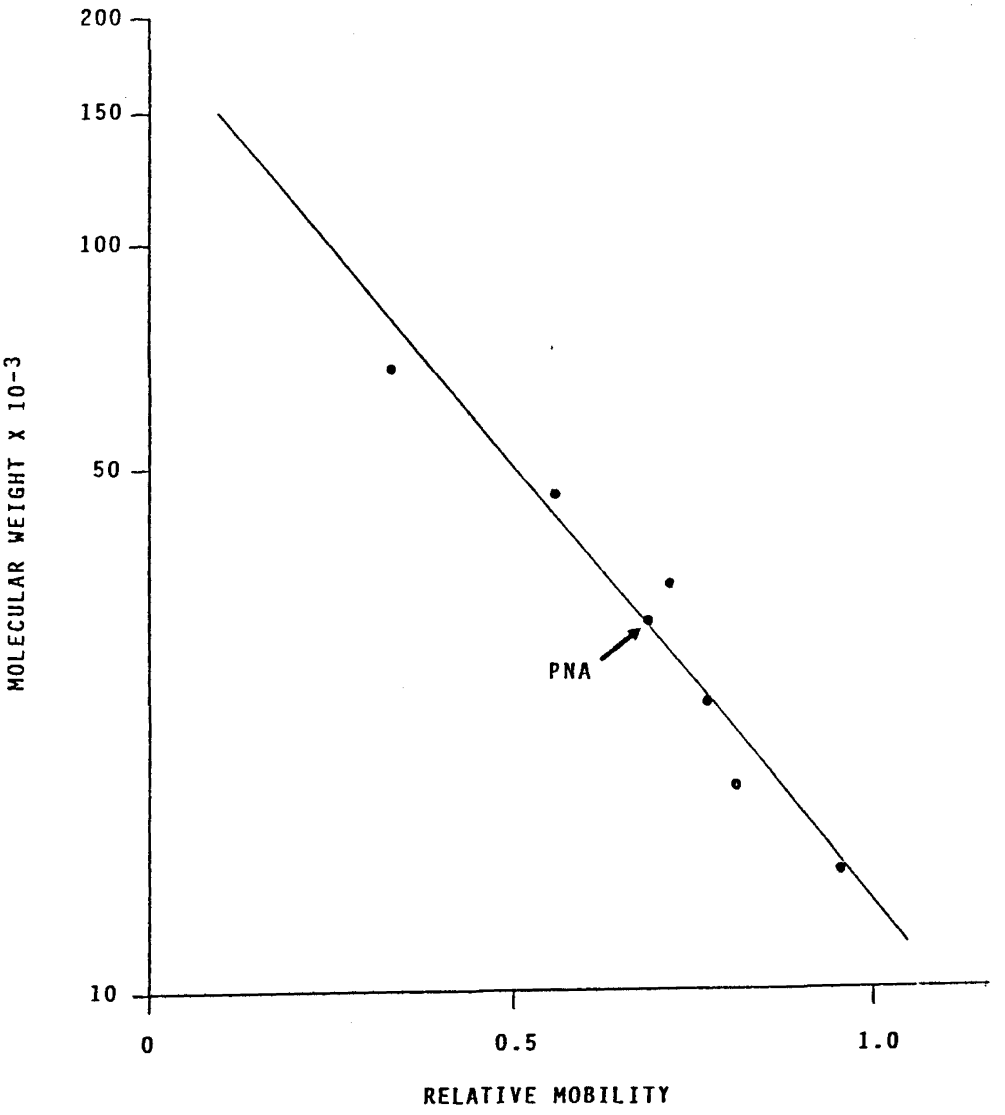

minutes was necessary for all protein material to migrate from the stacking gel. At shorter digestion times, some protein material remained in the sample well. The PNA samples used for SDS-PAGE were in a lyophilized form. Soybean agglutinin and concanavalin A are reported to form high molecular weight aggregates from lyophilization (110). Longer digestion times are consistent with the formation of high molecular weight aggregation of PNA. Protein homogeneity was also assayed by-urea denatured (Figure IV.6.) and native (Figure IV.7.) disc polyacrylamide electrophoresis. Both gels revealed a single protein band.

IV.B. THE PRIMARY STRUCTURE OF PEANUT AGGLUTININ

Amino Acid Composition

The amino acid composition of purified PNA (Table IV.1.) agrees with that previously reported by Lotan, et al. (53) and Miller (69). Peanut Agglutinin contains a high content of hydroxy and acidic amino acids, a low content of tryptophan and tyrosine, and is devoid of cystine or cysteine. No traces of amino sugars were detected by amino acid analysis. The values for the nearest integer were derived from an average value of two acid hydrolysates performed for 16, 24, and 72 hours, and assuming a subunit molecular weight of 27,500 daltons. A chromatogram of a 24 hour PNA hydrolyzate is shown in

Figure IV.6. Urea Polyacrylamide Disc Electrophoresis of Peanut Agglutinin

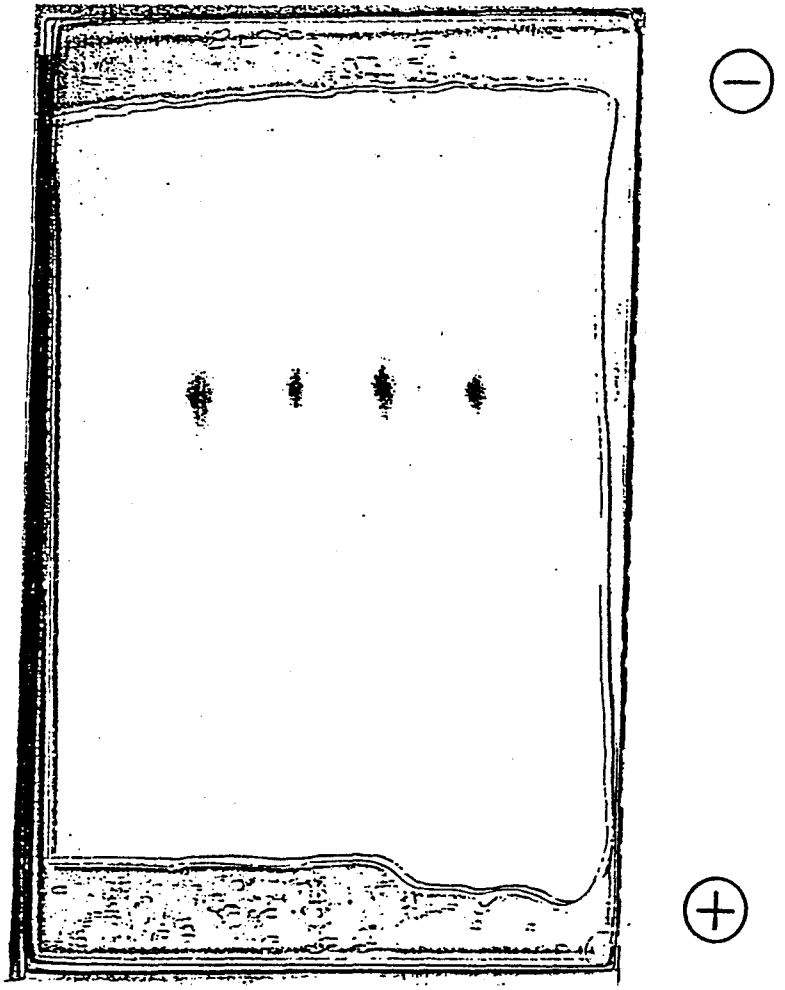

Urea PAGE of PNA (40 μg) was run in a resolving gel made 7.5% in acrylamide for 4.5 hours at 100 VDC and 25 mA.

Figure IV.7. Native Polyacrylamide Disc Electrophoresis of Peanut Agglutinin

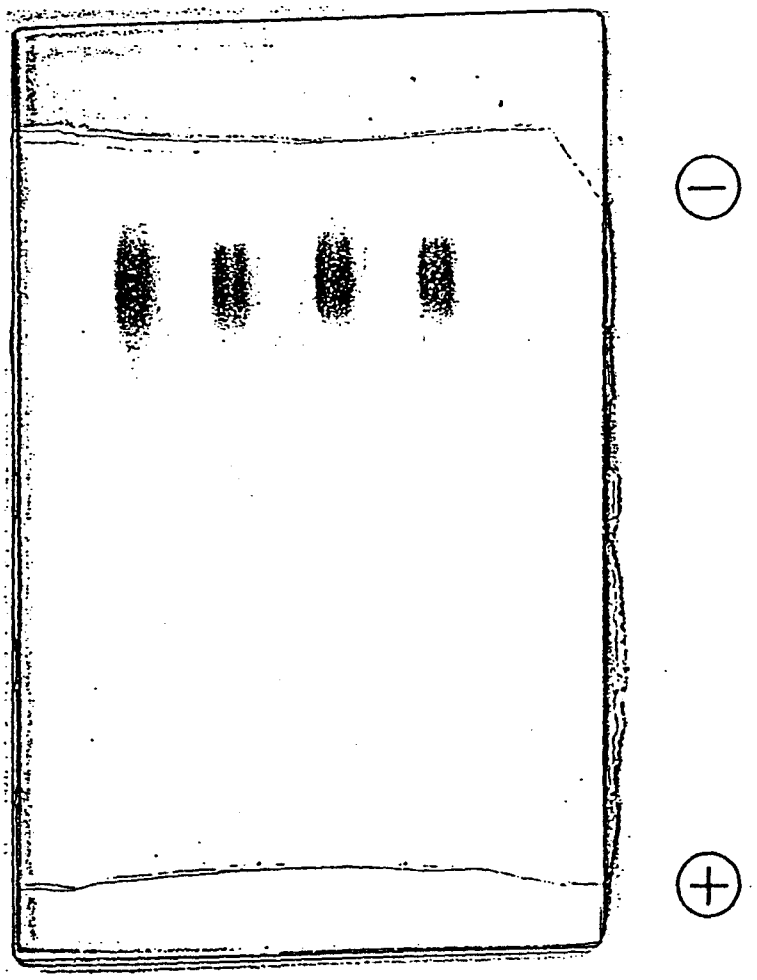

Native PAGE of PNA (40 μg) was run in a resolving gel made 10% in acrylamide for 6.0 hours at 100 VDC and 25 mA.

Table IV.1. Amino Acid Composition of Peanut Agglutinin(1)

	16 hr	24 hr	72 hr	nearest integer	Lotan (2)	Miller (3)
Asp	33.8	34.0	34.0	34	36	36
Thr	22.2	22.6	20.8	23	28	22
Ser	26.4	25.8	21.9	28	31	28
Glu	14.6	15.0	14.5	15	15	14
Pro	10.1	10.1	8.5	10	10	9
Gly	12.0	9.9	15.1	12	24	22
Ala	13.4	13.4	13.2	13	16	16
Cys	0	0	0	0	0	0
Val	23.2	24.7	25.8	25	25	28
Met	3.8	3.5	3.7	4	4	2
Ile	14.7	15.9	17.2	16	14	17
Leu	13.5	13.6	13.5	14	14	14
Tyr	7.2	6.7	6.4	7	6	6
Phe	15.9	15.8	15.4	16	14	16
His	3.9	3.8	3.7	4	3	3
Lys	11.6	11.4	11.4	11	10	11
Arg	8.0	8.0	7.6	8	7	8
Trp	-	-	-	2	2	3
Totals	234.3	234.2	232.7	242	259	255

1. All values shown in Table IV.1. were adjusted to represent the moles of amino acid per polypeptide assuming a subunit molecular weight of 27,500.
2. Ref. 53.
3. Ref. 69

Figure IV.8. Each residue was quantified in reference to the absorbance (peak area) of calibration standards (0.25 μmoles) programmed in the HP 3390A Reporting Integrator. Results were reported directly after the completion of each sample run. Corrections for the loss of threonine and serine during hydrolysis was made by extrapolation of the molar hydrolyzate yields to time zero. Hydrolysis of threonine and serine was estimated to be 7.8 and 18.5%, respectively, over a 72 hour period. Samples of PNA oxidized by performic acid showed no traces of cystine or cysteine present in the form of cysteic acid. Oxidation of methionine to methionine sulfone was observed by the loss of a methionine absorbance (r.t.=74.90 min) and the appearance of a characteristic methionine sulfone absorbance signal (r.t.=19.36 min). The absorption specturm after oxidation of the indole chromophore to oxindole by N-bromosuccinimide is shown in Figure IV.9. Estimation of tryptophan content was calculated by (120):

$$n = \frac{\mu\text{moles tryptophan}}{\mu\text{moles PNA}} = \frac{\Delta OD \times 1.31 \times M.W.}{OD \times a.f. \times 5500}$$

$$= \frac{(0.3080)(1.31)(27,500)}{(0.9359)(0.96)(5500)} = 2.21$$

where n=number of tryptophan residues per mole of protein, OD=initial optical density at 280 nm, ΔOD=change in optical density at 280 nm, a.f.=extinction coefficient of PNA at

Figure IV.8. Amino Acid Analysis of a PNA 24 Hydrolyzate

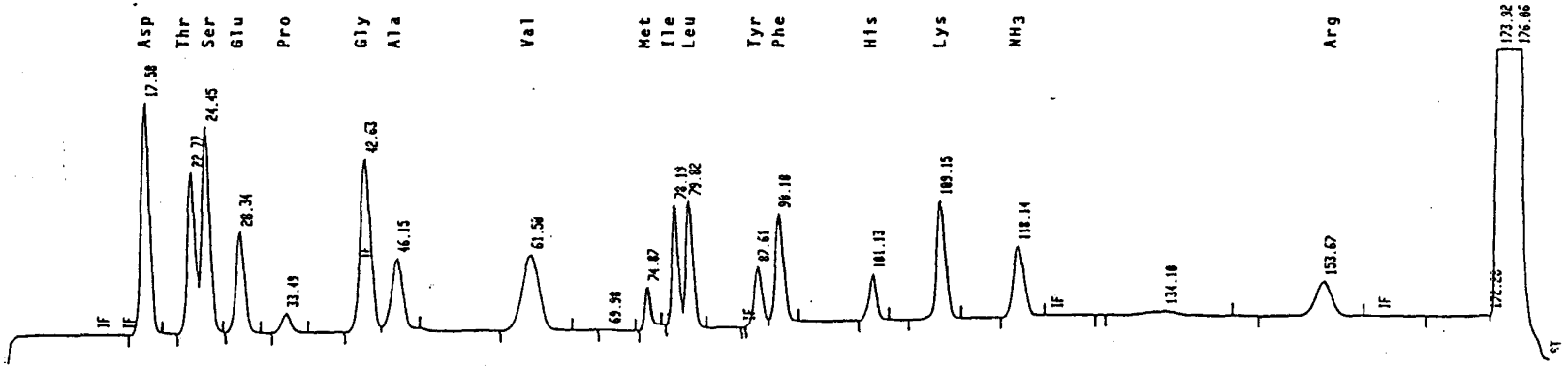

Figure IV.9. Indole-Oxindole Conversion of Tryptophan by N-Bromosuccinimide Oxidation

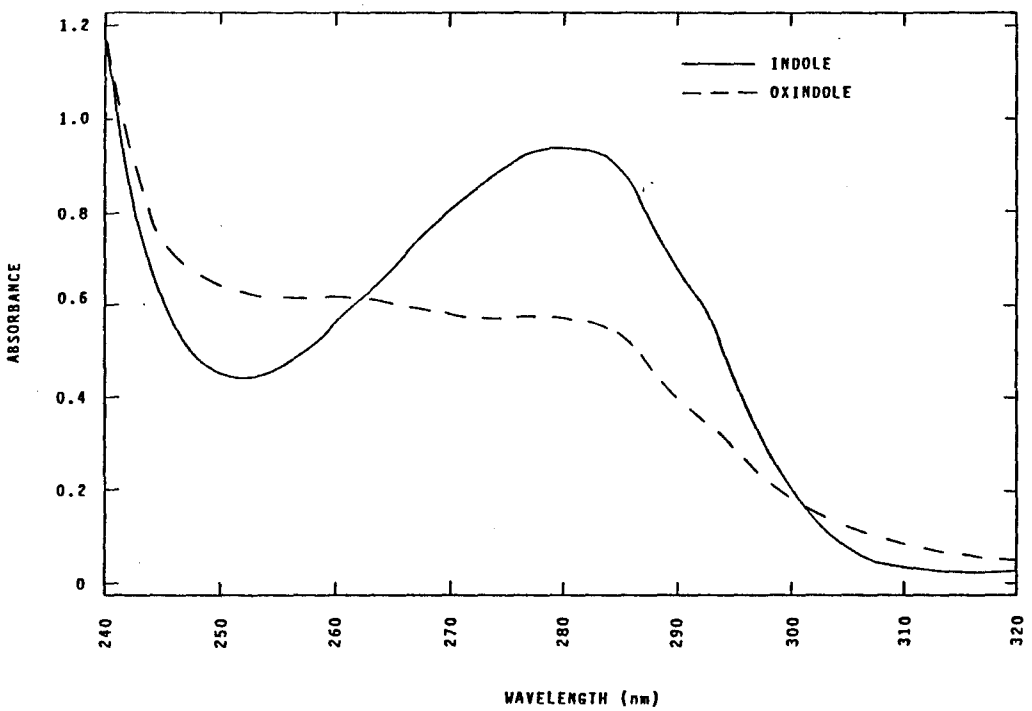

Indole absorption spectrum of PNA (1 mg) was recorded in 10M urea at pH=3.84. Oxindole absorption spectrum was recorded after conversion with 0.178 mg N-bromosuccinimide

280 nm in mg/ml, 1.31=an empirical factor which corrects for the absorption at 280 nm of the oxidation product of tryptophan (oxindole), M.W.=molecular weight of PNA, and 5500=molar absorptivity of tryptophan. In this expression, it is assumed that the molar absorptivity of free and bound tryptophan at 280 nm does not change.

Cyanogen Bromide Fractionation

Four poorly resolved bands (I-IV) were observed from gel chromatography of PNA digested with cyanogen bromide (Figure IV.10.). Fractionation of each band a second time using the same column produced four resolved bands, two of which were obtained from band II, IIa and IIb (Figure IV.11.), and two obtained from band III, IIIc and IIId (Figure IV.12.). Amino acid analysis of PNA revealed 4 methionine residues per subunit. Although 5 CNBr peptides was anticipated, a small peptide resulting from two closely spaced methionine residues, or a methionine residue near the carboxy or amino terminal could have eluded detection. Amino acid composition of the 4 isolated bands is shown in Table IV.2. The nearest integers were obtained for band IIa and IIb by normalization to the molar yield of histidine/2 and histidine, respectively. The nearest integers for band IIb and IIIc were obtained by normalization to the molar yield of arginine. The sum of the residues determined from amino acid analysis of the 4

Figure IV.10. Gel Chromatogram of Cyanogen Bromide Peptides of PNA

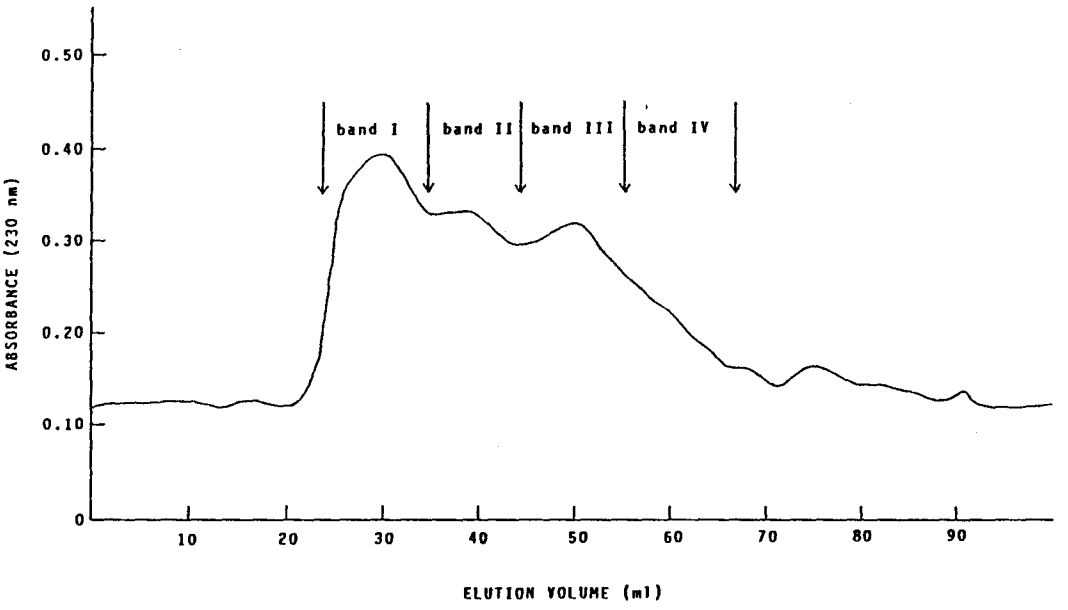

Isolation of CNBr peptides was on a 110 x 1 cm column of Sephadex G-25-300 gel equilibrated with 88% formic acid. Elution was with 88% formic acid at a flow rate of 3.3 ml/hr.

Figure IV.11. Gel Chromatogram of Cyanogen Bromide Band II

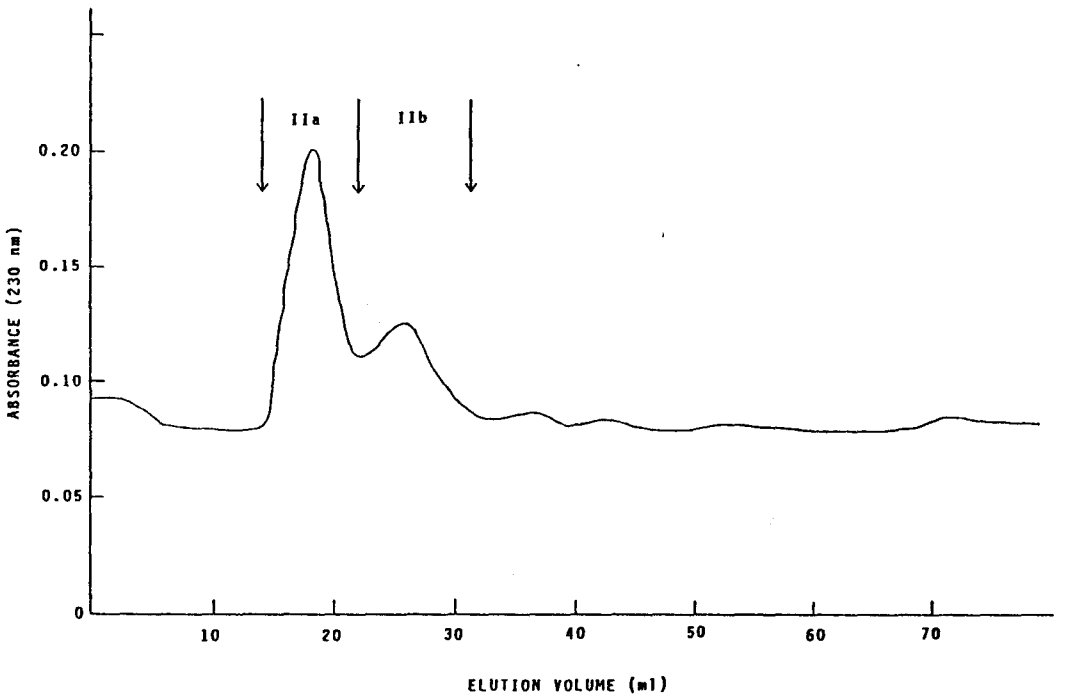

Conditions were as described for Figure IV.10.

Figure IV.12. Gel Chromatogram of Cyanogen Bromide Band III

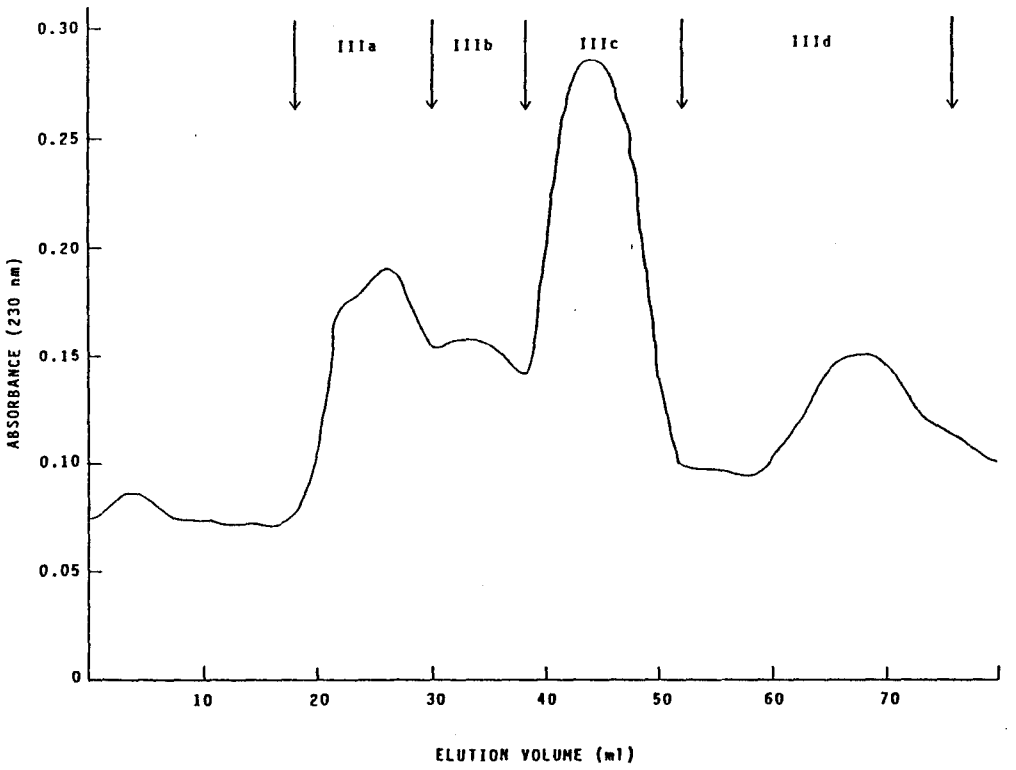

Conditions were as described for Figure IV.10.

Table IV.2. **Amino Acid Composition of Cyanogen Bromide Peptides of Peanut Agglutinin**

	PNA CNBr Fractions(1)					Native(2)	Young(3)	
	IIa	IIb	IIIc	IIId	Total	Total	CN1	CN2
Asp	14	11	2	8	35	34	10	1
Thr	12	4	2	2	20	23	3	2
Ser	14	6	5	4	29	28	5	5
Glu	6	5	2	3	16	15	4	1
Pro	4	2	2	0	8	10	1	1
Gly	12	9	2	4	27	12	4	1
Ala	8	4	3	2	17	13	3	2
Val	12	6	2	2	22	25	6	2
Ile	8	4	1	6	19	16	2	1
Leu	6	4	1	2	13	14	4	1
Tyr	4	2	0	2	8	7	1	0
Phe	6	5	4	2	17	16	4	3
His	2	1	0	1	4	4	0	0
Lys	6	2	0	4	12	11	1	0
Arg	4	1	1	1	7	8	1	1

1. Amino acid compositions of peptides isolated from PNA digestion with CNBr, this study.

2. Amino acid composition of native (undigested) PNA, this study.

3. Amino acid composition of two CNBr peptides reported in the PNA sequence of Young, et al. (41).
   CN1 = CNBr peptide spanning residues 1-50
   CN2 = CNBr peptide spanning residues 51-73

CNBr peptides agrees with the composition of native PNA (Table IV.2.) with the exception of glycine. This can be attributed to sample contamination by collagen commonly found in dust particles. In addition, amino acid compositions of CNBr bands IIb and IIIc agree with the sequence data of Young et al. (41), (Table IV.2.). Peptides generated from the CNBr digestion were not used for sequence analysis because of their insolubility. They were only soluble in concentrated (88%) formic acid. The CNBr peptides were not used for subsequent sequence analysis, because formic acid cannot be used as a medium for Edman degradations.

Trypsin Fractionation

Thirty two fractions were isolated from reverse phase HPLC of PNA digested with trypsin (final DPCC-trypsin to substrate ratio 3:100). Elution was monitored at 254 nm precluding acetate/acetonitrile gradient cut-off (Figure IV.13.). Despite prolonged (15 hrs) and vigorous (enzyme to substrate ratio 3:100 on a weight to weight basis) treatment of PNA with trypsin, a significant amount of protein remained undigested. The undigested material was identified as fraction T1 by SDSPAGE using PNA not treated with enzyme as a control. Those peaks occurring after fraction 32 were found to arise from the solvent. A trypsin self-digestion control performed at the same

Figure IV.13. HPLC Separation of Peptides Obtained from the Digestion of PNA with Trypsin.

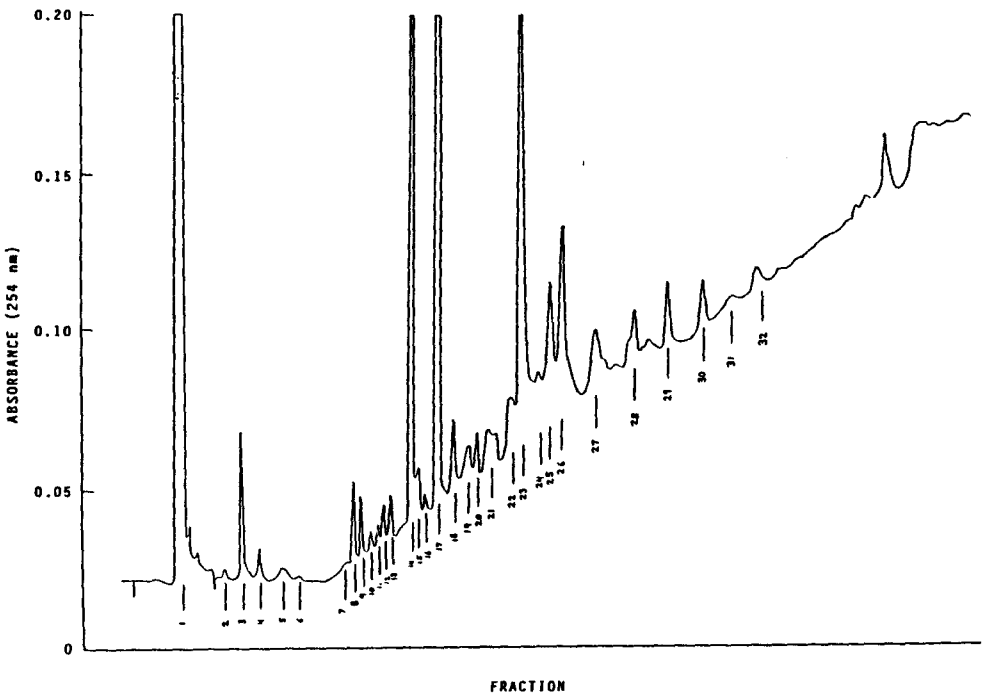

Elution of tryptic peptides on Ultrasphere-ODS C-18 column by a non-linear gradient of ammonium acetate/acetonitrile at pH=4.0 (0 to 70% acetonitrile in 60 min.).

trypsin concentration as the PNA digest was run simultaneously with the PNA tryptic digestion. This control identified 5 major peaks of the 32 fractions that were either not a PNA tryptic peptide (T18, T21, T22), or contaminated by peptides from trypsin self-digestion (T23, T28).

Amino acid composition of the isolated tryptic peptides is shown in Table IV.3. Amino acid analysis was performed on all fractions except T1 (undigested PNA) and fractions T18, T21, and T22 (trypsin self-digestion products). A comparison of the composition sum of isolated tryptic peptides to non-digested PNA (Table IV.4.) shows deviations in the amount of Gly, Met, Tyr, His, and Lys. The number of these residues are low (about 50%) in all cases except for Gly. Small peptides, or single amino acids, (expected to have short retention times) may have co-eluted and been lost in fraction I (also having a short retention time). This can account for such deficiencies. Analysis for tryptophan was not performed.

Sequence Analysis

The strategy for the determination of the amino acid sequence of PNA included manual and automated Edman degradation of the intact protein and polypeptides generated from digestion with trypsin. The peptide fragments were placed in sequence by homology to other

Table IV.3. **Amino Acid Composition of Tryptic Peptides of PNA**

	T2	T3	T4	T5	T8	T9	T10	T11	T12	T13	T14	T15
Asp	1	1				1	1	1	1			
Thr	1					1	1	2	1			1
Ser	2						1	2	2	1		2
Glu											1	
Pro											1	1
Gly	1						1	1	1	1		2
Ala	1						1				1	2
Val	1						1	2	2		1	1
Met												
Ile	1	1		1			1	1				
Leu		3									1	1
Tyr			1									
Phe					1				1	1		2
His												1
Lys		1										1
Arg	1			1				1			1	1

Table IV.3. Cont.

	T17	T19	T20	T23	T24	T25	T26	T27	T28	T29	T32
Asp	2	1	1	7	3	3	2	2	1	3	1
Thr			1	4	1	1	2	1	1		
Ser	4	1	1	5	2	2	1	1	1		
Glu	1	1	1	3	1	2	2	1	1		
Pro	1			2	1	2	1	1		1	
Gly	2		1	3	1	2	3	3	2	1	1
Ala	1			1		1	1	1	1	1	
Val	2	1	2	5	2	2	2	1	1		
Met		1									
Ile	1		1	3	1	2	2	1	1	1	1
Leu	1		2	3		1	1	1	1		
Tyr				1							
Phe		1		4	1	1	1	1	1	1	1
His				1							
Lys	1	1	1	1							
Arg	1										

Table IV.4. **Composition of PNA Tryptic Peptides Compared to Non-Digested PNA**

	Tryptic Peptides	Native PNA
Asp	32	34
Thr	18	23
Ser	28	28
Glu	14	15
Pro	11	10
Gly	26	12
Ala	12	13
Cys	0	0
Val	26	25
Met	1	4
Ile	19	16
Leu	15	14
Tyr	2	7
Phe	17	16
His	2	4
Lys	6	11
Arg	6	8
Trp	-	2

lectins.

A chromatogram of standard PTH amino acids used for calibration is shown in Figure IV.14. Molar yields (integrated values) of each Edman cycle were reported when it was necessary to distinguish among more than one residue in a particular cycle. Sequence data of both manual and automated Edman degradation is shown in Table IV.5. Placement of peptides is shown with respect to the primary structure of sainfoin lectin (39, Figure IV.15.), which is in the same chemical taxonomic tribe as peanut agglutinin. Peptides were also placed with respect to the primary structure of PNA reported by Young, et al. (41). Forty seven cycles of automated Edman degradation performed on PNA yielded 28 of the N-terminal residues. After cycle 28, excessive background interference made identification of additional residues questionable. The N-terminal sequence of PNA reported in this study was 50% identical to the N-terminal sequence of sainfoin determined by Hapner, et al. (39), 96% homologous to the N-terminal sequence of PNA reported by Lauwereys, et al. (40), and 100% homologous to the N-terminal sequence of PNA found by Young, et al. (41). Details to the sequence data shown in Table IV.5., and Figure IV.15. follows:

1. Peptide T29

The ten sequenced residues of peptide T29 were 40% homologous to the sequence spanning Ile-84 to Phe-93 of

Figure IV.14. HPLC Separation of Calibration Standard PTH Amino Acids.

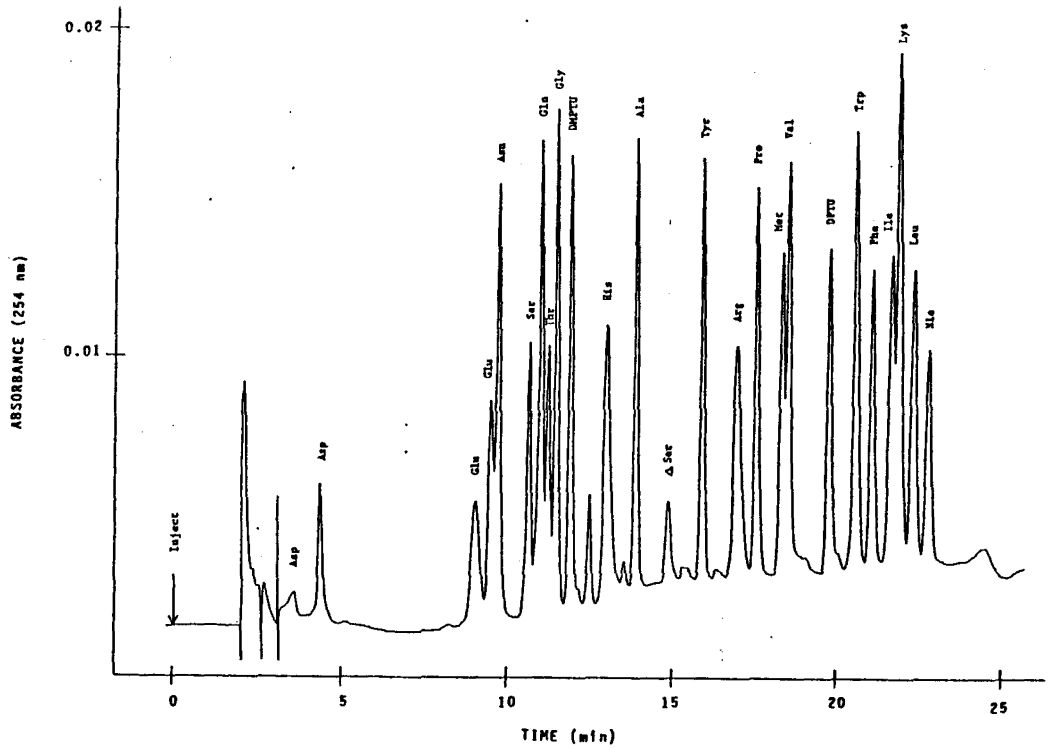

Elution of PTH amino acids on Ultrasphere-ODS C-18 column by a non-linear gradient of sodium acetate/acetonitrile at pH=5.16 (0 to 60% acetonitrile in 17.5 min., 60% acetonitrile for 10 min.).

Figure IV.15. Primary Structure of Peanut Agglutinin

```
Sainfoin                A-E-N-T-V-S-F-D-F-S-K-F-L-S-G-Q-E-N-
PNA (Young, et al.)     A-E[ ]T-V-S-F-N-F-N-S-F-S-E-G-N-P-A-
PNA (this study)        A-E[ ]T-V-S-F-N-F-N-S-F-S-E-G-N-P-A-

L-I-L-Q-G-D-T-V-T-D-D-S-N-R-C-L-V-L-T-R[ ]E-N-N-G-R-P-V-Q-
I-N-F-Q-G-D-V-T-V[ ]L-S-N-G-N-I-Q-L[ ]T-N-L[ ]N[      ]K-V-
I-N-F-Q-G-D-V-T-V[ ]L-S-

D-S-*-G-R-V-L-Y-Q-T-P-I-H-L-W-D-K-Q-I-D-K-E-A-S-F-E-T-S-F-
N-S-V-G-R-V-L-Y-A-M-P-V-R-I-W-S-S-A-T-G-N-V-A-S-F-L-T-S-F-
N-S-V-G-R-V-L-Y

T-F-F-I-Y-R-E-N-I-N-R-G-G-D-G-I-T-F-F-L-A-P-T-D-T-Q[ ]P[ ]
S-F-E-M-K-D-I-K-D-Y-D-P-A-D-G-I-I-F-F-I-A-P-E-D-T-Q-I-P-A-
S-F-E-M-K-      -D-Y-D-P-A-D-G-I-I-F-  -I-A-P-E-D-T-Q-I-P-A-
                                                (Q-F)

K-S[ ]G-G-G-Y-L-G-I-F-K-D[ ]A-E-S-N-E-T[    ]V-V-A-V-E-F-D-
G-S-I-G-G-G-T-L-G-V-S[ ]D-T-K[        ]G-A-G-H-V-G-V-E-F-D-
G-S-I-G-G-G-T-L-G-V-S[ ]D-T-K-

T-F-S-N-R[    ]W-D-P-A-N-P-H-I-G-I-N-V-N-S-V-K-S-K-I-T-T-P-
T-Y-S-N-S-E-Y-N-D-P-P-T-D-H-V-G-I-D-V-N-S-V-D-S-V-K-T-V-P-
   -S-N-S-E-Y-N-D-P-P-T-D-H-V-G-I-D-V-N-S-V-D-S-V-K-T-V-P-

W-G-L-K-N-D-Y-F[ ]T-V-T-I-T-Y-D-A-T[ ]R-S-L-S-V-S-S-F-Y-R-
W-N-S-V-S-G-A-V-V-K-V-T-V-I-Y-D-S-S-T-K-
                -V-K-V-                          -G-F-Y-R-
                                        - ( T4, S4, E2, G,

N-K-P-D-D-I-F-T-V-K-A-S[ ]V-H-L-R-D-A-L-P-Q-W-V-R-I-G-L-S-
                                                 -F-G-F-S-
          -I-F-T-V-T-A-S-G-N-D-L-K-A-L-G-P-E-  -V-R-
A3, L5, F3, R4 )  - M -  ( D8, T, E, A, V2, I4, Y2, K4 )-

A-A-T-G-D-L-V-E-Q-H-R-L[ ]Y-S-W-S-F-K-S-V-L-P-L-D-S-S-T
A-S-G-S-L-G-G-R-Q-I-H-L-I-R-S-W-L-F-Q-S-T-L
```

1. [] denotes deletions made to maximize homology.
2. Gaps denotes segments not sequenced.
3. () denotes predicted compositions of missing segments.

Table IV.5. Sequence Analysis of PNA Tryptic Peptides(1)

Intact PNA		T20						T23			
		T20I		T20II		T20III		T23I		T23II	
A	4354	V	1131	G	228	A	203	S	5557	I	19768
E	2376	L	860	S + ΔS		S + ΔS		N	6565	F	23513
T	2307	Y	458	I	119	G	44	S	2476	T	6230
V	3754			G	101	N	28	E	4079	V	4722
S	1047			G	89	D	56	Y	5886	T	3525
F	3132			G	83	L	24	N	2785		
N	2206			T	24	K	17	D	4682		
F	3036			L	53			P	2349		
N	2346			G	39			P	3048		
S	990			V	37			T	6931		
F	2393			ΔS				D	944		
S	994			D				H	699		
E	827			T				V	603		
G	1797			K				G	618		
N	1341							I	644		
P	1016							D			
A	1429							V			
I	1483							N			
N	1194							S + ΔS			
F	1271							V			
Q	895							D			
G								S + ΔS			
D								V			
V								K			
T											
V											
L											
S											

1. Values shown represent yields (nanomoles) of each automated Edman degradation cycle. ΔS represents detection of dehydroserine.

Table IV.5. Cont.

T26I		T26II		T26III	T25I		T25II		T29	
T	1461	I	318	L 260	S	525	I	440	D	2954
V	974	A	402	G 847	E	1146	A	623	Y	4585
P	847	P	837	E 178	G	1655	P	490	D	2483
		Q	135	G 772	N	940	E	381	P	3770
		F	343	N 116	P	1212	D	122	A	4654
		T	132	I 183	A	1544	T	210	D	2747
		Q	171	N 152	I	1211	Q	224	G	1499
		I	149	V 160	N	745	*		I	552
		P	160	K 45	F	718	P	301	I	336
		A	144	E 124			A	300	F	143
		G	237	G			G	221		
		S	+ ΔS	N 104			S	+ ΔS		
		I	86	E 96			I	178		
		G	82	Q 72			G	217		
		G	101	F 65			G	207		
							G	164		
							T			

Table IV.5. Cont.

T19				T17		T14		T19
T19I		T19II						
S	1355	V	2723	S	676	A	3474	D
F	2762	K	1579	G	313	L	4622	N
E	1946	V	845	I	294	G	1525	Y
M	2832			Q	331	P	1660	
K	1340			V	238	E	1178	
				R	84			

Table IV.5. Cont.

T11	T12	T15	T13	T32	T9
V	S	N	G	D	D
V	F	S	A	Y	N
D	P	V	Y	D	Y
V		G	R	P	
		R			

sainfoin, and 100% homologous to the corresponding sequence of PNA reported by Young, et al. (41). Occurrence of a C-terminal Phe is indication of chymotryptic activity in the trypsin digestion.

2. Peptide T15

A heptapeptide was sequenced from tryptic fraction T15. This peptide is 75% homologous to the segment spanning Asp-47 to Arg-51 in sainfoin, and 100% homologous to a corresponding PNA sequence reported by Young, et al. (41). Occurrence of a C-terminal Arg indicates this peptide resulted from tryptic cleavage.

3. Peptide T19

Two peptides, T19I, and T19II, were sequenced from fraction T19. The peptides were resolved in terms of the relative molar yields of their amino acids. The sequence of fraction T19I, a tryptic peptide, is found to be 20% homologous to the sequence spanning Thr-76 to Tyr-80 in sainfoin, and 100% homologous to the corresponding PNA sequence reported by Young, et al. (41). Fraction T19II, a chymotryptic tripeptide, could not be absolutely placed in the sainfoin lectin because of its small size, but is found in the corresponding PNA sequence reported by Young, et al. (41), that spans Phe-162 to Val-164 in sainfoin.

4. Peptide T32

The tetrapeptide sequenced from fraction T32 could not be placed in the sainfoin lectin sequence. However, it is in identity with the 4 N-terminal residues found in the decapeptide sequenced from fraction T29. Peptide T32 may have resulted from non-specific cleavage of peptide T29.

5. Peptide T25

Two peptides, T25I, and T25II, were sequenced from fraction T25. The nanopeptide T25I, is found to be a chymotryptic peptide. Its sequence is in identity to a nine amino acid segment found in the N-terminal of PNA that corresponds to residues 13 to 21 of sainfoin lectin. The 24 residue tryptic peptide T25II is found to be 52% homologous to the sequence spanning Leu-95 to Ala-115 in sainfoin, and 100% homologous to the corresponding sequence of PNA reported by Young, et al. (41). The eighth Edman degradation cycle of peptide T25II yielded only Asn. This residue is believed to result from peptide T25I because of its identity in the N-terminal sequence of PNA and its relative molar yield with respect to other residues in that peptide. Therefore, the eighth residue of fraction T25II was left unknown.

6. Peptide T26

Three peptides, T26I, T26II, and T26III, were sequenced from fraction T26. The tripeptide T26I was

resolved in terms of the relative molar yields of its amino acids. It is found to be 67% homologous to the sequence spanning Thr-152 to Pro-154 in sainfoin, and 100% homologous to the corresponding PNA sequence of Young, et al. (41). The remaining peptides were resolved by deleting the sequence of the segment spanning Leu-56 to Phe-70 in bovine trypsin (a chymotryptic peptide) from the combined sequence data of T26. This yielded the sequence of peptide T26III (a peptide from the self digestion of trypsin) and a 14 residue peptide T26II. Peptide T26II is found to be 67% homologous to the sequence spanning Leu-95 to Gly-106 of sainfoin and 87% homologous to the corresponding PNA sequence reported by Young, et al. (41). Peptide T26II is also found to be homologous to a 15 residue portion of PNA sequenced in peptide T25II with one exception. While the first five amino acids found in T25II are Ile-Ala-Pro-Glu-Asp-, the corresponding N-terminal sequence in T26II is Ile-Ala-Pro-Gln-Phe-. This alternate sequence is evidence for the existence of isolectins present in a single PNA preparation. The eighth Edman cycle of peptide T26II yielded Ile, a residue not determined in the sequence of T25II.

7. Peptide T20

Three peptides, T20I, T20II, and T20III were sequenced from tryptic fraction T20. The chymotryptic

tripeptide T20I was resolved in terms of the relative molar yields of its amino acids. It is found to be 100% homologous to both the sequence spanning Val-52 to Tyr-54 in sainfoin, and the corresponding PNA sequence of Young, et al. (41). The remaining tryptic peptides were resolved by deleting the sequence of the 14 carboxy terminal amino acids of T25II from the combined sequence data. This yielded a redundant sequence already found in T25II, and the sequence of a heptapeptide 43% homologous to the segment spanning Ala-192 to Arg-197 in sainfoin.

8. Peptide T23

Two peptides, T23I, and T23II were sequenced from tryptic fraction T23. The 24 residue tryptic peptide T23I is found to be homologous to the sequence spanning Ser-130 to Lys-150 of sainfoin, and 100% homologous to the corresponding PNA sequence of Young, et al. (41). The peptide T23II is found to be 80% homologous to the sequence spanning Ile-187 to Lys-191 of sainfoin.

9. Peptide T14

The total amino acid composition of PNA (Table IV.1.), yielded 10 residues of Pro. Seven of these 10 were placed from the sequence data of intact PNA, and peptides T29, T25II, T23I, and T26I. This leaves 3 residues of Pro not accounted for. The pentapeptide sequenced from fraction T14, -Ala-Leu-Gly-Pro-Glu-, was

placed in the segment spanning Asp-198 to Gln-202 in sainfoin. This region is completely conserved in the sequence -Pro-Glu- (with the exception of sainfoin containing the sequence -Pro-Gln-) in the other sequenced legume lectins (Figure IV.3.). Amino acid composition of peptide T14 yielded one residue of Val and Arg each. The sequence spanning Trp-203 to Arg-205 in sainfoin is also highly conserved in the other legume lectins. Then, using both the composition and Edman degradation data, the sequence of peptide T14 is believed to be -Ala-Leu-Gly-Pro-*-Val-Arg-. The Trp residue, conserved in the other lectins between Val and Arg, would not have been detected by amino acid analysis using acid hydrolysis due to destruction of the indole ring.

10. Peptide T13

A tetrapeptide was sequenced from tryptic peptide T13. This peptide is 75% homologous to the sequence spanning Ser-178 to Arg-181 in sainfoin.

The remaining peptides that were sequenced (T9, T11, T12, T17, and T19) could not be placed with confidence. The small number of residues making up these peptides made placement by homology questionable.

Amino acid composition of PNA (Table IV.1.) revealed 242 residues, including 11 Lys and 8 Arg amino acids (based on a subunit molecular weight of 27,500 daltons).

Digestion with trypsin would be expected to produce 20 peptides, 19 of which terminate in Lys or Arg (assuming complete and specific cleavage). Thirty two fractions of PNA were isolated from its digestion with trypsin (Figure IV.13.). A control digestion performed in the absence of PNA showed that some of the excess fractions were due to self-digestion of trypsin. Amino acid composition of the isolated fractions (excluding fractions identified as resulting from self-digestion of trypsin or the undigested fraction, T1, of PNA) showed that some peptides contained both Lys and Arg (T15 and T17), and many contained neither (T4, T8-T10, T12, T13, T24-T29, T32). This shows that both non-specific and incomplete cleavage had occurred in the tryptic digestion of PNA. Occurrence of a -Lys-Glu-bond not hydrolyzed was observed in peptide T26III. Amino acids containing a net negative charge (Asp or Glu) adjacent to a lysine or arginine residue have been reported to significantly reduce the rate of trypsin hydrolysis (127). Sequence analysis by both automated and manual Edman degradations showed that cleavage at Phe (T26III, T25I, and T29), and Tyr (T20I, T19, and T9) had occurred. This is often a result of chymotrypsin contamination of trypsin. Peptides with carboxy terminal Val (T19II, T11), Thr (T25III), Gly (T26II), and Pro (T26I, T12, T32), and Glu (T14), were also sequenced from the tryptic digestion of PNA. Non-specific hydrolysis by trypsin has been reported

to occur at peptide bonds formed by Val, Thr, and Gly (127). Other types of non-specific cleavage can also result from chymotryptic activity at high ratios of enzyme to substrate and long digestion periods (127). The occurrence of chymotryptic activity can result from two sources. The first comes from contaminated trypsin. Commercial preparations of trypsin are known to contain chymotrypsin. Trypsin is treated with an inhibitor specific for chymotrypsin such as L-(1-tosylamido-2-phenyl)ethyl chloromethyl ketone (TPCK), or diphenylcarbamyl chloride (DPCC), to eliminate chymotryptic activity. The trypsin used in this study was DPCC treated, which is reported to be less effective than TPCK treated trypsin in eliminating chymotryptic activity (127). The second source of chymotryptic activity can result from the structural change that occurs from the autodigestion of trypsin. An interchain split between Lys-131 and Ser-132 of trypsin leads to the formation of α-trypsin. Further degradation of α-trypsin leads to the formation of pseudotrypsin (ψ-trypsin), in which an additional bond between Lys-176 and Asp-177 is hydrolyzed. Cleavage at Lys-131 and Ser-132 (leading to α-trypsin) does not change the specificity of trypsin. However, cleavage between Lys-176 and Asp-177 in α-trypsin (leading to ψ-trypsin) allows the enzyme to hydrolyze bonds adjacent to aromatic amino acid residues (128). Both of these sources of chymotryptic

-like activity can explain the types of non-specific cleavage that occurred in the tryptic digestion of PNA.

The partial sequence of PNA reported by Lauwereys, et al. (40), placed 161 residues (67%) of the total amino acids making up its primary structure. Sequence strategy included trypsin digestions (enzyme to substrate ratio of 1:100 on a weight to weight basis) in the absence and presence of 0.1% SDS and 2M urea. Attempts to fully sequence the protein failed because of its resistance to hydrolysis, low solubility, and microheterogeneity due to the existence of isolectins.

The partial sequence of PNA reported by Young, et al. (41), placed 197 residues (81%) of the total amino acids making up its primary structure. Sequence strategy of Young, et al. (41), included a preliminary acid hydrolysis using 50% formic acid. Three fragments were obtained and separated by gel filtration. The peptides were further cleaved with trypsin or chymotrypsin. Two of the smaller fragments were fully sequenced, and the third only partially. Completion of the PNA sequence has recently been reported (N. M. Young, private communication). The sequences reported by Lauwereys, et al. (40), and Young, et al. (41), were in 75% agreement. Lacking in both these primary structures is a fragment consisting of about 33 amino acids (corresponding to residues 173 to 205 in sainfoin (Figure IV.15.).

The present study sequenced 128 residues of PNA (53%) by homologous placement of tryptic peptides to other leguminous lectins. Aside from microheterogeneity, as compared to the partial sequence of PNA reported by Young, et al. (41), there is 100% agreement between placement of amino acids. Subtracting the PNA sequence composition of Young, et al. (41), from the total composition of PNA (Table IV.6.), 45 residues are not accounted for. This suggests that in addition to the 33 residue segment missing within the sequence of PNA, about 12 residues of the carboxy terminal also remain unknown. Eight of these 45 amino acids are either Lys or Arg. Enzymatic digestion using trypsin would yield 9 peptides, with a average size of about 5 amino acids. This can explain why they were not detected. Small hydrophilic peptides are expected to have short retention times when separated by reverse phase HPLC. A significant amount of PNA was resistant to digestion by trypsin. The missing peptides may have co-eluted with intact PNA, eluting as a large, broad fraction with a short retention time also. Despite this, four peptides (23 amino acids) were sequenced and placed by homology within the missing primary structure of PNA in this study.

The amino acid composition of CNBr band IIb and IIIc (Table IV.2.) agree with the two complete cyanogen bromide peptides predicted from the sequence data of Young, et al. (41). Two partial CNBr peptides can also be generated from

Table IV.6. Total Amino Acid Composition of Segments not Sequenced in the Primary Structure of PNA

	Total Composition of PNA (1)	Partial Sequence Composition (2)	Residues not Sequenced (3)
Asp	34	27	7
Thr	23	14	9
Ser	28	25	3
Glu	15	11	4
Pro	10	8	2
Gly	12	20	-8
Ala	13	11	2
Cys	0	0	0
Val	25	21	4
Met	4	2	2
Ile	16	13	3
Leu	14	10	4
Tyr	7	5	2
Phe	16	13	3
His	4	3	1
Lys	11	7	4
Arg	8	4	4
Trp	2	3	-1

1. This study.
2. Composition of PNA determined from the sequence data of Young, et al. (41). Asn and Gln are reported as Asp and Glu, respectively.
3. Residues not sequenced were determined by subtracting the partial sequence composition data from the total composition data. Negative values indicate a deficiency of residues determined by amino acid analysis as compared to sequence analysis.

between Tyr-80 to Arg-172 of sainfoin. The second (PP2) spans the segment between Ile-206 and Leu-230 of sainfoin (Table IV.7.). The composition of PP1 most closely resembles that of CNBr fraction IIa, and PP2 that of CNBr fraction IIId. Subtracting the composition of PP1 and PP2 from CNBr fractions IIa and IIId, respectively, yields an estimate of the composition of the missing segments (Table IV.7.). Values for the number of Asp, Pro, and Val residues in CNBr fraction IIa, and Ser, Leu, Phe, and Arg, in CNBr fraction IIId appear in slight excess (negative differences). The sum of the placed residues within the missing sequence of PNA can be accounted for in the difference of the actual (this study) versus sequence (Young, et al.) composition of CNBr peptides (Table IV.6.).

IV.C. THE BINDING OF LIGANDS TO PEANUT AGGLUTININ

Preparation of N-Dansylgalactosamine

The reaction scheme for the preparation of 2-amino-2-deoxy-N-(5-dimethylamino-1-naphthalene sulfonyl)-galactose (N-dansylgalactosamine or DnsGalN) is shown in Figure IV.16. Three fluorescent products were detected from the reaction mixture after thin layer chromatography on silica gel (Figure IV.17.). The R_f values of the products were 0.16, 0.65, and 0.98, which fluoresce with a yellow-green, yellow, and blue color, respectively, when irradiated with short wave uv light. Control experiments

Table IV.7. **Predicted Composition of Cyanogen Bromide Peptides Not Fully Sequenced**

	PP1 (1)	CNBr IIa (3)	Residues Not Sequenced (4)	PP2 (2)	CNBr IIId (3)	Residues Not Sequenced (4)
Asp	16	14	-2	0	8	8
Thr	8	12	4	1	2	1
Ser	10	14	4	5	4	-1
Glu	4	6	2	2	3	1
Pro	6	4	-2	0	0	0
Gly	11	12	1	4	4	0
Ala	5	8	3	1	2	1
Val	13	12	-1	0	2	2
Ile	8	8	0	2	6	4
Leu	1	6	5	4	2	-2
Tyr	4	4	0	0	2	2
Phe	3	6	3	3	2	-1
His	2	2	0	1	1	0
Lys	6	6	0	0	4	4
Arg	0	4	4	2	1	-1

1. PP1 = segment of PNA sequence of Young, et al. (41), spanning Tyr-80 to Arg-172 of sainfoin. Asn and Gln reported as Asp and Glu.
2. PP2 = segment of PNA sequence of Young, et al. (41), spanning Ile-206 to Leu-230 of sainfoin. Asn and Gln reported as Asp and Glu.
3. Total amino acid composition of cyanogen bromide peptide IIa or IIId, this study.
4. Residues not sequenced determined by subtracting partial sequence composition data from total composition data. Negative values indicate a deficiency of residues determined by amino acid analysis as compared to sequence analysis.

Figure IV.16. Reaction Scheme for the Preparation (1) of N-Dansylgalactosamine

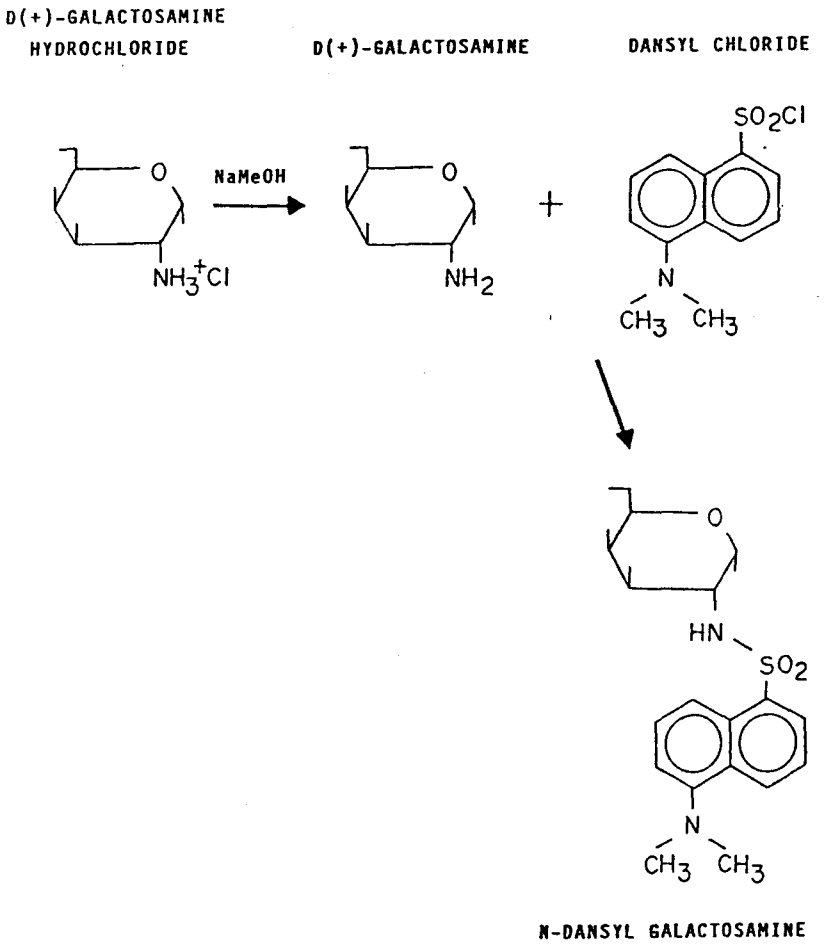

1. Ref. 125.

Figure IV.17. Thin Layer Chromatography of N-Dansyl-Galactosamine Reaction Mixture

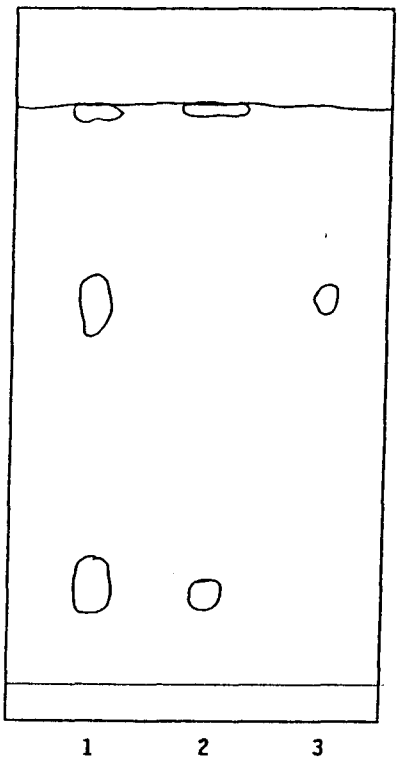

1. DnsGalN Reaction Mixture
2. Dansyl Chloride Control
3. HPLC Purified DnsGalN

Silica gel TLC developed in 10% methanol in methylene chloride. Detection was by short wave uv light.

showed that the products with R_f values of 0.16 and 0.98 were due to unreacted or hydrolyzed dansyl chloride (Figure IV.17.). HPLC separation of reaction mixture products yielded three bands (Figure IV.18.) with retention times of 84 sec (blue fraction), 156 sec (yellow fraction), and 516 sec (yellow-green fraction). Chromatography on silica gel separated the same three products but in a reversed elution order from reverse phase HPLC. Isolation of DnsGalN by either HPLC or silica gel chromatography yielded a single product as indicated by thin layer chromatography (Figure IV.17.).

The N-dansylgalactosamine was green and crystalline with a melting point of 81.0°C (decomposed at 168°C). Absorption bands were found in the ultra violet region at 248 and 328 nm (Figure IV.19.) in methanol. The proton NMR spectrum (Figure IV.20.) in DMSO d_6 agreed with that reported by Lartey, et al. (125) for N-dansylglucosamine, and is consistent with the structure of N-dansyl-galactosamine. Fluorescence excitation and emission maxima of the compound were found at 328 and 540 nm, respectively, in NaCl-TRIS buffer.

Binding of Fluorescent Ligands to PNA

The interaction of a protein and complexing agent can be followed by fluorescence spectroscopy. The wavelengths of maximal activation and emission, quantum

Figure IV.18. Reverse Phase HPLC of N-Dansylgalactosamine Reaction Mixture

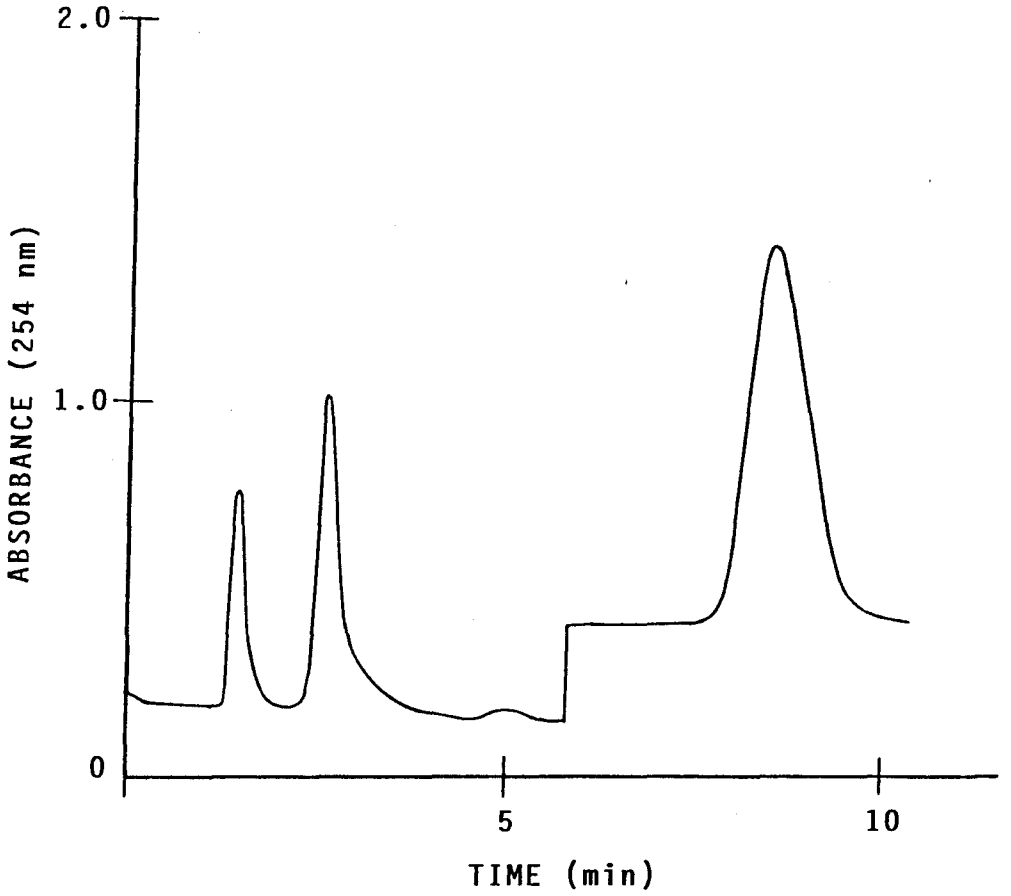

Separation of DnsGalN by isocratic elution using Whatman C-18 column and 70% methanol.

Figure IV.19. Ultra Violet Absorption Spectrum of N-Dansylgalactosamine in Methanol

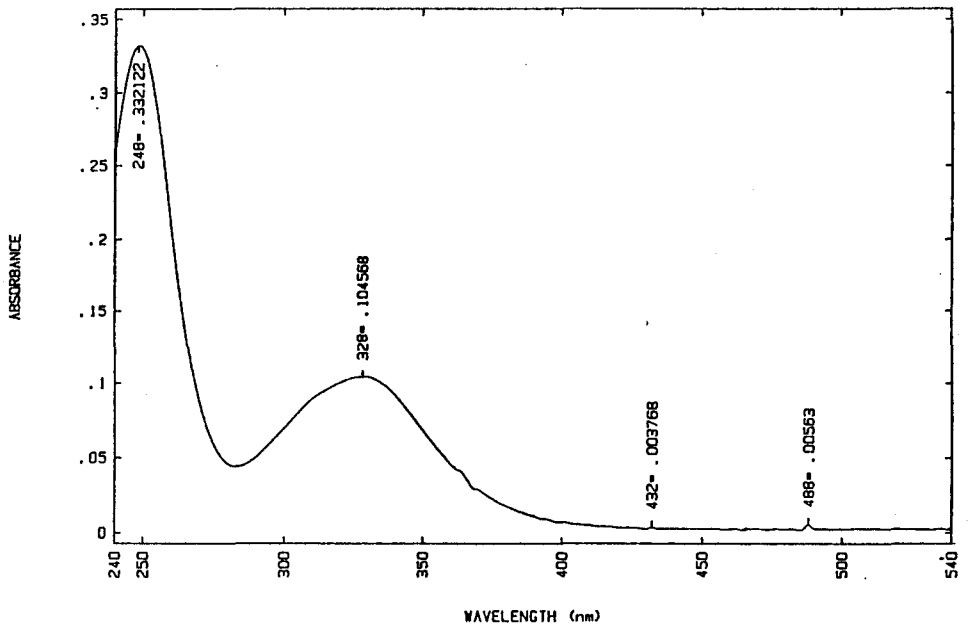

Figure IV.20. Proton NMR Spectrum of N-Dansyl-Galactosamine

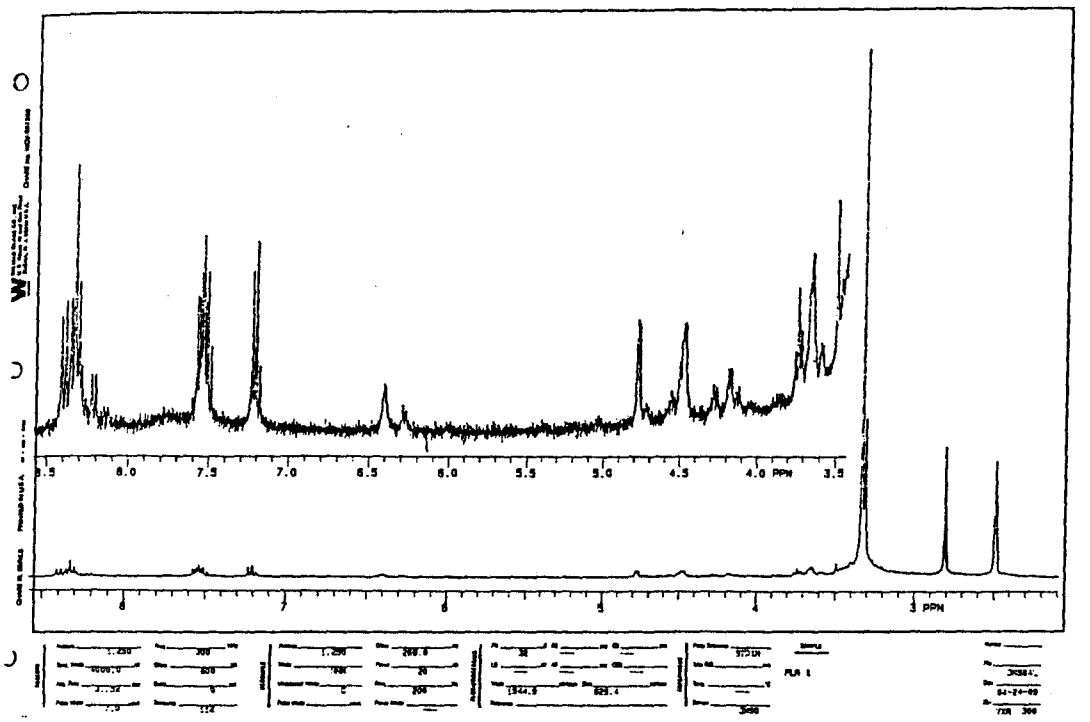

NMR spectrum of DnsGalN recorded in DMSO-d_6 after exchange with D_2O on Varian VXR300

yield, fluorescence lifetime, and degree of polarization are sensitive to subtle changes in the environment of a fluorophore. The fluorescent probes 2,6-toluidinyl-naphthalene sulfonate (TNS) and 1,8-anilino-naphthalene sulfonate (ANS) were used to study the hydrophobic binding properties of PNA. In addition, DnsGalN was used to study the carbohydrate binding of PNA, and interactions between the hydrophobic and carbohydrate binding sites. Structures for these fluorescent probes are shown in Figure IV.21.

The property that makes TNS, ANS, and DnsGalN useful is that they are all only weakly fluorescent in aqueous buffers, but show a strong enhancement of fluorescence quantum yield upon transfer to a non-polar solvent. Since the active site of many proteins are found within hydrophobic regions of the macromolecule, the binding of probes like TNS, ANS, and DnsGalN can be followed by enhancement of the fluorescence they exhibit upon complexation. The binding of non-fluorescent probes can also be studied if the binding is competitive with the fluorescent probe. In this instance, a fixed concentration of protein, complexed with the fluorescent probe, would show a decrease in fluorescence (quenching) when titrated with a non-fluorescent competitive inhibitor.

1. Binding of DnsGalN and Lactose to PNA

The fluorescence of DnsGalN increased about 120-fold

Figure IV.21. Molecular Structure of Probes Used in PNA Binding Assays

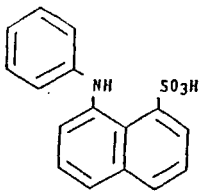

1,8-anilinonaphthalenesulfonic acid (ANS)

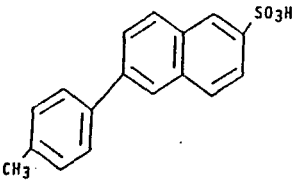

2,6-toluidinylnaphthalenesulfonic acid (TNS)

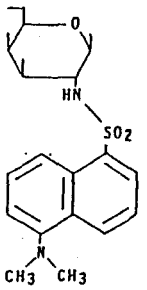

N-dansylgalactosamine (DnsGalN)

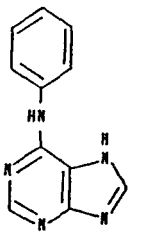

N^6-benzyladenine (BAP)

with a blue shift of 13 nm in the presence of PNA (Figure IV.22.). Ligand binding is represented according to the Hill equation (131). In all fluorescence binding assays, it is assumed that the change in fluorescence intensity is proportional to the concentration of complex formed. The fluorescence intensity at infinite protein concentration (Fi) was obtained from a double reciprocal plot of the fluorescence intensity (F) at a particular protein concentration (Figure IV.23.). The fluorescence data was analyzed according to the following reaction scheme (132):

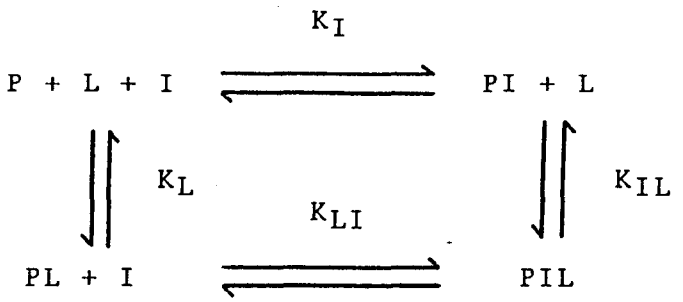

where P, L, and I refer to PNA, the fluorescent probe, and the inhibitory probe, respectively. When log[P]f, where [P]f is the concentration of unbound protein (tetramer), is plotted against log[(F-Fo)/(Fi-F)], where Fo is the fluorescence intensity in the absence of protein, and [(F-Fo)/(Fi-F)] is the fraction of binding sites occupied by the fluorescent probe, the intercept on the x axis yields the pKa value for the protein-fluorescent probe interaction. This is equated to (133):

$$\log[(F-Fo)/(Fi-F)] = \log Ka + \log\{[P]f - [L]t * \Delta F/\Delta Fi\}$$

where $\Delta F = (F-Fo)$ and $\Delta Fi = (Fi-Fo)$ are the change in fluorescence intensity at a particular and infinite protein concentrations, respectively, and [L]t is the total concentration of fluorescent probe. A titration curve obtained from the fluorescence intensity change of DnsGalN as a function of added protein is shown in Figure IV.24. A graphical representation for the determination of the association constant ($Ka = 10.6 \pm 1.2 \times 10^3\ M^{-1}$) of DnsGalN to PNA is shown in Figure IV.25.

The binding of lactose to PNA was studied by following the quenching of fluorescence from PNA-DnsGalN complex (Figure IV.26.), due to the release of DnsGalN from lactose inhibition. Since the binding of DnsGalN can be completely inhibited by the addition of lactose, [PIL] = 0, and association constants K_{LI} and $K_{IL} = 0$. The reaction scheme can then be characterized by (133):

$$\{[P]t/[PL] - 1\} * [L]f = (K_I / K_L) * [I]f + 1/K_L$$

where [P]t = total PNA concentration (tetramer), [PL] = concentration of PNA/DnsGalN complex, and [L]f and [I]f are the concentrations of free DnsGalN and lactose. The concentration of free fluorescent probe was obtained from

[L]f = ([L]t - (ΔF/ΔFi) * [L]t), where [L]t is the total concentration of DnsGalN. The concentration of free lactose was obtained from [I]f = ([I]t - (ΔF'/ΔFi) * [P]t), where [I]t is the total concentration of lactose, and ΔF' is the fluorescence change induced by the addition of lactose to the PNA/DnsGalN complex. The slope and intercept of a plot of (([P]t/[PL]-1) * [L]f) verses [I]f provides values for the association constant of the fluorescent probe (K_L) and the inhibitory sugar (K_I). A titration curve obtained from the fluorescence intensity change of PNA-DnsGalN complex as a function of added lactose is shown in Figure IV.27. A graphical representation for the determination of the association constant (Ka = 1.5 $\pm$ 0.3 x 10^3 M^{-1}) of lactose to PNA is shown in figure IV.28.

Control experiments using dansyl amide in place of N-dansylgalactosamine show no fluorescence enhancement in the presence of PNA. This indicates that the binding of DnsGalN is through the galactose, rather than the dansyl moiety. No binding of DnsGalN is observed from fluorescence enhancement in the presence of 10 mM lactose. This suggests a competitive binding of DnsGalN and lactose to PNA.

2. Binding of TNS and N^6-Benzylaminopurine to PNA

The emission maximum of TNS is 500 nm in water and

Figure IV.22. Fluorescence Emission Enhancement of DnsGalN in the Presence of PNA

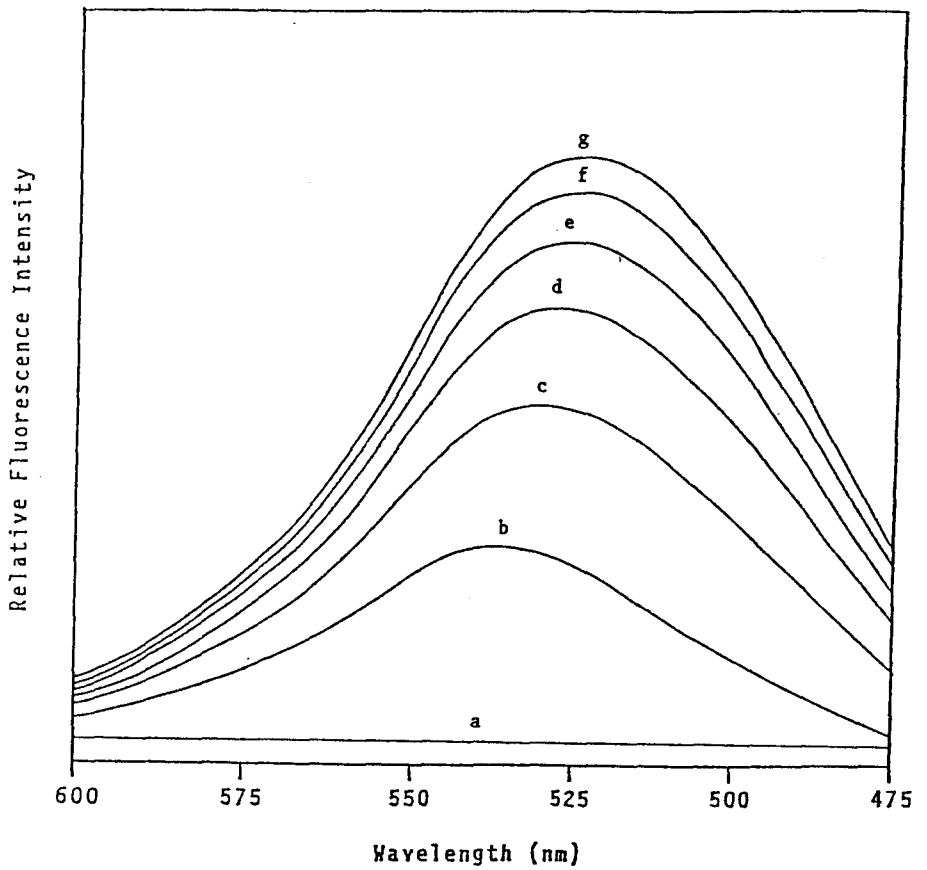

Fluorescence emission spectra for DnsGalN were determined at 22.0°C with excitation at 328 nm. (a) buffer blank, (b) 850 μl of 5.0 μM DnsGalN, (c) - (g) 20 μl additions of 185 μM PNA.

Figure IV.23. Fluorescence Emission Intensity of DnsGalN Extrapolated to Infinite PNA Concentration

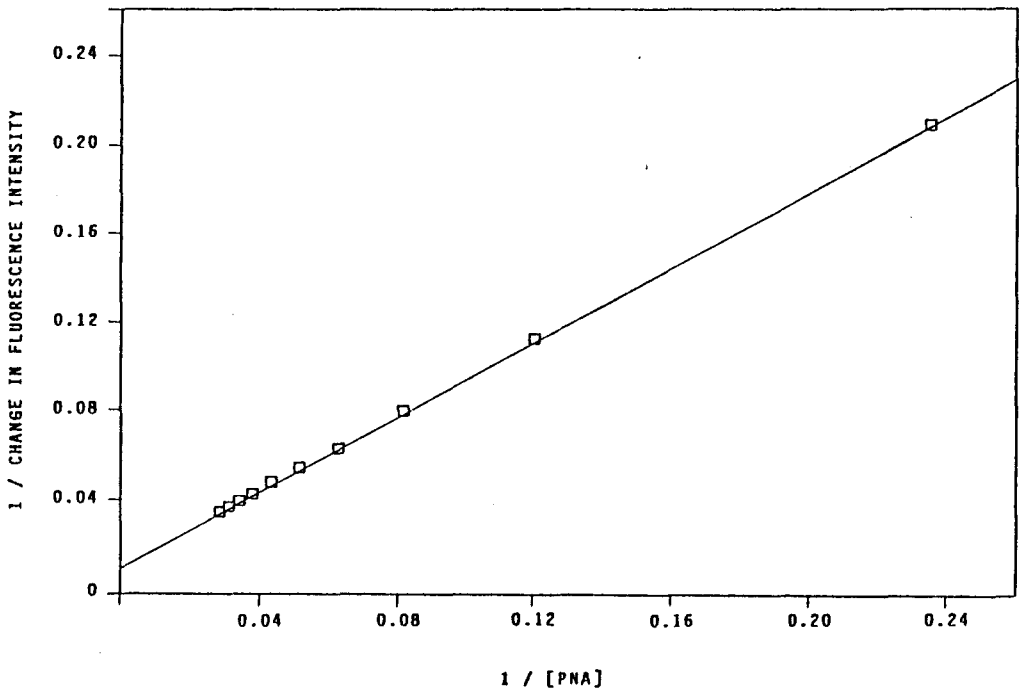

Double reciprocal plot of the fluorescence enhancement titration data shown in Figure IV.22.

Figure IV.24. Titration of DnsGalN with PNA

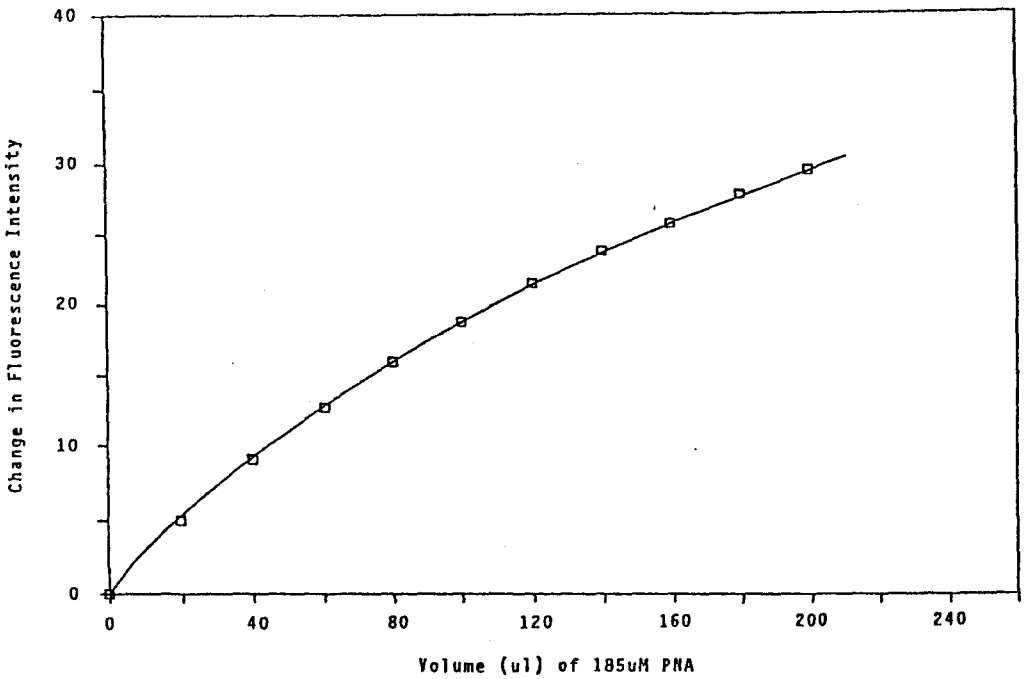

Fluorescence enhancement titrations of DnsGalN (850 μl, 5.0 μM) with PNA (20 μl additions of 185 μM PNA). Emission was recorded at 540 nm with excitation at 328 nm. Corrections were made for blank fluorescence and dilution.

Figure IV.25. Graphical Representation for the Determination of the Association Constant of DnsGalN Binding to PNA

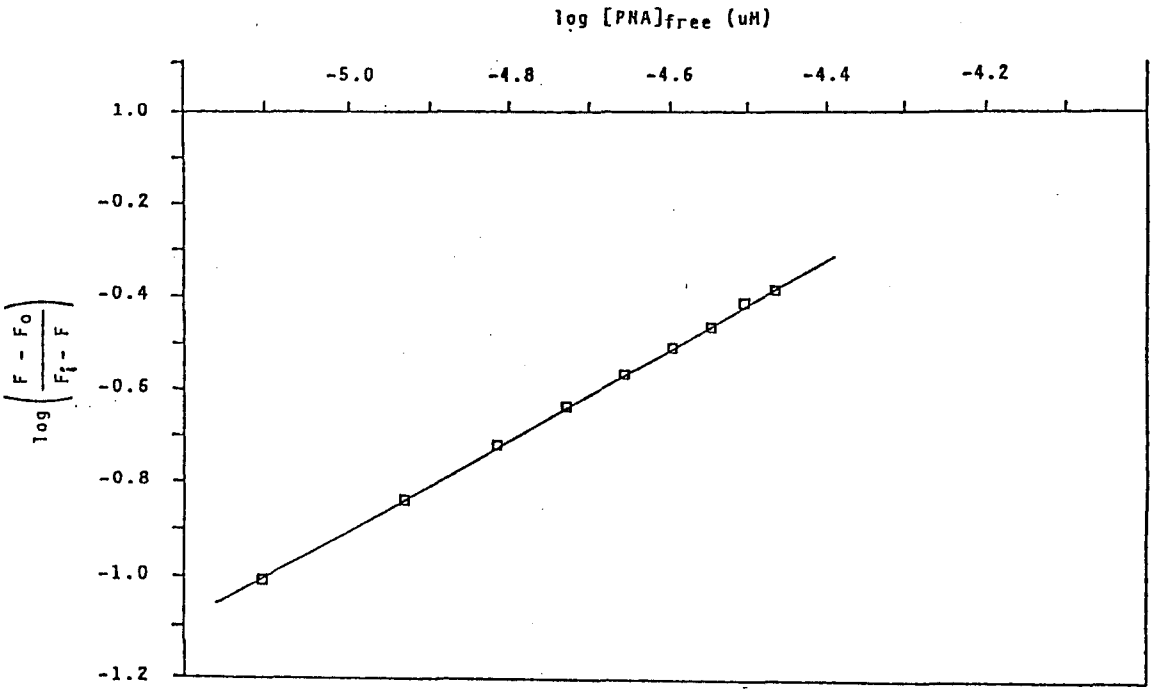

Figure IV.26. Fluorescence Emission Quenching of PNA-DnsGaln Complex by Lactose

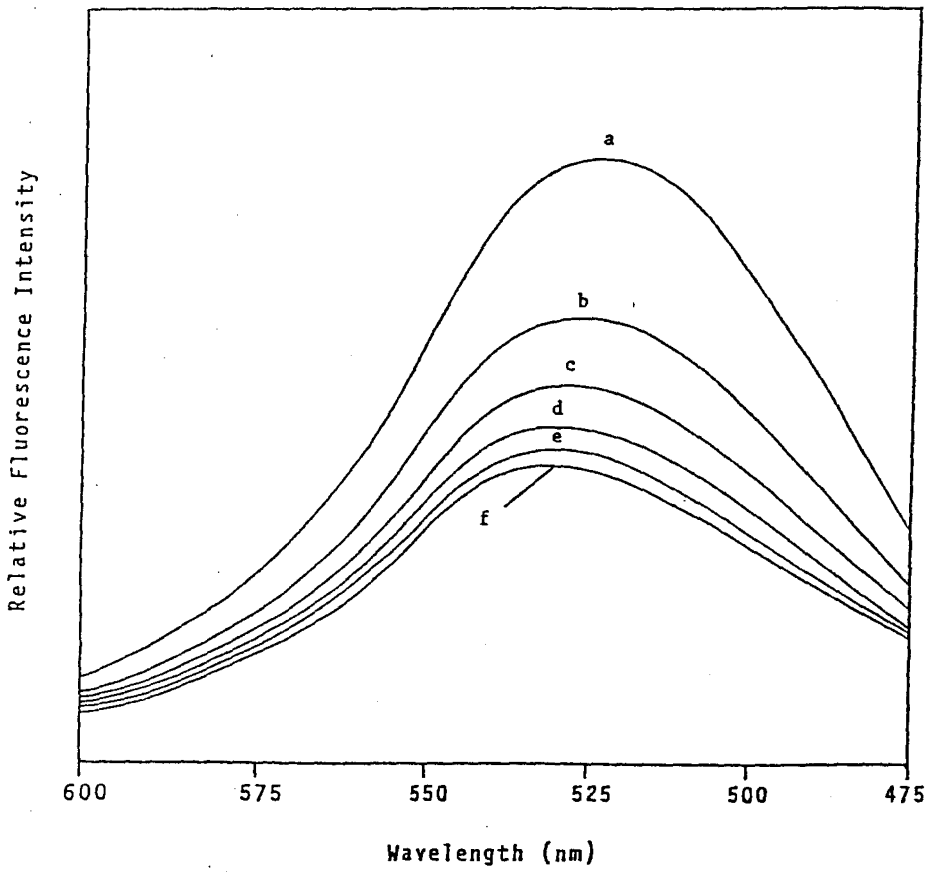

Fluorescence emission spectra for PNA-DnsGalN were determined at 22°C with excitation at 328 nm. (a) 1050 μl of 35.2 μM PNA and 4.05 μM DnsGalN, (b) - (f) 3.0 μl additions of 100 mM lactose.

Figure IV.27. Titration of PNA-DnsGalN Complex with Lactose

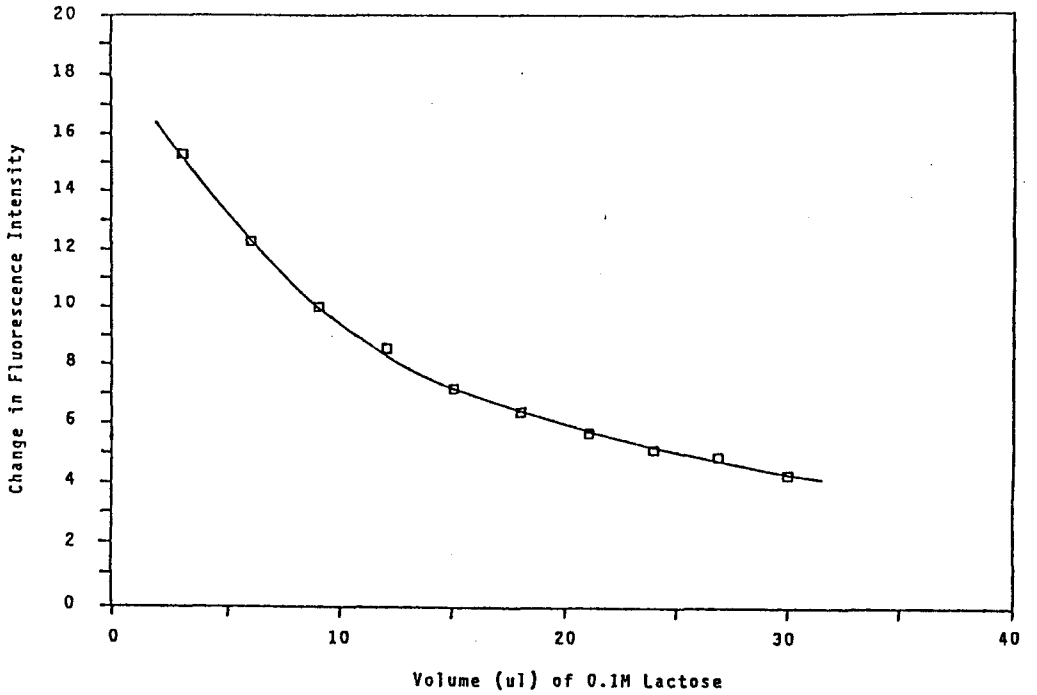

Fluorescence quenching titrations of PNA-DnsGalN complex (1050 μl containing 35.2 μM PNA and 4.05 μM DnsGalN) with lactose (3.0 μl additions of 100 mM lactose). Emission was recorded at 540 nm with excitation at 328 nm. Corrections were made for blank fluorescence and dilution.

Figure IV.28. Graphical Representation for the Determination of the Association Constant from the Competitive Binding of Lactose to PNA-DnsGalN Complex

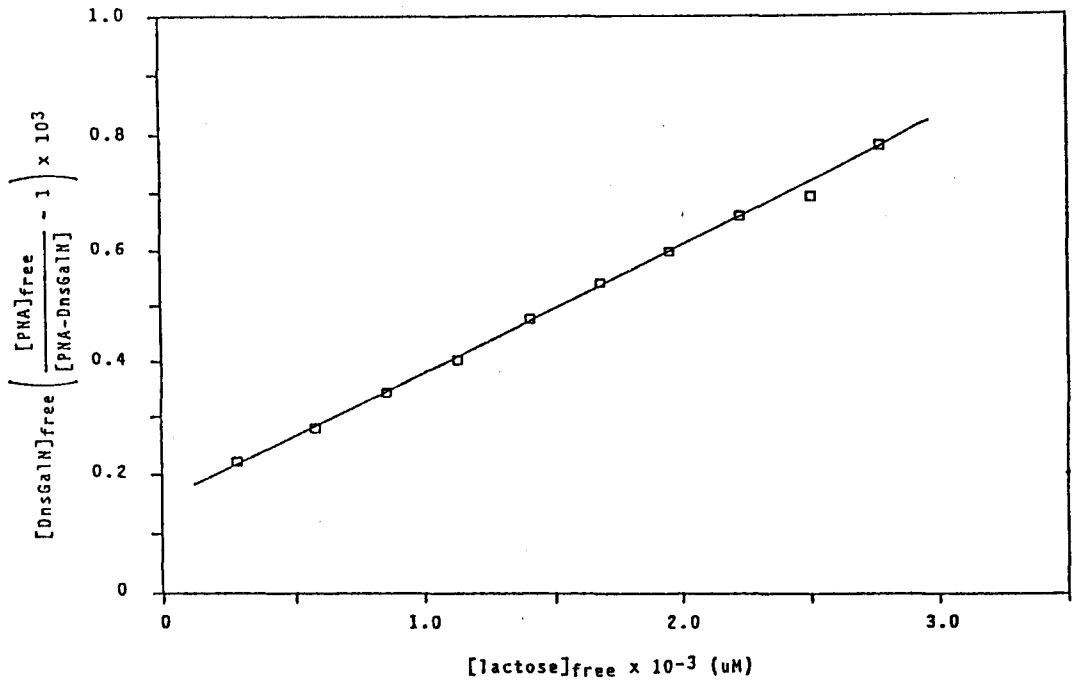

486 nm in NaCl-TRIS buffer. The fluorescence of TNS increased about 330-fold with a blue shift of 51 nm in the presence of PNA (Figure IV.29.). Treatment of data analysis for the binding of TNS to PNA was as described for the DnsGalN-PNA interaction. A double reciprocal plot of fluorescence intensity and PNA concentration was linear and gave the fluorescence intensity at a infinite protein concentration. Figure IV.30. shows a titration curve obtained from the fluorescence intensity change of TNS as a function of added protein. A graphical representation for the determination of the association constant (Ka = 9.1 ± 0.2 x 10^3 M^{-1}) of TNS binding to PNA is shown in Figure IV.31.

The binding of N^6-benzylaminopurine (BAP) to PNA was studied by following the quenching of fluorescence from PNA-TNS complex (Figure IV.32.), due to the release of TNS from BAP inhibition. Treatment of data analysis was as described for the binding of lactose to the PNA-DnsGalN complex. A titration curve obtained from the fluorescence intensity change of PNA-TNS complex as a function of added BAP is shown in Figure IV.33. A graphical representation for the determination of the association constant (Ka = 0.21 ± 0.04 x 10^3 M^{-1}) of BAP binding to PNA is shown in Figure IV.34.

Figure IV.29. Fluorescence Emission Enhancement of TNS in the Presence of PNA

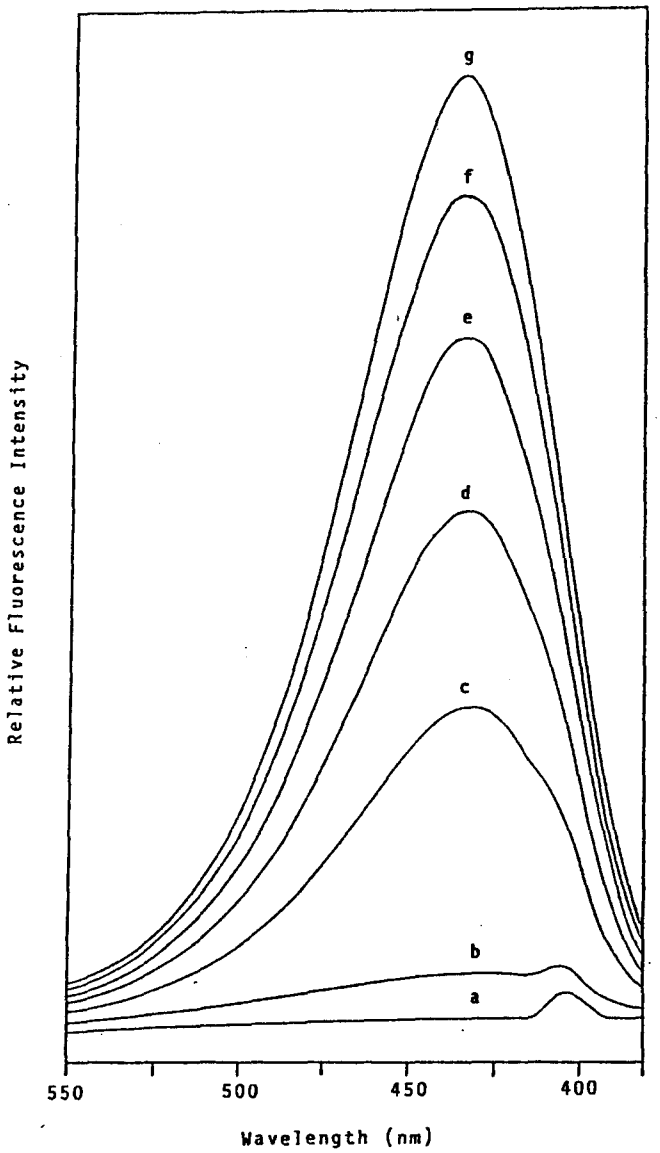

Fluorescence emission spectra for TNS were determined at 22.0°C with excitation at 350 nm. (a) buffer blank, (b) 890 μl of 11.66 μM TNS, (c) - (g) 40 μl additions of 183 μM PNA.

Figure IV.30. Titration of TNS with PNA

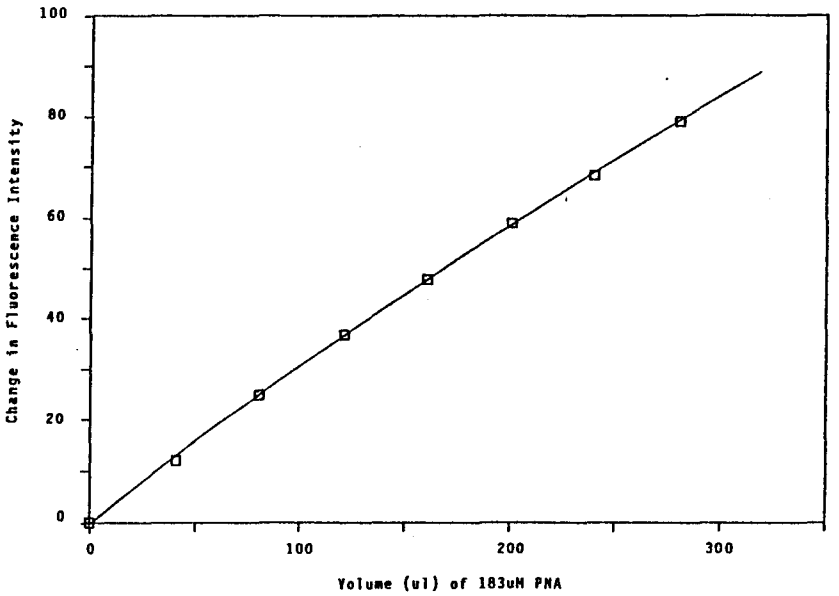

Fluorescence enhancement titrations of TNS (890 μl, 11.66 μM TNS) with PNA (40 μl additions of 183 μM PNA). Emission was recorded at 425 nm with excitation at 350 nm. Corrections were made for blank fluorescence and dilution.

Figure IV.31. Graphical Representation for the Determination of the Association Constant of TNS Binding to PNA.

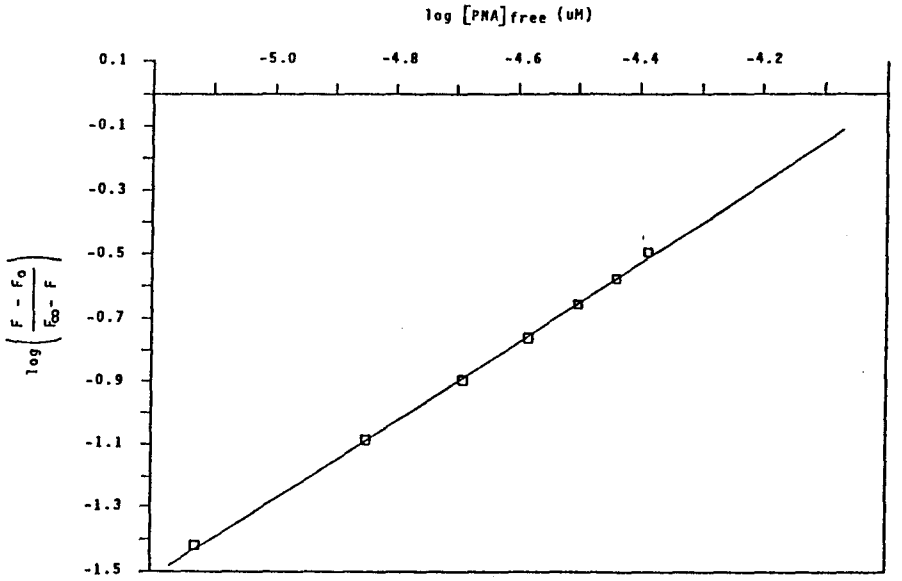

Figure IV.32. Fluorescence Emission Quenching of PNA-TNS Complex by BAP

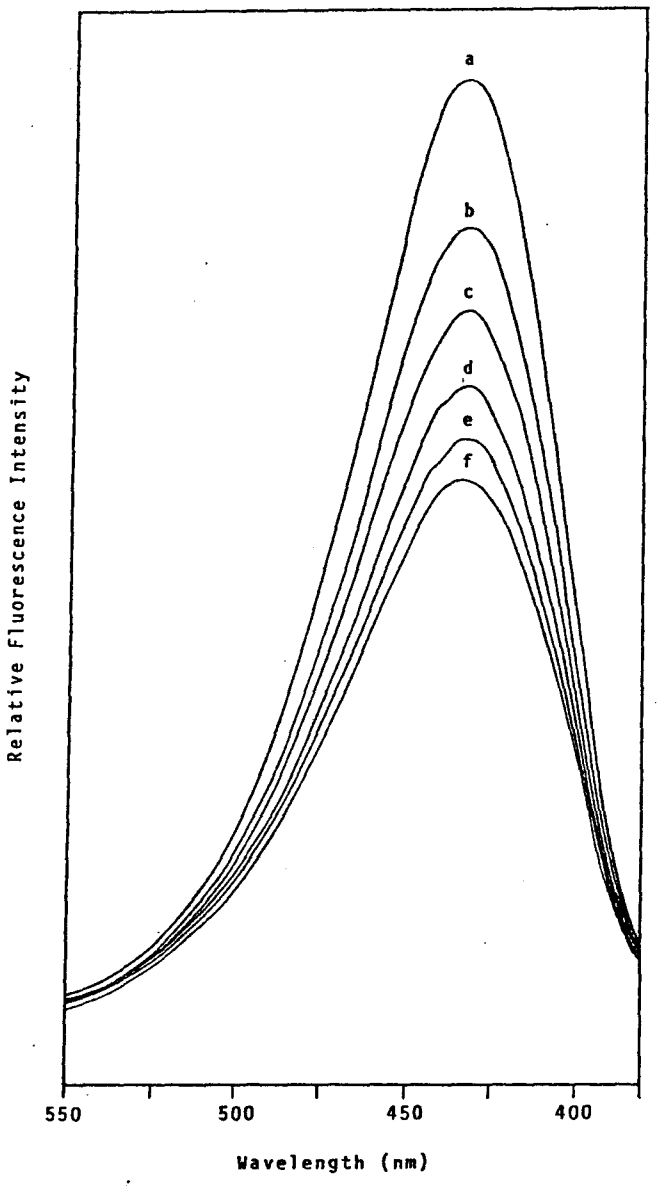

Fluorescence emission spectra for PNA-TNS were determined at 22.0°C with excitation at 350 nm. (a) 1170 μl of 43.80 μM PNA and 8.87 μM TNS, (b) - (f) 30 μl additions of 8.00 μM BAP.

Figure IV.33. Titration of PNA-TNS Complex with BAP

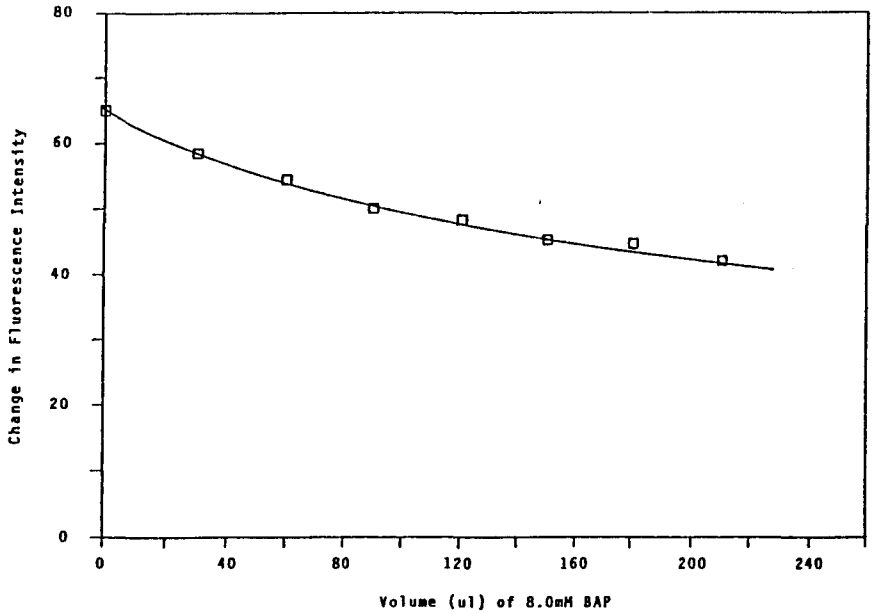

Fluorescence quenching titrations of PNA-TNS complex (1170 μl containing 43.8 μM PNA and 8.87 μM TNS) with BAP (30 μl additions of 8.0 mM BAP). Emission was recorded at 425 nm with excitation at 350 nm. Corrections were made for blank fluorescence and dilution.

Figure IV.34. Graphical Representation for Determination of the Association Constant from the Competitive Binding of BAP to PNA-TNS Complex

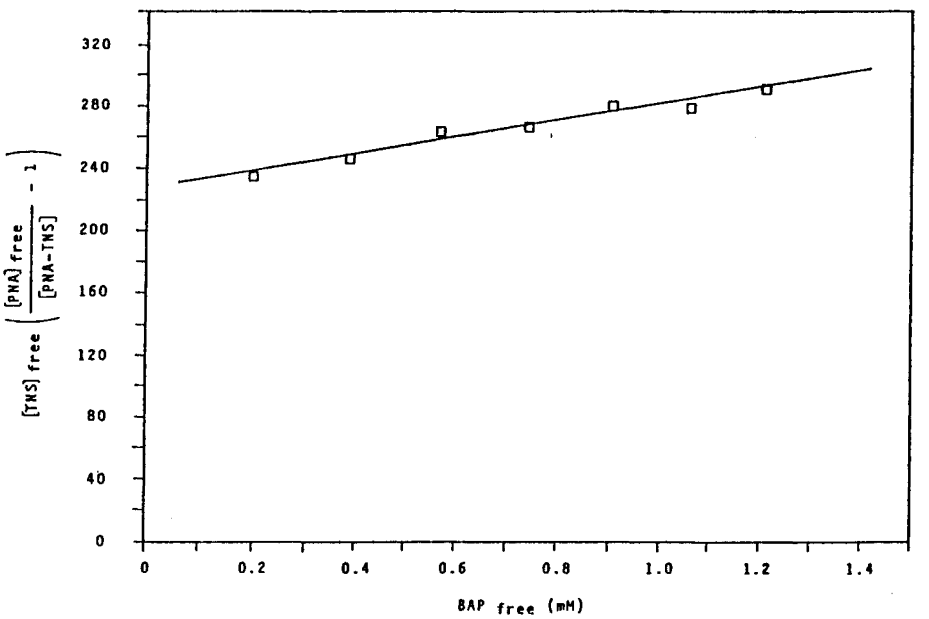

3. Binding of ANS to PNA

The emission maximum of ANS is 515 nm in water and NaCl-TRIS buffer. The fluorescence intensity of ANS increased about 300-fold with a blue shift of 45 nm in the presence of PNA. Analysis of data for the binding of ANS to PNA was as described for the PNA-DnsGalN interaction. A double reciprocal plot of fluorescence intensity and protein concentration was linear and gave the fluorescence intensity at infinite protein concentration. An association constant of Ka = 24.2 ± 1.5 x 10^3 M^{-1} was obtained for the binding of ANS to PNA. BAP did inhibit ANS binding to PNA. However, concentrations of BAP needed to obtain sufficient fluorescence quenching of the PNA-ANS complex for data analysis could not be attained because of its insolubility.

4. The Effect of BAP on DnsGalN Binding to PNA

The interaction of carbohydrate and hydrophobic binding of PNA was analyzed by titrations of DnsGalN with PNA in the presence of BAP. Because of the insolubility of BAP in water, titrations were performed in solutions made 6% in ethanol. Control experiments show no effect of 6% ethanol on DnsGalN binding to PNA in the absence of BAP. Association constants of 6.9, 9.4, 10.9, and 12.4 x 10^3 M^{-1} were obtained for the binding of DnsGalN to PNA in the presence of 0, 0.1, 0.5, and 1.0 mM BAP, respectively (see

appendix for graphical representation). This relative enhancement of DnsGalN binding to PNA in the presence of increasing amounts of BAP was duplicated in two sets of experiments. Association constants obtained in the absence of BAP were, however, less than previously determined. Protein samples used for analysis of carbohydrate-hydrophobic interactions were from a separate preparation. Variations in association constants may result from different origins of protein source.

5. Determination of Ligand Stoichiometry

The stoichiometry of ligand binding was estimated following the assay described by Wang and Edelman (143). The dissociation constant and number of binding sites of a fluorescent ligand, L, to a protein, P, with n independent sites can be determined from the following model:

$$P + L \underset{}{\overset{K}{\rightleftharpoons}} PL$$

where K is the dissociation constant for the binary complex PL. If only the PL complex possess significant fluorescence, then empirically, at a fixed total concentration of protein, Po, and an arbitrary concentration of fluorescent ligand, L,

$$\frac{I}{Imax} = \frac{\psi PF}{\psi nPo} = \frac{PF}{nPo}$$

where I is the observed fluorescence intensity after self-absorption correction, Imax is the maximum fluorescence intensity when the ligand concentration is made infinitely large, and ψ is a proportionality constant relating the fluorescence intensity to the concentration of ligand-protein complex. By applying the law of mass action and substituting PF and Po = P + PF,

$$\frac{1}{I} = \frac{1}{Imax} + \frac{K}{Imax}\,\frac{1}{F}$$

When Fo>>Po, and F≈Fo, a plot of 1/I verses 1/Fo will yield Imax and K from the intercept and slope, respectively. To determine the stoichiometry of binding, a series of titrations are performed at various concentrations of Po and constant Fo. By substituting in the expression for the mass action law,

$$\frac{Lo}{I} = \frac{1}{\psi} + \frac{K}{\psi(nPo - PF)}$$

Under the conditions that nPo>>PF,

$$\frac{Lo}{I} = \frac{1}{\psi} + \frac{K}{\psi nPo}$$

and an estimate of the number of binding sites can be obtained from a plot of Lo/I versus 1/Po. The association constants determined by this method (titrating a fixed amount of protein with ligand) were $13.6 \pm 2.4 \times 10^3$ and

29.1 ± 7.0 x 10^3 M^{-1} for TNS and ANS, respectively. These agree with the association constants of 9.1 ± 0.21 x 10^3 M^{-1} (TNS) and 24.2 ± 1.5 x 10^3 M^{-1} (ANS) previously obtained by titrating fixed amounts of ligand with protein. The stoichiometry of TNS binding to PNA was estimated to be 0.91 ± 0.14 sites/tetramer. Because experimental data of ANS ligand stoichiometry was inconsistent, the number of ANS binding sites could not be determined.

IV.D. CRYSTALLOGRAPHY OF PEANUT AGGLUTININ

Crystallization of Peanut Agglutinin-Lactose

Crystals of PNA formed in the presence of lactose varied in size from about 0.2 x 0.4 x 0.8 mm to less than 0.05 mm in the largest dimension. The large crystals formed in two to three weeks as single rectangular prisms (Figure IV.35.). Smaller crystals, which appeared in shorter periods of time (two to eight days), often formed as clusters of needles or thin flat plates. The most suitable crystals for x-ray analysis formed in solutions of PEG6000 (5.0%) after small portions of saturated ammonium sulfate was added. The salt solution may influence the crystallization process, or slow the rate of growth, or both.

Figure IV.35. Crystals of PNA Grown in the Presence of Lactose

PNA-lactose crystals shown were grown at pH=7.0 in 50% PEG6000. [PNA]=6.5 mg/ml, [lactose]=5.0 mM.

Crystallization of Peanut Agglutinin-N^6-Benzylaminopurine

Crystals of PNA formed in the presence of BAP were in the shape of rhombohedra, with an average size of about 0.4 mm in any dimension (Figure IV.36.). The molar ratio of BAP to PNA was 38:1. Because of the insolubility of BAP in aqueous buffers, the crystallization medium was made 17.8% in methanol. The presence of methanol can explain the lower concentration of PEG6000 (3.6%) needed to induce crystallization when compared to the PNA-lactose complex. Crystals of the PNA-BAP complex took six to eight weeks to develop fully.

Heavy Atom Derivatization of Peanut Agglutinin

The strategy followed for the preparation of heavy atom derivatives of PNA was similar to that used for Con A and pea lectin (134,89). For Con A, six derivatives were prepared: $Pb(NO_3)_2$, K_2PtCl_4, $Sm(NO_3)_3$, $UO_2(NO_3)_2$, sodium mersalyl, and β-(o-iodophenyl)-D-glucopyranoside. Two derivatives, $UO_2(NO_3)_2$, and p-chloromercuribenzene sulfonate (pCMB), were successfully prepared for pea lectin. Derivatization of PNA by crystal soaking required a 9.5% PEG6000 medium to prevent crystal dissolution and cracking. Both the K_2PtCl_4 and K_2PtCl_6 salts formed solutions that were colored (yellow-orange). PNA crystals soaked in these solutions acquired a more intense color than that of the mother liquor. The color became more

Figure IV.36. Crystals of PNA Grown in the Presence of N^6-Benzylaminopurine

PNA-BAP crystals shown were grown at pH=7.2 in 4.0% PEG6000. [PNA]=6.36 mg/ml, [BAP]=1.56 mM.

intense with time. It is known that platinum compounds react strongly with sulfhydryl groups (133), but also show a reactivity toward methionine and, to some extent, histidine. Although PNA is devoid of cystine, amino acid analysis yielded four methionine and four histidine residues that could react with the tetrachloroplatinate complex. Uranyl, lead, and samarium ions have been found to bind primarily to carboxylate groups and occasionally to the hydroxyl side chains of serine and threonine. Both nitrate and acetate salts of uranyl ion were used for possible heavy atom derivatives of PNA. Nitrate coordinates less strongly to the uranyl ion and its salts can give more extreme effects (133). A total of eight binding sites for uranyl nitrate were located in the pea lectin (89), and three in Con A (134). Eight binding sites were also located in Con A for samarium.

Co-crystallization of PNA in the presence of pCMB was attempted to produce a isomorphous derivative. Fluorescence binding studies show PNA to possess several classes of hydrophobic binding sites which can accommodate pCMB. Since pCMB is more soluble in high ionic strength solutions, co-crystallization media were made 6.0M in ammonium sulfate.

Diffraction Data Analysis

1. PNA-Lactose Complex

The space group of the PNA-lactose crystals, $P2_12_12$, was confirmed by observed extinctions (h00: h=2n+1, and 0k0: k=2n+1, ref.135) of data measured on the diffractometer. Cell parameters (Table IV.8.) calculated by a least squares analysis of the angular settings for 10 reflections agree with those found by Olsen, et al. (111), and Salunke, et al. (112). A total of 29,148 reflections (26,222 unique) were collected on three crystals labeled 8N, 2N, and 3N (excluding decay and alignment standards), in 2θ shells of 2.7° to 23.0°, 23.0° to 28.0°, and 28.0° to 30.5°, respectively. An initial 1000 intense reflections were collected on each crystal for the purpose of scaling data sets together. Crystal decay was corrected by assuming a linear decrease in reflection intensity with time. Intensity decay was found to be 19.8%, 15.6%, and 12.0%, for crystals 8N, 2N, and 3N, respectively. Relative absorption corrections derived from χ scans at ψ=90° were from 1.0 to 0.93 for crystal 8N, 1.0 to 0.52 for crystal 2N, and 1.0 to 0.84 for crystal 3N. Data sets were merged with their initial 1000 reflections and scaled together using the SHELX76 program for the determination of crystal structures (136). Scaling factors of 0.6442, 0.4769, and 0.7053 were obtained for crystals 8N, 2N, and 3N, respectively. An R_{int} factor (degree of agreement from merging equivalent reflections) of 0.0645 was also determined from SHELX76 for the complete PNA-lactose data

Table IV.8. Lattice Parameters of PNA-Lactose Crystals

	Crystal		
Cell Constant	8N	2N	3N
a (Å)	129.02(5)	128.83(9)	128.87(3)
b (Å)	126.04(3)	126.09(8)	125.94(9)
c (Å)	76.09(7)	76.10(3)	76.00(2)
$\alpha=\beta=\gamma$ (deg)	90.00	90.00	90.00
Volume ($Å^3 \times 10^{-3}$)	1.23(7)	1.23(6)	1.23(4)

set. The collected data set extends to 2.93 Å resolution.

The average unit cell volume is 1.23(6) x 10^6 $Å^3$, and it contains four asymmetric units per unit cell. Assuming one tetramer of PNA per asymmetric unit, the ratio of the unit cell volume to protein molecular weight (Vm) is 2.81 $Å^3$/dalton (using PNA subunit molecular weight of 27,500 daltons). This is within the range of previously observed values (1.68 to 3.53 $Å^3$/dalton) and near the average of 2.40 $Å^3$/dalton (137).

2. PNA-N^6-Benzylaminopurine Complex

Precession photography was used to determine the space group of PNA-BAP crystals. Precession photographs indicate a monoclinic cell is present. Comparison of h01, hk0, h11, and hk1 precession photographs revealed the absence of systematic extinctions. Only three monoclinic space groups, P2, P2/m, and Pm, have no conditions for systematically absent reflections. Since the mirror symmetry of P2/m and Pm requires that the contents of the unit cell contain of both enantiomorphs, they are not possible for a protein crystal. Thus the space group of the PNA-BAP crystals is uniquely defined as P2. Figures IV.37. and IV.38. shows the reciprocal lattice of the h01 and hk0 sections of PNA-BAP crystals. Cell parameters were determined from films as a=67.0(3) Å, b=35.2(8) Å, c=65.8(9) Å, and β=68.6(7)°. The calculated unit cell

Figure IV.37. X-ray Precession Photograph (μ=10°) of the h01 Reciprocal Lattice Section of PNA-BAP Complex

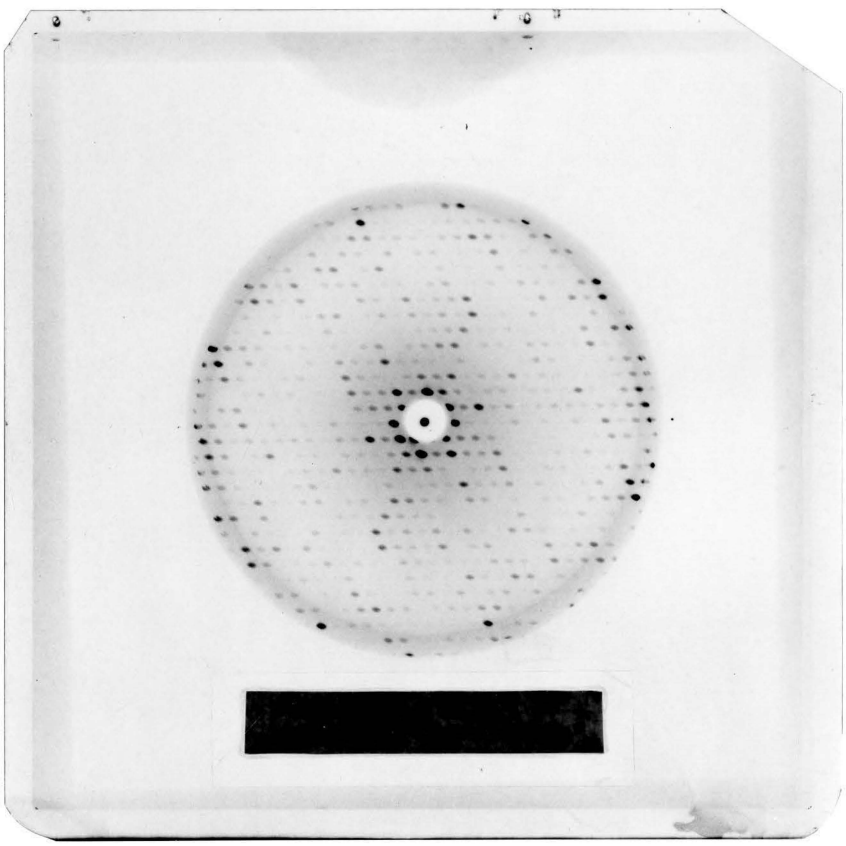

Figure IV.38. X-ray Precession Photograph (μ=10°) of the hk0 Reciprocal Lattice Section of PNA-BAP Complex

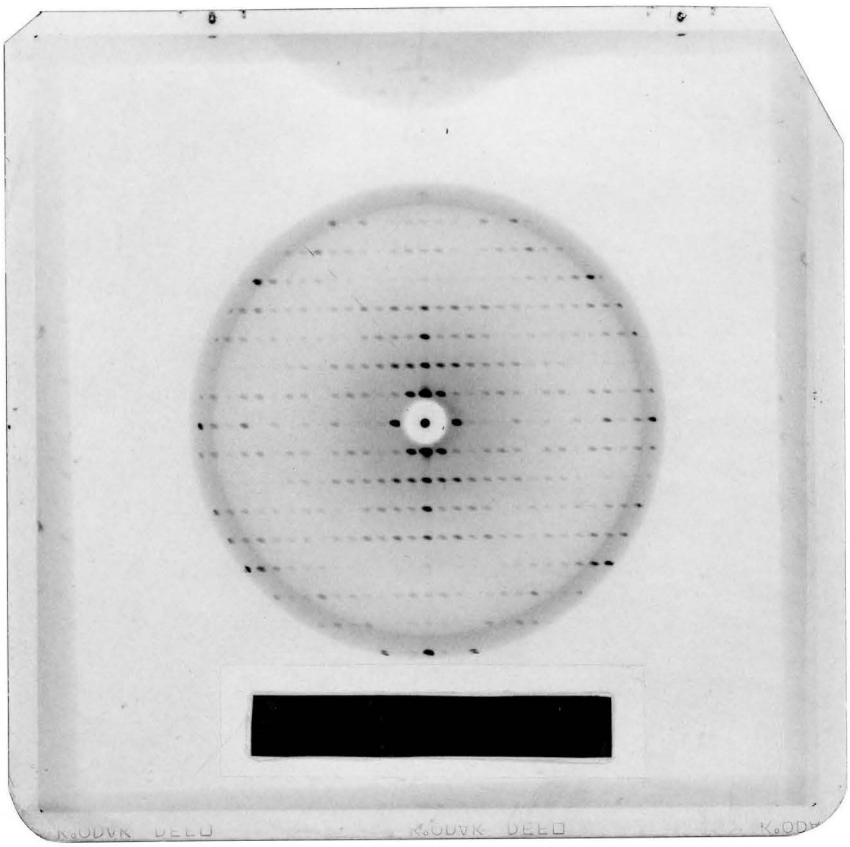

volume is 1.44(4) x 10^5 $Å^3$, and it contains 2 asymmetric units per unit cell. Assuming one monomer of PNA per asymmetric unit, the ratio of the unit cell volume to protein molecular weight is 2.62 $Å^3$/dalton (using PNA subunit molecular weight of 27,500 daltons). This demonstrates that while the PNA-lactose complex crystallizes as a tetramer in the asymmetric unit, the PNA-BAP complex crystallizes as a monomer in the asymmetric unit. By using the crystallographic two-fold axis as a molecular axis, PNA may exist as a dimer in the unit cell.

Crystals of PNA-BAP complex formed in the presence of 17.8% methanol. Crystallization mother liquors required methanol to solubilize the BAP. Gel filtration of PNA in the presence of 17.8% methanol was performed to ascertain the effects of alcohol on the quaternary structure of PNA. Dissociation of PNA into dimers was not observed (Figure IV.39.). To prevent interaction of PNA with the agarose (Sephadex G150) resin, it was necessary to perform gel filtration experiments with buffers made 200 mM in lactose. The effect of BAP on the quaternary structure of PNA could not be determined by Shepadex gel filtration. This is because the presence of 200 mM lactose in the elution buffer made the BAP insoluble. This can be a result of the lactose 'salting out' the BAP. Gel filtration of PNA in the presence of BAP was also attempted using columns of polyacrylamide. Although these columns were not found to

Figure IV.39. Gel Filtration of PNA in the Presence of 17.8% Methanol and 200 mM lactose on Sephadex G100-50

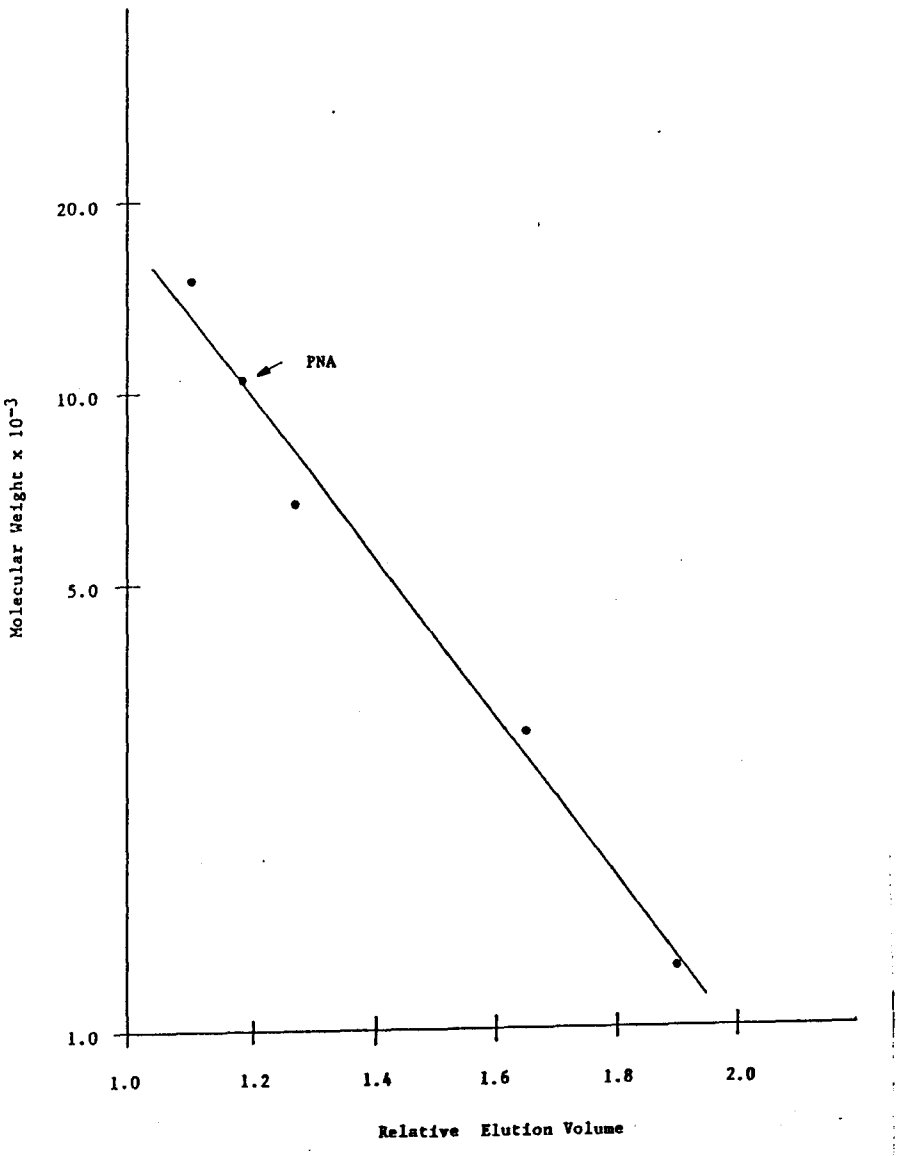

interact with PNA, the presence of methanol caused flow rates to be inconsistent. Therefore, the molecular weight of PNA could not be assessed in the presence of BAP by gel filtration.

Heavy Atom Derivative Assays

A comparison of diffraction data collected from native PNA crystals, and those exposed to heavy atom compounds, were used to determine if an isomorphous derivative of PNA had been prepared. If the heavy atom was bound specifically to the crystallized protein, then the intensities of reflections in the diffraction pattern would be altered relative to the native protein. Changes in the diffraction pattern were sought in comparative diffractometer scans of the crystallographic axes. If any differences were noted, then more data were collected on the heavy atom treated PNA crystal. Relative intensities of data collected on heavy atom treated PNA crystals were compared to the same data collected on native PNA by the program SHELX76 (136). Table IV.9. compares reflection intensities of three PNA-lactose crystals (used to collect the native data set) to PNA treated with heavy atom compounds. Only the K_2PtCl_4, $Pb(NO_3)_2$, and pCMB treated crystals show significant intensity differences. Table IV.10. compares the R factors between the 1000 reflections collected on native PNA and PNA exposed to the platinum,

lead, and mercury compounds. Data was collected on a single crystal to 2θ=21.0° for the $Pb(NO_3)_2$ treated crystals, to 2θ=12.0° for the K_2PtCl_4 treated crystals, and to 2θ=18.5° for the pCMB treated PNA. These correspond to resolutions of 4.2 Å for $Pb(NO_3)_2$-PNA, 7.4 Å for K_2PtCl_4-PNA, and 4.8 Å for pCMB-PNA data. The degree of agreement factor for other successfully derivatized proteins vary from about 0.10 to 0.30 (138). The significant differences in the diffraction intensities caused by the treatment of PNA crystals with $Pb(NO_3)_2$ makes this derivative the most promising.

Table IV.9. Axis Intensity (1) Scans of Native PNA Compared to Heavy Atom Treated PNA

2θ	8N	2N	3N	$Pb(NO_3)_2$	K_2PtCl_4	pCMB
			(100 Axis)			
2.73	8800	7000	7700	26700	6000	6800
4.04	160	120	170	160	160	170
5.39	60	60	60	260	-	60
6.85	70	60	80	210	40	60
9.63	-	-	-	60	-	-
10.98	20	20	-	120	60	40
12.39	60	50	60	80	70	60
15.04	30	-	-	60	40	30
17.89	50	30	60	100	60	60
19.24	190	120	140	500	120	120
			(001 Axis)			
2.35	11800	7500	13900	25400	10700	11000
3.52	200	110	230	750	170	180
5.87	100	50	140	300	210	160
7.00	80	50	110	400	50	80
8.18	110	60	120	180	70	130
9.31	30	-	-	50	-	-
10.49	70	40	100	100	60	80
11.69	100	80	110	100	60	120
12.83	60	40	50	120	50	40
14.00	150	80	150	140	120	130
			(010 Axis)			
2.85	2200	1500	1900	2700	2300	1800
4.26	150	100	120	130	160	180
7.07	300	220	280	210	220	260
8.46	40	-	-	30	20	30
9.89	130	100	130	220	120	130
11.25	20	-	30	-	30	30
12.71	100	60	100	90	60	100
14.09	60	30	60	60	30	50
18.34	30	40	30	50	50	40
19.80	70	40	70	90	40	80

1. Intensities shown as counts (photons) per second.

Table IV.10. Degree of Agreement Between Equivalent Reflections of PNA-Lactose (1) and Heavy Atom Treated PNA

Compared Data	R-Factor
PNA-lactose 2N vs PNA-lactose 3N	0.0751
PNA-lactose 2N vs PNA-lactose 8N	0.0678
PNA-lactose 2N vs PNA-pCMB	0.0752
PNA-Lactose 2N vs PNA-$Pb(NO_3)_2$	0.1387
PNA-Lactose 2N vs PNA-K_2PtCl_4	0.0873

1. All comparisons made with respect to PNA-lactose 2N.

V. CONCLUSIONS

Macromolecular Properties of Peanut Agglutinin

The purification of peanut agglutinin by affinity chromatography using lactosyl-Sepharose gels afforded a homogeneous protein by native and denaturing polyacrylamide gel electrophoresis. The molecular weight of PNA determined by SDS-PAGE is estimated at 30,000 ± 3000 daltons. Gel chromatography of PNA at neutral pH yields a species with a molecular weight of 102,000 ± 16,000 daltons. Other values reported for the molecular weight of PNA vary from 98,000 to 110,000 at neutral pH, and 24,500 to 27,500 in the presence of denaturants (109, 53). These data suggest that PNA exists as a tetramer of equal sized subunits at neutral pH. Amino terminal sequencing of PNA gave single amino acid residues suggesting that the four subunits comprising the lectin are identical. This makes peanut agglutinin similar to concanavalin A, soybean, kidney bean, and horse gram lectins in its native molecular weight, and its native molecular form. Amino acid analysis of PNA shows a high content of acidic and hydroxyamino acids, and a low content of methionine, tryptophan, and

histidine, and the absence of cysteine and cystine which are also characteristic of other legume lectins. No traces of covalently bound amino sugars are observed by amino acid analysis. Although many other leguminous lectins are found to be glycosylated, a few such as Con A, pea, and lentil lectin are not.

Primary Structure of Peanut Agglutinin

Two partial sequences have been reported for PNA. The first placed 161 residues (67%) by overlapping homologous segments of tryptic peptides to other leguminous lectins (40). Although the tryptic digestions were performed in the presence of denaturants, the protein was still resistant to enzymatic hydrolysis. Low solubility of peptides and microheterogeneity from isolectin interference were also cited in the failure to fully sequence the protein. The second reported partial sequence placed 197 residues (81%), also by overlapping homologous segments of peptides to other leguminous lectins (41). These peptides were generated by a preliminary formic acid hydrolysis and gel filtration separation followed by digestion with trypsin or chymotrypsin. This second partial sequence of PNA is reported to be completed (N. M. Young, private communication).

In this study, 128 residues (53%) of peptides generated by the digestion of PNA with trypsin were placed

by homology. To ensure that PNA was sufficiently hydrolyzed, long digestion times and high enzyme-to-substrate ratios were employed. Despite prolonged (15 hrs) and vigorous (3% trypsin on a weight to weight basis) treatment of PNA with the enzyme, a significant amount of protein remained undigested. This is probably a result of the stability of PNA towards denaturation. Chemical pre-denaturation of PNA was avoided to prevent deactivation of the enzyme. A thermal pre-denaturation of PNA was not attempted. This might have resulted in a more complete digestion of the protein.

Several difficulties were encountered in the sequence analysis of PNA. The high weight ratio of trypsin in the digestion mixture resulted in contamination of samples used for analysis by enzyme self digestion products. Additional interference from this self digestion was also evident from the non-specific cleavages that occurred. Products from interchain hydrolysis of trypsin are known to change the specificity of the enzyme (128).

The amino acid composition and reported sequence data of PNA shows the missing segments to be comprised of about 45 residues containing a high content of lysine, arginine, phenylalanine, and tyrosine. In consideration of both the tryptic and chymotryptic activity observed in a single enzymatic digestion of PNA, this would lead to a large number of small peptides generated from these

segments. Loss of these small fragments from co-elution with other peptides or undigested PNA can explain the failure to fully sequence the protein in all attempts. A further interference from isolectin microheterogeneity was observed in the sequence analysis undertaken in this study. Although small changes from alternate sequences would not have made placement of peptides by homology more difficult, it did complicate the separation of peptides from the digestion mixture.

Amino acid analysis of the peptides generated by digestion of PNA with cyanogen bromide agree with the total composition data and published partial sequences available for the protein. Amino acid analysis revealed 4 methionine residues per subunit of PNA. This should have yielded 5 CNBr peptides, but only 4 were isolated. Because of the good agreement between total and CNBr peptide composition, it is likely that the remaining peptide results from two closely spaced methionine residues, or a methionine residue near the carboxy terminal which eluded detection. Secondary digestions of CNBr peptides were not performed because of general insolubility. Only concentrated (88%) formic acid solubilized the CNBr peptides.

Common to both partial sequences of PNA previously reported is a missing segment estimated to be 33 residues which spans residues 173 to 205 in sainfoin lectin. Subtraction of the sequence of Young, et al. (41) from the

total amino acid composition of PNA leaves 45 residues not accounted for. This suggests that in addition to the 33 residue segment missing within the primary structure of PNA, about 12 residues of the carboxy terminal also remain unknown. Four peptides consisting of 23 amino acids were sequenced and placed by homology within the missing primary structure of PNA in this study. In addition, the composition of segments for which no sequence information is available was obtained from reported sequences, the total composition of PNA, and the CNBr peptide composition data.

Hydrophobic Binding of PNA

The binding of hydrophobic ligands to legume lectins have been described using a variety of methods. Interactions of 1,8-anilinonaphthalenesulfonic acid (ANS) and 2,6-toluidinylnaphthalenesulfonic acid (TNS) to a series of legume lectins has been studied by lectin induced alterations in the emission spectra of the fluorescent probe (93,94,96). The binding of non-fluorescent ligands such as adenine and many adenine analogs to lima bean lectin were examined using UV-difference spectroscopy and a competition assay based on the ability of a particular probe to enhance or quench the emission of a fluorescent ligand (94, 139, 140). Equilibrium dialysis was conducted using radiolabeled adenine on lima bean, soybean, Phaseolus

vulgaris, and Dolichos biflorus seed lectin. A spin labeled analogue of adenine, N^6-(2,2,6,6-tetramethyl-1-oxypiperidin-4-yl)adenine, was shown to interact strongly with lima bean, Dolichos biflorus, and Phaseolus vulgaris seed lectin by electron spin resonance spectroscopy (141). The photoaffinity probe, 8-azidoadenine, was used to label the region of adenine binding of lima bean and kidney bean lectin (97). Finally, a crystallographic study of concanavalin A complexed with β-(o-iodophenyl)-D-glucopyranoside has identified the subunit hydrophobic binding pocket (95). The residues making up the subunit binding pocket in Con A are not homologous to the photoaffinity labeled region of lima bean or kidney bean lectin (97).

The most complete studies of hydrophobic binding to legume lectins are with Con A and lima bean lectin (Table V.1.). Fluorescence spectroscopy shows that both lectins possess a single hydrophobic site (high affinity site) which binds TNS in the stoichiometry of 1 ligand per tetramer. In addition, a non-polar site (subunit site) that interacts with ANS in the stoichiometry of 1 ligand per protomer was found for lima bean lectin. Binding of TNS to Con A, lima bean, and most other legume lectins is about one order of magnitude greater than that of ANS. In lima bean lectin, the subunit site can bind both ANS and TNS with similar affinities. The high affinity site,

TABLE V.1. Properties of Interactions Between Lectins and Hydrophobic Ligands

	Con A (93,96)	Lima Bean Lectin (93)	PNA (this study)
ANS			
Ka	2.8 ± 0.4	3.9	24.2 ± 1.5
n	-	0.95/protomer	-
TNS			
Ka	19	K1= 79 ± 1.2 K2=2.2 ± 0.8	9.1 ± 0.2
n	1.0/tetramer	0.27/protomer	0.91/tetramer
BAP			
Ka	-	36	0.21 ± 0.04

notes:
1. all Ka values (association constants) in $M^{-1} \times 10^{-3}$
2. n is stoichiometry of ligand binding

however, is specific of TNS alone (94). The molecular weight and sedimentation coefficient of Con A in the presence of TNS was not significantly altered in the presence of TNS. Dimeric succinyl-Con A also binds one mole of TNS but with a 2-fold increase in the association constant (96). Addition of haptenic sugars did not inhibit binding of ANS to lima bean lectin, or TNS to Con A as measured by fluorescence titrations. TNS did not inhibit hemagglutinating activity of Con A (96), and ANS did not inhibit hemagglutinating activity of lima bean lectin (94). This suggests that the hydrophobic and carbohydrate sites are non-interacting. N^6-benzylaminopurine appears to bind competitively with TNS in the case of lima bean lectin (139). Due to heterogeneity of TNS binding, the effect of BAP on high affinity binding could not be quantified. Enhancement of ANS binding was observed in the presence of BAP, adenine, and a number of related ligands. This effect was used to screen several adenine analogs for binding to lima bean lectin. But this assay is only an indirect measure of ligand binding, and the relationship between ANS and adenine binding may not be linear. However, binding parameters assessed by radiolabeled adenine and equilibrium dialysis agree with fluorescent measurements in the analysis of lima bean lectin (139).

In this study, fluorescence spectroscopy was used to

show that PNA interacts with both ANS and TNS. Analysis of binding data obtained by equilibrium dialysis was inconsistent. Other studies have reported that TNS binds very strongly to dialysis tubing, and that this method cannot be used to assay TNS binding (147). Association constants for the binding of ANS ($24.2 \pm 1.5 \times 10^3$ M^{-1}), and TNS ($9.1 \pm 0.2 \times 10^3$ M^{-1}), to PNA were determined from fluorescence titrations according to the Hill equation. Unlike most other lectins, the binding of ANS and TNS to PNA are of the same order of magnitude. Non-linear Scatchard plots of both ANS and TNS binding to lima bean lectin indicate site heterogeneity. One explanation for the unusual stoichiometry of one binding site of TNS per tetramer of Con A is a strong negative cooperativity. This may be caused by conformational changes induced in the macromolecule by the binding of one TNS ligand at any of the four identical sites (96). In this study, Hill coefficients of 1.4 ± 0.08 and 1.21 ± 0.02 were obtained for the binding of ANS and TNS to PNA, respectively. Heterogeneous binding sites, multiple equilibria, or negative cooperativity of hydrophobic ligand binding to PNA would be approximated by Hill coefficients of less than unity. But Hill coefficients greater than unity suggest that ANS and TNS exhibit, to some extent, a positive cooperativty upon binding to PNA. Thus initial ligand binding enhances subsequent ligand binding to the

macromolecule.

Adenine, adenosine, and N^6-benzylaminopurine all showed perturbations in their UV-difference spectrum with PNA. In all cases, however, the change in absorbance was small ($\Delta A < 0.01$) and subject to instrumental and Beer's law limitations. The binding of BAP was examined in an assay based on its ability to displace a competing fluorescent probe from PNA. Titrations of a PNA-TNS or PNA-ANS mixture show a quenching of complex fluorescence. This quenching is consistent with selective inhibition of TNS and ANS binding due to competition with BAP.

Fluorescent probes like ANS and TNS generally exhibit a blue shift in emission maximum, a decrease in emission bandwidth, and a increase in emission quantum yield when transferred from a polar to non-polar medium (144). This has been used to estimate the polarity of binding sites on a number of proteins (144 - 147). Although the effect of solvent on the quantum yield of arylaminonaphthalene sulfonates is much more dramatic than shifts of the emission maximum, the variety of possible quenching mechanisms available makes changes in emission intensity less reliable. For this reason, the change in emission wavelength has been used, with excellent correlation, to estimate the polarity of macromolecule binding sites (146). The fluorescence maxima for ANS decreased by 51 nm in the presence of lima bean lectin

(94), and 45 nm in the presence of PNA (this study). The fluorescence maxima for TNS decreased by 80 nm in the presence of Con A, and 77 nm in the presence of lima bean lectin (94). In contrast, the fluorescence maxima of TNS only decreased by 51 nm in the presence of PNA. The similarity in association constants, fluorescence emission maxima shifts, and inhibition of complex formation by BAP, correlate well with the binding of TNS and ANS to the same site on PNA. Although there is very good agreement between emission maxima shifts of TNS in the presence of Con A and lima bean lectin, the finding of a smaller wavelength shift of TNS in the presence of PNA suggests a difference in its TNS binding site. This is an indication that the local environment of the TNS binding site in PNA is more polar in reference to that of Con A or lima bean lectin. As found for Con A and lima bean lectin, the stoichiometry of TNS binding to PNA is estimated at 0.91 ± 0.14 sites/tetramer.

In order to examine the relationship between hydrophobic and carbohydrate binding of PNA, the fluorescently labeled sugar N-dansylgalactosamine (DnsGalN) was prepared. Hill plots from fluorescence titration experiments yielded an association constant of 10.6 ± 1.2 x 10^3 M^{-1} for the binding of DnsGalN to PNA. A Hill coefficient of 0.99 ± 0.03 suggest the probe binds to a single, non-interacting site. Control experiments using

dansyl amide in place of DnsGalN show no fluorescence enhancement which indicates the labeled probe interacts through the galactose, rather than the dansyl moiety. Titrations of DnsGalN with PNA performed at several fixed concentrations of lactose show a competitive binding of DnsGalN and lactose. A competition assay based on the fluorescence quenching of PNA-DnsGalN complex by lactose yielded an association constant of $1.5 \pm 0.3 \times 10^3$ M^{-1}. This agrees well with the values of 1.3×10^3 M^{-1} (25°C) and 0.92×10^3 M^{-1} (20°C) obtained by others using UV-difference spectroscopy (68, 142).

The enhanced association of DnsGalN over lactose for PNA suggest a non-polar binding site adjacent to the carbohydrate binding site as proposed for Con A and soybean agglutinin (24,25). Previous studies excluded this type of non-polar interaction since aromatic aglycons of galactose did not inhibit the hemagglutination activity of PNA over methyl galactosides (53). But hemagglutination experiments are much less sensitive than spectroscopic methods of analysis. Perturbations in the UV spectrum of PNA by lactose have been attributed to macromolecular conformational changes that affect tyrosine residues at or near the sugar binding site (107). Greater affinities would be expected from pi-pi interactions that can occur between DnsGalN and tyrosine residues of the sugar binding site of PNA.

The effect of BAP on the interaction of DnsGalN and PNA is to enhance binding. Association constants of 6.9, 9.4, 10.9, and 12.4 x 10^3 M^{-1} were obtained for the binding of DnsGalN in the presence of 0, 0.1, 0.5, and 1.0 mM BAP, respectively. Control experiments showed BAP does not influence the fluorescence of DnsGalN at concentrations used for analysis. Insolubility of BAP in aqueous solutions prevented further inhibition studies. Association constants obtained in the absence of BAP were less than previously determined. Protein samples used for carbohydrate-hydrophobic interactions were, however, from a separate preparation. Variations in association constants may result from different origins of protein samples.

The physiological functions of both the carbohydrate and hydrophobic binding exhibited by lectins remains unknown. Binding of N-arylaminonaphthalenesulfonates have been found to occur at the hydrophobic active site of many proteins (145,147). However, ANS and TNS are not naturally occurring ligands, and in some cases, do not interact with the known functional sites in proteins. The finding that legume lectins can bind ligands such as adenine derivatives (cytokinins) at a hydrophobic site may be of some physiological importance, since these compounds are present in plants and are known to serve an important role as phytohormones.

Investigation into the effect of hydrophobic binding

on carbohydrate binding was initiated to explore the possibility of hormonal regulation of lectin-carbohydrate interactions. Although an effect of sugar binding was observed in the presence of varying amounts of BAP, the interaction was small with respect to the molar ratios of hydrophobic ligand and protein that were used (PNA concentrations between 0 and 40 μM, BAP concentrations between 0 and 1000 μM). With lectins constituting a major portion of the protein in many plants, especially the legumes, hormonal control of sugar binding would be expected at much lower concentrations of cytokinin. But interactions of carbohydrate binding may be more pronounced with different cytokinin.

Crystallography of Peanut Agglutinin

Data collected on native crystals of PNA grown in the presence of lactose extends to at least 2.93 Å. The degree of agreement obtained from merging symmetry equivalent reflections (R_{int}) from the three crystals used to collect the data set is 0.0645. This can be used as a measure of the quality of the data. In comparison, values reported for R_{int} from other macromolecules are of the order of 5% (148). The average R_{int} for the native data set of Con A was 0.078 (134).

Experiments were performed to prepare heavy atom derivatives of PNA in order to obtain a crystal structure

phasing model using the method of isomorphous replacement. Diffraction data of crystals soaked in $Pb(NO_3)_2$ solutions gave a symmetry R factor of 0.14 in comparison to the native PNA data set suggesting that this heavy atom was incorporated into PNA isomorphously. Low resolution data of crystals soaked in K_2PtCl_4, and crystals grown in the presence of pCMB also show indications of isomorphous binding which extends the possibility of using isomorphous replacement in the solution of the PNA three dimensional structure. The success in the solution of other lectin structures such as favin by obtaining a phasing model using the method of molecular replacement is another possibility in completing the PNA structure. Progress is underway in the analysis of diffraction data to obtain a phasing model for PNA.

Preliminary crystallographic results of PNA grown in the presence of BAP show profound changes in unit cell parameters. A space group change from orthorhombic ($P2_12_12$) to monoclinic (P2) is observed in addition to a substantial decrease in unit cell volume. Analysis of unit cell volume to protein molecular weight ratios show that crystals of PNA formed in the absence of BAP, and in the presence of lactose, crystallize as tetramers in the unit cell. However, PNA crystals formed in the presence of BAP crystallize as dimers.

Fluorescence enhancement titrations of Con A, lima

bean lectin, and PNA with TNS suggest an unusual stoichiometry of one binding site per tetramer. It has been suggested that the TNS binding site of Con A may be at or near the unique point of 222 symmetry in the center of the tetramer. Crystallographic studies show that there is a fairly hydrophobic cavity in this subunit contact region. Molecular modeling shows that it is accessible to solvent and large enough to accommodate only 1 TNS molecule (96). A tetramer composed of 4 identical subunits would be expected to possess an equal number of potential active sites. If these sites are situated in a cavity restricted in size, there would be a limitation to the number of sites available. Since BAP lacks any symmetry, the 2-fold axis observed in the diffraction pattern of PNA-BAP complex crystals implies one binding site per protomer. However, previous fluorescence experiments suggest that BAP and TNS bind competitively, and that there is a single TNS binding site per tetramer of PNA. One explanation for these results is that upon binding BAP, PNA dissociates into dimers which exposes additional hydrophobic sites that are not readily accessible in the native tetrameric form of PNA. Gel filtration experiments were performed as another means to ascertain whether PNA dissociates from the tetrameric native state to dimers upon binding BAP. Sephadex gel filtration columns are found to interact with PNA and gave consistent molecular weights when the elution

buffer, made similar to that used for the crystallization of PNA-BAP complex, contained 200 mM lactose. Since BAP is not soluble in this elution buffer, the effect of BAP on the quaternary structure could not be confirmed by gel filtration. These results did show, however, that PNA does not dissociate in a 17.8% methanol medium needed to solubilize BAP. Attempts were also made at determining the molecular weight of PNA in the presence and absence of BAP using gel filtration columns of polyacrylamide. But these columns were not stable in the 17.8% methanol elution buffer.

Although lectins have been known to exist for over 100 years, their biological functions remain unknown. Most of the proposed functions are related to their carbohydrate binding activity. The recent finding that legume lectins can also bind a variety of hydrophobic ligands, especially adenine derivatives, will undoubtedly have many physiological implications. But many questions about the number, location, and site restrictions of the hydrophobic binding regions remain to be answered. A crystallographic study of the cytokinin binding region offers the best means of providing for these answers.

REFERENCES

1. Stillmark, H. (1888). Thesis, University of Dorpat, Dorpat (Tartu).

2. Kocourek, J. (1986). In "The Lectins, Properties, Functions, and Applications in Biology and Medicine" (I. E. Liener, N. Sharon, and I. J. Goldstein, eds.), pp 11-18. Academic Press, Inc:, Orlando.

3. Sumner, J. B., and Howell, S. F. (1936). J. Bacteriol. 32, 227-237.

4. Watkins, W. M., and Morgan, W. T. J. (1952). Nature(London) 196, 825-826.

5. Boyd, W. C., and Shapleigh, E. (1954). Science 119, 419.

6. Goldstein, I. J., Hughes, R. C., Monsigny, M., Osawa, T., and Sharon, N. (1980). Nature 285, 66.

7. Dixon, H. B. F. (1981). Nature 292, 192.

8. Etzler, M. E. (1986). Ref. 2, pp 371-392.

9. Talbot, C. F., and Etzler, M. E. (1978). Biochemistry 17, 1474-1479.

10. Pueppke, S. G. (1979). Plant Physiol. 64, 575-580.

11. Barondes, S. H. (1986). Ref. 2, pp 438-462.

12. Sharon, N. (1986). Ref. 2, pp 494-522.

13. Wright, C. S., Gavilanes, F., and Peterson, D. L. (1984). Biochemistry 23, 280-287.

14. Marchalonis, J. J., and Edelman, G. M. (1968). J. Mol. Biol. 32, 453-465.

15. Sakakibara, M., Noguchi, H., and Makino, S. (1979). Agric. Biol. Chem. 43, 1647-1658.

16. Hammarstrom, S., and Kabat, E. A. (1971). Biochemistry 10, 1684-1692.

17. Goldstein, I. J., and Poretz, R. D. (1970). Biochemistry 9(14), 2890-2896.

18. Lis, H., Sela, B., Sachs, L., and Sharon, N. (1970). Biochim. Biophys. Acta 211, 582-585.

19. Hassing, G. S. Goldstein, I. J., and Marini, M. (1971). Biochim. Biophys. Acta 243, 90-97.

20. Hardman, K. D., and Ainsworth, C. F. (1976). Biochemistry, 15, 1120-1128.

21. Reeke, G. N. Jr., and Becker, J. W. (1986). Science 234, 1108-1111.

22. Kronis, K. A., and Carver, J. P. (1985). Biochemistry 24, 834-840.

23. Baker, D. A., Sugii, S., Kabat, E. A., Ratcliffe, R. M., Hermentin, P., and Lemieux, R. U. (1983). Biochemistry 22, 2741-2750.

24. Poretz, R. D., and Goldstein, I. J., (1971). Biochem. Pharmacol. 20, 2727-2739.

25. Pereira, M. E. A., Kabat, E., and Sharon, N. (1971). Carbohydr. Res. 37, 89-102.

26. Etzler, M. E. (1983). In "Chemical Taxonomy, Molecular Biology, and Functions of Plant Lectins" (I. J. Goldstein, and M. E. Etzler, eds.), pp 1-5. Alan R. Liss, Inc. New York.

27. Barondes, S. H. (1981). Ann. Rev. Biochem. 50, 207-231.

28. Barondes, S. H. (1980). In "Cell Adhesion and Motility" (A. S. G. Curtis and J. Pitts, eds.), pp 309-328. Cambridge University Press, Cambridge.

29. Sharon, N. (1986). Ref. 2. pp 494-522.

30. Lis, H., and Sharon, N. (1986). Ref. 2. pp 354

31. Bird, G. W. G. (1951). Curr. Sci. 20, 298-299.

32. Burger, M. M. (1969). Proc. Nat. Acad. Sci. USA 62, 994.

33. Inbar, M., and Sachs, L. (1969). Nature 223, 710.

34. Sela, B. A., Lis, H., Sharon, N., and Sachs, L. (1970). J. Membrane Biol. 3, 267.

35. Sharon, N. (1977). Sci. Am. 236, 108-119.

36. Lis, H., and Sharon, N. (1977). In "The Antigens" (M. Sela, ed.), pp 429-529. Academic Press, New York.

37. Strosberg, A. D., Buffard, D., Lauwereys, M., and Foriers, A. (1986). Ref. 2. pp 249-263.

38. Edelman, G. M., Cunningham, B. A., Reeke, G. N. Jr., Becker, J. W., Waxdal, M. J., and Wang, J. L. (1972). Proc. Nat. Acad. Sci. USA 69(9), 2580-2584.

39. Hapner, K. D., Kouchalakos, R. N., and Bradshaw, R. A. (1983). Ref. 26. pp 255-258.

40. Lauwereys, M., Foriers, A., Sharon, N., and Strosberg, A. D. (1985). FEBS Lett. 181(2), 241-244.

41. Young, N. M., Johnston, R. A. Z., Watson, D. C. (1988). In "Lectins-Biology, Biochemistry, Clinical Biochemistry" (T. C. Bog-Hansen and D. L. J. Freed, eds.), vol. 6, pp 349-353. Sigma Chemical Company, St. Louis, MI., USA.

42. Vodkin, L. O., Rhodes, P. R., and Goldberg, R. B. (1983). Cell, 34, 1023-1031.

43. Hoffman, L. M., and Donaldson, D. D. (1985). EMBO Journal 4(4), 883-889.

44. Schnell, D. J., and Etzler, M. E. (1987). J. Biol. Chem. 262(15), 7220-7225.

45. Foriers, A., Lebrun, E., Van Rappenbusch, R., DeNeve, R., and Strosberg, A. D. (1981). J. Biol. Chem. 256, 5550-5560.

46. Hopp. T. P., Hemperly, J. J., and Cunningham, B. A. (1982). J. Biol. Chem. 257(8), 4473-4483.

47. Higgins, T. J. V., Chandler, P. M., Zurawski, G., Button, S. C., and Spencer, D. (1983). J. Biol. Chem. 258, 9544-9549.

48. Olsen, K. W. (1983). Biochim. Biophys. Acta 743, 212-218.

49. Hemperly, J. J., and Cunningham, B. A. (1983). Trends Biochem. Sci. 8, 100-102.

50. McKenzie, G. H., Sawyer, W. H., and Nichol, L. W. (1972). Biochim. Biophys. Acta 263, 283-293.

51. Wang, J. L., Cunningham, B. A., and Edelman, G. M. (1971). Proc. Nat. Acad. Sci. USA 68, 1130-1134.

52. Lönnerdal, B. Borrebaek, C. A. K., Etzlet, M. E., and Ersson, B. (1983). Biochem. Biophys. Res. Commun. 115(3), 1069-1074.

53. Lotan, R., Skutelsky, E., Dannon, D., and Sharon, N. (1975). J. Biol. Chem. 250, 8518-8523.

54. Young, N. M., Williams, R. E., Roy, C., and Yaguchi, M. (1982). Can. J. BIochem. 60, 933-941.

55. Kouchalakos, R. N., Bates, O. J., Bradshaw, R. A., and Hapner, K. D. (1984). Biochemistry 23, 1824-1830.

56. Lotan, R., Siegelman, H. W., Lis, H., and Sharon, N. (1974). J. Biol. Chem. 249, 1219-1224.

57. Jaffe, C. L., Ehrlich-Rogoziñski, S., Lis, H., and Sharon, N. (1977). FEBS Lett. 82, 191-196.

58. Weber, T. H., Aro, H., and Nordman, C. T. (1972). Biochim. Biophys. Acta 263, 94-105.

59. Räsänen, V., Weber, T. H., and Grasbeck, R. (1973). Eur. J. Biochem. 38, 193-200.

60. Carter, W. G., and Etzler, M. E. (1975). J. Biol. Chem. 250, 2256-2762.

61. Kocourek, J., Jamieson, G. A., Votruba, T., and Horejsi, V. (1977). Biochim. Biophys. Acta 500, 344-360.

62. Trowbridge, I. S. (1974). J. Biol. Chem. 249, 6004-6012.

63. Higgens, T. J. V., Chandler, P. M., Zurawski, G., Button, S. C., and Spencer, D. (1983). J. Biol. Chem. 258, 9544-9549.

64. Hemperly, J. J., Hopp, T. P., Becker, J. W., and Cunningham, B. A. (1979). J. Biol. Chem. 254, 6803-6810.

65. Goldstein, I. J., and Poretz, R. D. (1986). Ref. 2. pp 33-34.

66. Yariv, J., Kallb, A. J., and Leuitski, A. (1968). Biochim. Biophys. Acta 165, 303.

67. Strosberg, A. D., Buffard, D., Lauwereys, M., Foriers, A. (1986). Ref. 2. pp 261.

68. Neurohr, K. J., Young, N. M., and Mantsch, H. H. (1980). J. Biol. Chem. 255, 9205-9209.

69. Miller, R. L. (1983). Anal. Biochem. 131, 438-446.

70. Namen, A. E., and Hapner, K. D. (1979). Biochim. Biophys. Acta 580, 198.

71. DeBoeck, H., Lis, H., van Tilbeurgh, H., Sharon, N., and Loontiens, F. G. (1984). J. Biol. Chem. 259, 7067-7074.

72. Catsimpoolas, N., and Meyer, E. W. (1969). Arch. Biochem. Biophys. 132, 279-288.

73. Lis, H., and Sharon, N. (1978). J. Biol. Chem. 253, 3468-3476.

74. Miller, J. B., Noyes, C., Heinrikson, R., Kingdon, H. S., and Yachnin, S. (1973). J. Exp. Med. 138, 939-951.

75. Miller, J. B., Hsu, R., Heinrikson, R., and Yachnin, S. (1975). Proc. Nat. Acad. Sci. USA 72, 1388-1391.

76. Etzler, M. E., Gupta, S., and Borrebaeck, C. (1981). J. Biol. Chem. 256, 2367-2370.

77. Etzler, M. E., and Kabat, E. A. (1970). Biochemistry 9, 869-877.

78. Stein, M. D., Howard, I. K., and Sage, H. J. (1971). Arch. Biochem. Biophys. 146, 353-355.

79. Howard, I. K., Sage, H. J., Stein, M. D., Young, N. M., Leon, M. A., and Dyckes, D. F. (1971). J. Biol. Chem. 246, 1590-1595.

80. Matsumoto, I., Uehara, Y., Jimbo, A., and Seno, N. (1983). J. Biochem. (Tokyo) 93, 763-769.

81. Baumann, C., Rudiger, H., and Strosberg, A. D. (1979). FEBS Lett. 102, 216-218.

82. Rigas, D. A., and Head, C. (1969). Biochem. Biophys. Res. Commun. 34, 633-639.

83. Rini, J. M., Hofmann, T., Carver, J. P. (1987). Biochem. Cell Biol. 65, 338-344.

84. Schnell, D. J., and Etzler, M. E. (1987). J. Biol. Chem. 262(15), 7220-7225.

85. Bowles, D. J., and Pappin, D. J. (1988). TIBS 13, 60-64.

86. Bhattacharyya, L., Brewer, F. C., Brown, R. D., and Koenig, S. H. (1985). Biochemistry 24, 4974-4980.

87. Brewer, F. C., Brown, R. D., Koenig, S. H. (1983). J. Biomol. Struct. Dyn. 1, 961-997.

88. Reeke, G. N., Jr., Becker, J. W., Edelman, G. M. (1975). J. Biol. Chem. 250(4), 1525-1547.

89. Einsphar, H., Parks, E. H., Suguna, K., Subramanian, E., and Suddath, F. L. (1986). J. Biol. Chem. 261(35), 16518-16527.

90. Reeke, G. N., Jr., and Becker, J. W. (1986). Science 234, 1108-1111.

91. Bessler, W., Shafer, J. A., and Goldstein, I. J. (1974). J. Biol. Chem. 249, 2819-2822.

92. Carver, J. P., Mackenzie, and Hardman, K. D. (1985). Biopolymers 24, 49-63.

93. Roberts, D. D., and Goldstein, I. J. (1983). Arch. Biochem. Biophys. 224, 479-484.

94. Roberts, D. D., and Goldstein, I. J. (1982). J. Biol. Chem. 257(19), 11274-11277.

95. Edelman, G. M., and Wang, J. L. (1978). J. Biol. Chem. 253(9), 3016-3022.

96. Yang, D. C. H., Gall, W. E., and Edelman, G. M. (1974). J. Biol. Chem. 249(21), 7018-7023.

97. Maliarik, M. J., and Goldstein, I. J., (1988). J. Biol. Chem. 263(23), 11274-11279.

98. Sharon, N., and Lis, H. (1979). Biochem. Soc. Trans. 7, 783-799.

99. Marshall, R. D. (1972). Annu. Rev. Biochem. 41, 673-702.

100. Becker, J. W., Cunningham, B. A., and Hemperly, J. J. (1983). Ref. 26. pp 31-45.

101. Hardman, K. D., Agarwal, R. C., and Freiser, M. J. (1982). J. Mol. Biol. 157, 69-86.

102. Olsen, K. W. (1983). BIochim. Biophys. Acta 743, 212-218.

103. Bird, G. W. G. (1964). Vox Sang. 9, 748-749.

104. Pueppke, S. G. (1981). Arch. Biochem. Biophys. 212(1), 254-261.

105. Pereira, M. E. A., Kabat, E. A., Lotan, R., and Sharon, N. (1976). Carbohy. Res. 51, 107-118.

106. So, L. L., and Goldstein, I. J. (1968). J. Biol. Chem. 243, 2003-2007.

107. Neurohr, K. J., Young, N. M., and Mantsch, H. H. (1980). J. Biol. Chem. 255(19), 9205-9209.

108. Neurohr, K. J., Bundle, D. R., Young, N. M., and Mantsch, H. H. (1982). Eur. J. Biochem. 123, 305-310.

109. Fish, W. W., Hamlin, L. M., and Miller, R. L. (1978). Arch. Biochem. Biophys. 190(2), 693-698.

110. Decastel, M., DeBoeck, H., Goussault, Y., DeBruyne, C. K., Loontiens, F. G., and Frenoy, J-P. (1985). Arch. Biochem. Biophys. 240(2), 811-819.

111. Olsen, K. W., and Miller, R. L. (1982). FEBS Lett. 145(2), 303-307.

112. Salunke, D. M., Khan, M. I., Surolia, A., and Vijayan, M. (1982). J. Mol. Biol. 154, 177-178.

113. Salunke, D. M., Khan, M. I., Surolia, A., and Vijayan, M. (1983). FEBS Lett. 156(1), 127-129.

114. Salunke, D. M., Swamy, M. J., Khan, M. I., Mande, S. C., Surolia, A., and Vijayan, M. (1985). J. Biol. Chem. 260(5), 13576-13579.

115. Bhagwat, A. A., and Thomas, J. (1980). J. Gen. Microbiol. 117, 119-125.

116. Sundberg, L., and Porath, J. (1974). J. Chrom. 90, 87-98.

117. Hames, B. D. (1981). In "Gel Electrophoresis of Proteins" (B. D. Hames and D. Rickwood, eds.), Ch. 1., pp 23-40. IRL Press, Oxford.

118. Darbre, Andre (1986). In "Practical Protein Chemistry-A Handbook" (A. Darbre, ed.), Ch. 8.6.1. John Wiley & Sons Ltd., New York.

119. Darbre, Andre (1986). Ref. 118. Ch. 8.9.1.

120. Spande, T. F. and Witkop, B. (1967). In "Methods in Enzymology" (C. H. W. Hirs, ed.), Vol. XI, Ch 58, Academic Press, New York.

121. Fonta, A., and Gross, E. (1986). Ref. 120. Ch. 2.4.1.

122. Wilkinson J. M. (1986). Ref. 120. Ch. 3.5.1.

123. Tarr, G. E. (1977). In "Methods in Enzymology" (C. H. W. Hirs and S. N. Timasheff, eds.), Vol. XLVII, Part E, Ch. 34, Academic Press, New York.

124. Tarr, G. E. (1975). Anal. Biochem. 63, 361-370.

125. Lartey, P. A. and Derechin, M. (1979). Prep. Biochem. 9(1), 85-95.

126. DeBoeck, H., Loontiens, F. G., Lis, H., and Sharon, N. (1984). Arch. Biochem. Biophys. 254, 297-304.

127. Kasper, C. B. (1970). In "Protein Sequence Determination" (S. B. Needleman, ed.), Ch.6.III., Springer-Verlag, New York.

128. Keil-Dlouha, V., Zylber, N., Imhoff, J. M., Tong, N. T., and Keil, B. (1971). FEBS Lett. 16(4), 291-295.

129. Turner, O. C., and Brand, L. (1968). Biochemistry 7, 3381-3390.

130. Brand, L., and Gohlke, J. R. (1972). Annu. Rev. Biochem. 41, 843-868.

131. Hill, A. V. (1910). J. Physiol. (London) 90, iv-vii.

132. Bessler, W., Shafer, J. A., and Goldstein, I. J. (1974). J. Biol. Chem. 249(9), 2819-2822.

133. Blundell, T. L., and Johnson, L. N. (1976). In "Protein Crystallography" Ch. 8.6. Academic Press, New York.

134. Becker, J. W. Reeke, G. N. Jr., Wang, J. L., Cunningham, B. A., and Edelman, G. M. (1975). J. Biol. Chem. 250(4), 1513-1524.

135. International Tables for X-Ray Crystallography (1974). Vol. IV. Birmingham:Kynoch Press (present distributor Kluwer Academic Publishers, Dordreht).

136. Sheldrick, G. M. (1976). SHELX76. Program for Crystal Structure Determination. Univ. of Cambridge, England.

137. Matthews, B. W. (1968). J. Mol. Biol. 33, 491-497.

138. McPherson, A. (1982). In "Preparation and Analysis of Protein Crystals" (A. McPherson, ed.), p 184. John Wiley & Sons, New York.

139. Roberts, D. D., and Goldstein, I. J. (1983). J. Biol. Chem. 258(22), 13820-13824.

140. Roberts, D. D., Arjunan, P., Townsend, L. B., and Goldstein, I. J. (1986). Phytochemistry, 25(3), 589-593.

141. Maliarik, M., Plessas, N. R., and Goldstein, I. J. (1988). Biochemistry, 28, 912-917.

142. Caron, M., Ohanessian, J., Becquart, J., and Gillier-Pandraud, H. (1982). Biochim. Biophys. Acta, 717, 432-438.

143. Wang, J. L., and Edelman, G. M. (1971). J. Biol. Chem. 246(5), 1185-1191.

144. Brand, L., and Gohlke, J. R. (1972). Annu. Rev. Biochem. 41, 843-868.

145. Stryer, L. (1965). J. Mol. Biol. 13, 482-495.

146. Turner, D. C., and Brand, L. (1968). Biochemistry 7(10), 3381-3390.

147. Barel, A. O., Turneer, Mireille, and Dolmans, M. (1972). Eur. J. Biochem. 30, 26-32.

148. Blundell, T. L., and Johnson, L. N. (1976). Ref. 133, p 331.

149. Scatchard, G. (1949). Ann. NY Acad. Sci. 51, 660-672.

150. Gunther, G. R., Wang, J. L., Yahara, I, Cunningham, B. A., and Edelman, G. M. (1973). Proc. Nat. Acad. Sci. USA 70(4), 1012-1016.

APPENDIX

BINDING OF HYDROPHOBIC LIGANDS TO PEANUT AGGLUTININ

1. Scatchard Analysis of TNS/ANS Binding to PNA

Experimental

Solutions of NaCl-TRIS buffer made 1.5, 3.0, 6.0, 9.0, and 12.0 mg/ml in PNA (for TNS) or 1.0, 2.0, 3.0, and 4.0, (for ANS), were titrated with 272 μM TNS (30 μl additions x 6) or 1000 υM ANS (5 μl additions x 6) respectively. An initial volume of 900 μl was used in each titration. Excitation was at 350 nm (10 nm slit), and emission was at 450 nm (TNS) or 480 nm (ANS) with a 10 nm slit. The concentration of TNS or ANS were determined by adding a weighed amount to a fixed volume of buffer. Parallel titrations of NaCl-TRIS buffer was used to correct for the background fluorescence of either probe.

Results

Data were plotted according to the method of Scatchard (149), which yielded association constants of $12.0 \pm 0.61 \times 10^3$ M^{-1} for TNS and $27.7 \pm 2.1 \times 10^3$ M^{-1} for ANS. Site stoichiometry was estimated from these plots as 1.1 ± 0.20 sites/tetramer for TNS and 0.98 ± 0.08 sites/tetramer for ANS (using a molecular weight of 110,000

daltons for PNA). A Scatchard plot for the binding of TNS to PNA is shown in Figure A.1.

2. Binding of DnsGalN to PNA in the Presence of BAP

The results for the binding of DnsGalN to PNA in the presence of fixed amounts of BAP, Ch.IV.C.4., are plotted according to the method described in Ch.IV.C.1. A representative plot, shown in Figure A.2., indicates that in the presence of increasing amounts of BAP, DnsGalN binds with increased affinity to PNA.

3. Hydrophobic Binding Interactions of PNA

Binding interactions of PNA with various probes are shown in Table A.1. In the presence of PNA, both TNS and ANS show about a 300-fold enhancement of fluorescence, and about a 50-fold nm blue shift in emission maximum, compared to that observed in water. The fluorescence enhancement and blue shift of DnsGalN are, however less. These results are consistent with the binding of TNS and ANS to a similar (or the same) site, and the DnsGalN binding to a more polar site (when compared to the TNS or ANS site) on PNA. Scatchard analysis shows that both TNS and ANS bind with a stoichiometry estimated at one site/tetramer. A model of PNA which can describe the binding of ligands like TNS and ANS (determined fluorometrically) and BAP (determined crystallographically) is shown in Figure A.3. In this model, PNA exists as a tetramer with one binding site for TNS or ANS. In the presence of BAP, PNA dissociates into

Figure A.1. Scatchard Analysis of TNS Binding to PNA

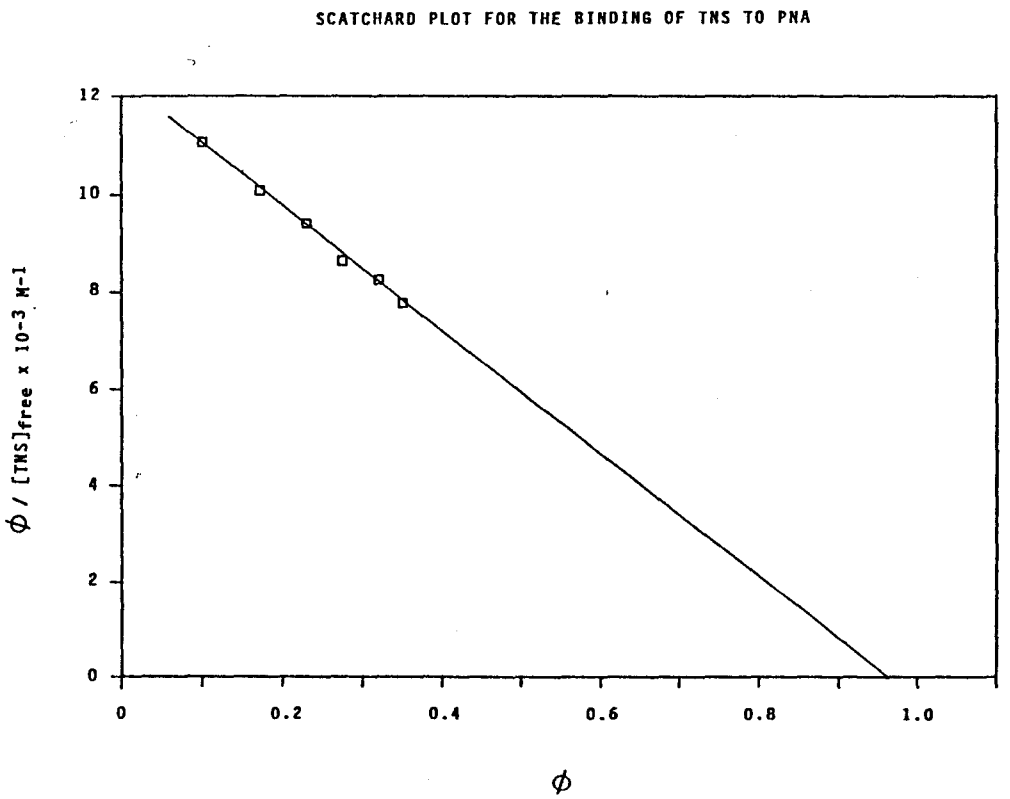

A fixed amount of PNA (6 mg/ml) was titrated with 272 μM TNS (30 μl additions x 6). Parallel titrations of NaCl-TRIS buffer was used to correct for blank fluorescence.

Figure A.2. Graphical Representation for the Determination of the Association Constant of DnsGalN Binding to PNA in the Presence of BAP

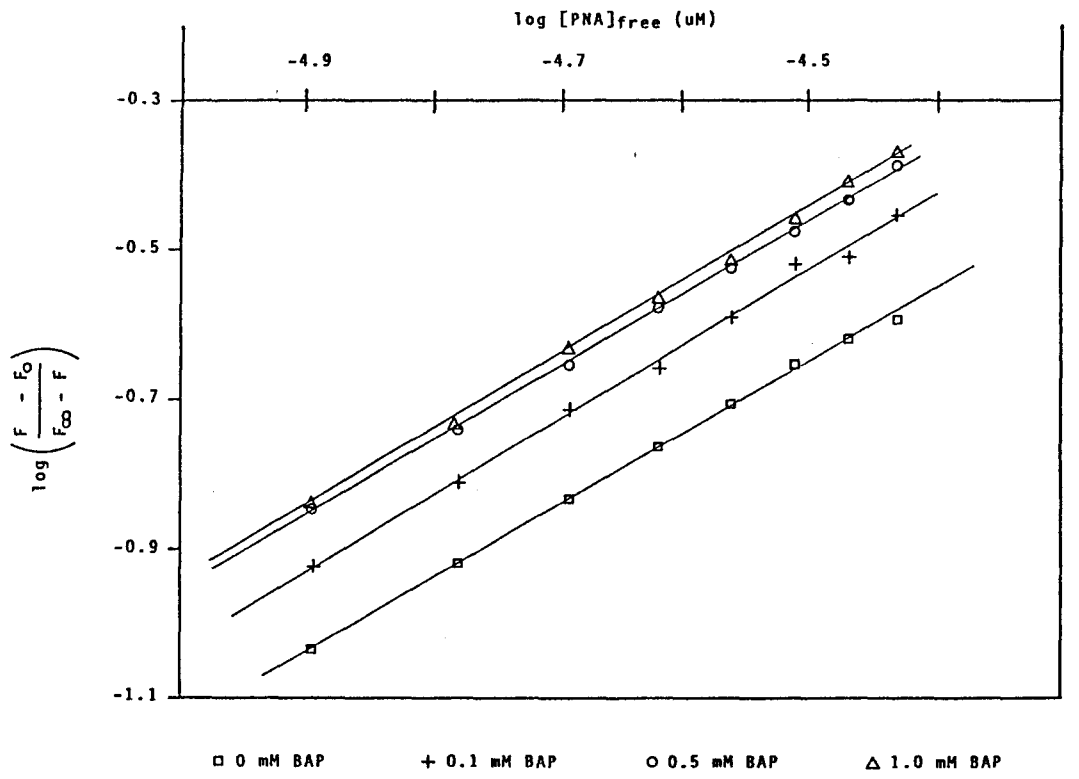

Table A.1. Hydrophobic Binding Interactions of PNA

PROPERTIES OF PNA BINDING INTERACTIONS

ligand	fluorescence enhancement	wavelength shift	Ka ($M^{-1} \times 10^{-3}$)	# sites/tetramer
TNS	330 x's	-51 nm	9.1 ± 0.2	1.1 ± 0.02
BAP			0.21 ± 0.04	
ANS	300 x's	-45 nm	24.2 ± 1.5	0.98 ± 0.08
DnsGalN	120 x's	-13 nm	10.6 ± 1.2	
lactose			1.5 ± 0.3	

Figure A.3. Model for the PNA Based on its Hydrophobic Binding Interactions

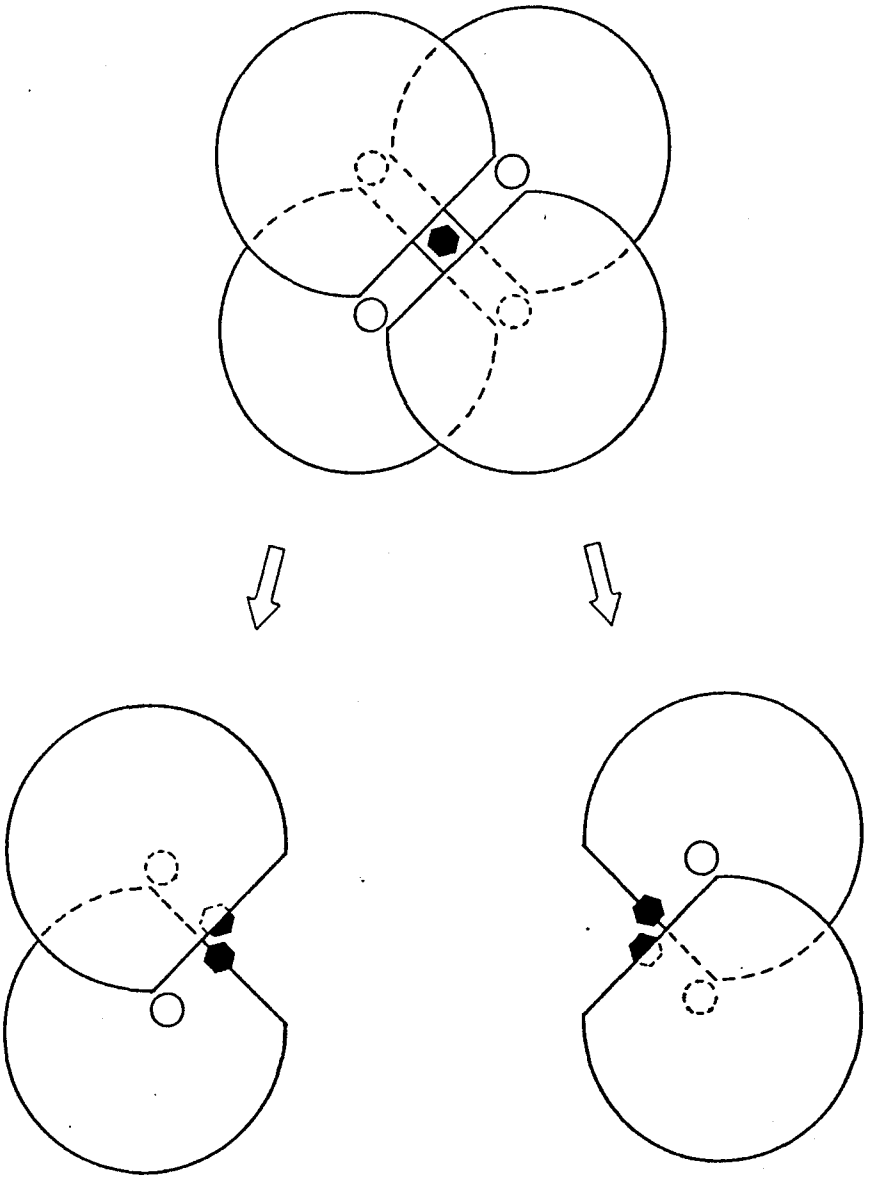

dimers, facilitating the binding of additional BAP ligands. From space group requirements, BAP binds to PNA in the stoichiometry of 1 ligand/monomer.

A change in carbohydrate binding valence would accompany the dissociation of tetrameric PNA into dimers. Tetrameric concanavalin A was shown to have significantly altered biological properties after treatment with succinic anhydride which converts the protein to a dimeric molecule (150). In the dimeric form, the hemagglutinating ability of Con A is drastically reduced. This was suggested to be a consequence of its lower carbohydrate valence when it exists as dimers (150). PNA is one of the Legume lectins which interacts with the rhizobium which can nodulate the peanut plant (115). The dissociation of PNA by BAP suggests that cytokinins may provide a means of regulating the rhizobium-lectin interaction in legume plants. The effect of BAP on the binding of DnsGalN to PNA was small (about a 2.5 enhancement in the presence of a 28:1 molar ratio of BAP to PNA). It is possible that dissociation of PNA from tetramers into dimers better facilitates the binding of DnsGalN. This may occur from alterations in the carbohydrate binding site from either quaternary structural changes, or rearrangements in subunit structure.

APPROVAL SHEET

This dissertation submitted by Eugene J. Zaluzec has been read and approved by the following committee:

Dr. Kenneth W. Olsen, Research Director
Associate Professor of Chemistry
Department of Chemistry
Loyola University of Chicago

Dr. Stephen F. Pavkovic
Professor of Chemistry
Department of Chemistry
Loyola University of Chicago

Dr. Albert W. Herlinger
Associate Professor of Chemistry
Department of Chemistry
Loyola University of Chicago

Dr. Duarte Mota de Freitas
Assistant Professor of Chemistry
Department of Chemistry
Loyola University of Chicago

Dr. Mir Shamsuddin
Department of Clinical Pathology
Children's Memorial Hospital (Chicago)

The final copies have been examined by the director of the dissertation and the signature which appears below verifies the fact that any necessary changes have been incorporated and that the dissertation is now given final approval by the Committee with reference to content and form.

The dissertation is therefore accepted in partial fulfillment of the requirement for the degree of Doctor of Philosophy.

Date 9/20/89 Director's Signature